

AN INVESTIGATION INTO THE PARAMETERS EFFECTING
THE PERFORMANCE OF TUBE MILLS:

THE BEHAVIOUR OF A SINGLE PARTICLE ON THE
INSIDE OF A ROTATING CYLINDER.

M. B. NATES

September 1989

Submitted to the University of Cape Town
in part fulfillment of the requirements
for the degree of Master of Science in Me-
chanical Engineering.

The University of Cape Town has been given
the right to reproduce this thesis in whole
or in part. Copyright is held by the author.

The copyright of this thesis vests in the author. No quotation from it or information derived from it is to be published without full acknowledgement of the source. The thesis is to be used for private study or non-commercial research purposes only.

Published by the University of Cape Town (UCT) in terms of the non-exclusive license granted to UCT by the author.

I, M. B. Nates, submit this thesis in part fulfillment of the requirements for the degree of Master of Science in Mechanical Engineering. I claim that this is my original work and has not been submitted in this or any other form for a degree at any university.

University of Cape Town

ACKNOWLEDGEMENTS

Thanks are due to ESKOM, whose support of this project is much appreciated, in particular Mr. A. Robinson of the Milling division. The assistance and suggestions from Dr. G. Nurick, project supervisor, and Prof. D. Reddy are acknowledged with much gratitude. Thanks are also due to the technical staff of the department of Mechanical Engineering for their assistance during the experimental phase of the project.

University of Cape Town

SYNOPSIS

This thesis is the first stage of a project to investigate the parameters effecting the performance of tube mills. The main topics that the project will cover are the motion of mill charge and the wear characteristics of the balls and the mill liners. A literature survey highlighted that no examination had been performed that investigated the motion of a particle with specific emphasis on the response to changes in the coefficient of friction between the particle and the liner. This thesis concentrates on the motion of a single particle moving on the inside of a smooth rotating cylinder.

Three formulations are presented that model the motion of the particle. The first model assumes that the particle slides along the cylinder. To ensure that it slides, and does not roll, a block shaped particle is modelled. The second motion type assumes that a spherical shaped particle rolls along the cylinder. The assumption that is made, is that the point of contact between the ball and the cylinder does not slip or skid. This mode of rolling has been defined as Pure Rolling. A third model is proposed that is a combination of the sliding and rolling models. The formulation attempts to incorporate both actions, rolling and sliding. In this way the motion of the particle is dependent on both the rolling and sliding interactions.

The governing equations for the Sliding and Rolling models are solved numerically, using an Euler Forward Approximation. Both models are solved by a computer implementation of the resulting numerical equations. The Sliding program has been extended to animate the response of the block on the inside of the cylinder. The theoretical predictions from the two numerical solutions are presented and discussed.

Experiments were done to validate the theoretical models. The rationale for the experimentation and the experimental procedure are discussed. Emphasis was placed on the Sliding model and with a less intensive investigation being completed on the Rolling model. The correlation of the theoretical predictions of the Sliding model were in close agreement with the experimental data. All the experimental results are presented and discussed with respect to the relevant theoretical predictions.

The conclusions and recommendations that are presented include the following. The first is that the Sliding formulation is competently able to model the basic response of a block. The model allows the amount and onset of slipping between the block and the cylinder to be analysed. The amount of slipping predicted by this formulation is significantly more than previously suspected. This result has implications on particle and liner wear.

The Rolling model is not adequate, as its period of validity only extends over the ball's initial motion. The time period before it breaks down is of the order of 1 second. The attempt at a simple combination of the two models was not possible. The resulting simple combination neglects the effects of the particle's spin on its translational motion.

University of Cape Town

TABLE OF CONTENTS

	<u>Page</u>
ACKNOWLEDGEMENTS	i
SYNOPSIS	ii
LIST OF ILLUSTRATIONS	vi
NOMENCLATURE	viii
GLOSSARY	ix
1. INTRODUCTION	1
2. LITERATURE SURVEY	3
2.1 General Terminology employed in Milling	3
2.2 Ball Paths and Trajectories in a Rotary Mill	6
2.3 Charge Slippage in a Rotary Mill	16
2.4 Charge Surging in a Rotary Mill	25
2.5 Radial Segregation in a Rotary Mill	29
2.6 General Discussion of Reviewed Literature	33
3. DERIVATION AND DISCUSSION OF THEORETICAL MODELS	35
3.1 Sliding Model	35
3.1.1 Derivation of Sliding Equations	36
3.1.2 Numerical Solution of Sliding Equations	38
3.1.3 Examination of the End Conditions of a Sliding Block	39
3.1.4 Computer Implementation of the Numerical Solution to the Sliding Equations	41
3.1.5 Discussion of the Results from the Numerical Solution of the Slid- ing Equations	44
3.2 Rolling Model	54
3.2.1 Derivation of the Equations for a Ball moving with Pure Rolling	54
3.2.2 Numerical Solution of the Rolling Equations	56
3.2.3 Discussion of the Results from the Numerical Solution of the Roll- ing Equations	56
3.3 Combination of the Rolling and Sliding Models	62

4. EXPERIMENTAL RATIONALE AND PROCEDURE	64
4.1 Experimental Rationale	64
4.2 Experimental Apparatus	65
4.3 Experimental Procedure	69
5. PRESENTATION AND DISCUSSION OF THE EXPERIMENTAL RESULTS	71
5.1 Determination of Coefficient of Friction for each Surface	71
5.2 Results of the Angle of Departure of a Single Block	72
5.3 Discussion of the Results of the Slip Angle of a Single Block	76
5.4 A Brief Discussion of the Experimentally observed Centrifuge Speeds of a Single Block.	81
5.5 A Brief Discussion of the Results of the Rolling Scenario	83
6. CONCLUSIONS AND RECOMMENDATIONS	84
6.1 Conclusions	84
6.2 Recommendations	86
7. REFERENCES	88
8. BIBLIOGRAPHY	90
9. APPENDICES	
APPENDIX 1: Resume of Reviewed Literature	
APPENDIX 2: Resume of Mathematical Formulations	
APPENDIX 3: Solution of the Sliding Governing Equations using an Euler Forward Approximation.	
APPENDIX 4: Worked Example of the Numerical Solution of the Sliding Equations	
APPENDIX 5: Derivation of the Toppling Equations.	
APPENDIX 6: Solution of the Rolling Governing Equations using an Euler Forward Approximation.	
APPENDIX 7: Listing of Experimental and Theoretical Results	
APPENDIX 8: Listing of Computer Program used for the Solution and Animation of the Sliding Equations.	
APPENDIX 9: Listing of Computer Program used for the Solution of the Rolling Equations.	

LIST OF ILLUSTRATIONSFigures

2.1	Section through a Ball Mill	4
2.2	Formulation of the Forces acting on a Ball.....	6
2.3	Distinct Ball paths according to White [1].....	8
2.4	Paths of travel of Particles in Ball Mill. (Davis [2]).....	9
2.5	Ball Paths at Various Speeds according to the Davis and the Gow et al [4] Formulations.	10
2.6	Ball paths before and after inclusion of the effects of adhesion, according to Vermuelen [8].....	13
2.7	Ball paths in a Mill with the effects of Lifter Bars included, as per Vermuelen [9].....	14
2.8	Charge Shapes at various Loads and Speeds as recorded by Gow et al [4].....	16
2.9	Arrangement of the Measuring Instruments, δ_s is the distance between the probes. (Manz [13]).....	18
2.10	Pickup Ratio and Slip plotted against angle for a smooth Mill. [13].....	19
2.11	Average Pickup and Slip Ratios plotted against Speed Ratio for a Smooth Mill with different Charge Ratios. (Manz [13]).....	20
2.12	Average Pickup and Slip Ratio plotted against number of Lifters for various Charge Ratios. (Manz [13]).....	20
2.14	Bed Behaviour Diagram of Nickel Oxide [14]	22
2.15	Reproduction of experimental results from Vermuelen and Howat [15].....	23
2.16	Graphical depiction of the dependence of Surge on the Milling Parameters [6].....	26
2.17	Tracings from the film strip of the rod configurations during a cascading phase of the charge motion [16].....	28
2.18	Radial Segregation for different types of bed motion [18].....	30
3.1	Orientation of the forces acting on a Block.....	36
3.2	Flow Chart of Computer Program.....	42
3.3	Two Graphs of μ versus ϵ , for various Ω_m	46
3.4	Graphs illustrating the possible End Conditions of a Block on a Smooth Liner.	48
3.5	Graphs illustrating the trends of R and T versus ϵ for a Block on a Smooth Liner.	49
3.6	The Parabolic Trajectories of a Block for varying μ and constant Ω_m	51

3.7	The Parabolic Trajectories of a Block for varying Ω_m and constant μ	52
3.8	Orientation of the forces acting on a Ball	55
3.9	Graph of θ versus time for a Ball moving with pure Rolling on a smooth liner with $\mu=\infty$	57
3.10	Graph of $\dot{\theta}$ and ω versus time for a Ball moving with pure Rolling on a smooth liner	58
3.11	Graph of R versus time for a Ball moving with pure Rolling on a smooth liner	60
3.12	Graph of T/R versus time for a Ball moving with pure Rolling on a smooth liner	60
4.1	Photograph of Experimental Apparatus	66
4.2	Photograph of Information Panel and Camera position	67
4.3	Photograph of a Sample Video Recorded Frame	69
5.1	Graph of Angular Rise versus Mill Speed for three different blocks on a steel surface	73
5.2	Graph of Angular Rise versus Mill Speed, with the 90% confidence range	74
5.3	Graph of Angular Rise versus Mill Speed, with the mean sample values and the theoretical predictions	75
5.4	Graph of Slip Angle versus Mill Speed	77
5.5	Graph of Angular Displacement of a Block and the Mill Liner versus Time	78
5.6	Graph of the Slip Angle versus Mill Speed on the Steel Surface	80
5.7	Graph of the Slip Angle versus Mill Speed on the Cloth Surface	80
7.1	Mill with a Sinusoidal Liner Shape	87
A5.1	Orientation of forces acting on a Block on the Point of Toppling ($\dot{\theta}=\Omega_m$)	A5.1
A5.2	Orientation of forces acting on a Block on the Point of Toppling ($\dot{\theta}\neq\Omega_m$)	A5.3

Tables

5.1	Tabulation of the Uncertainty in μ	71
5.2	Tabulation of Data obtained from Figure 5.5	79
5.3	Tabulation of Experimental and Theoretical Centrifuge Speeds	82

NOMENCLATURE

a	=	Ball Diameter	(m)
a_n	=	Normal Acceleration	(m/s ²)
a_t	=	Tangential Acceleration	(m/s ²)
g	=	Acceleration due to Gravity (9,81m/s ²)	(m/s ²)
m	=	Mass	(kg)
h	=	Time Increment for Euler Step (δt)	(seconds)
l_r	=	Block width in the radial direction	(m)
l_t	=	Block width in the tangential direction	(m)
t	=	Time	(seconds)
x, y	=	Coordinates of the centre of a particle	(m)
Fr	=	Froude Dimensionless Number (u^2/lg)	
I	=	Second Moment of Inertia	(kgm ²)
J	=	Percentage Fill of the Mill	(%)
L	=	Mill Length	(m)
N	=	Mill rotational Speed	(rpm)
N_c	=	Davis Critical Velocity	(rpm)
R	=	Normal Reaction of the Liner on a Particle	(N)
T	=	Tangetial Force along Liner (Friction)	(N)
V	=	Liner Velocity	(m/s)
W	=	Weight of the particle due to gravity	(N)
W_r	=	Weight Component in the radial direction	(N)
W_t	=	Weight Component in the tangential direction	(N)
α	=	The Davis Angle of Depature	(°)
μ	=	General Coefficient of Friction	
μ_s	=	Static Coefficient of Friction	
μ_k	=	Kinetic Coefficient of Friction	
θ	=	Angular Position of a Particle on the Liner	(°)
$\dot{\theta}$	=	Angular Velocity about the Mill Centre	(rad/s)
$\ddot{\theta}$	=	Angular Accleration about the Mill Centre	(rad/s ²)
ω	=	Angular Velocity of a Ball about its own centre (spin)	(rad/s)
$\dot{\omega}$	=	Angular Acceleration about Ball Centre	(rad/s ²)
π	=	Pi (3.141592654)	
Ω_m	=	Mill Velocity	(rad/s)
R	=	Mill Radius	(m)
R'	=	Effective Radius of roatation	(m)

GLOSSARY

- AOD : Angle of Departure of the particle from the liner
- Cascading : Term used to describe a particle that is rolling down the face of the 'en masse' region.
- Cataracting : Term used to describe a particle that is in flight above the body of the charge
- Critical Velocity : The mill velocity at which a particle becomes centrifuged to the liner
- POD : Point of Departure of the particle from the liner
- POR or POI : Point of Return or Impact of the particle onto the liner.
- N_c : The Davis Critical Velocity of the mill for centrifuging to occur.
- θ_{slip} : Slipping Angle of a Block for $\dot{e} = Q_m$
- θ_{topple} : Toppling Angle of a Block for $\dot{e} = Q_m$
- Keyed in : Term used to describe a charge that is moving at the same speed as the liner.
- Shoulder of Charge : The uppermost part of the charge, from where the particles depart and start to cataract.
- Toe of Charge : The lowest part of the charge, onto which the cataracting balls impact.

1. INTRODUCTION

The power production and mining industries of South Africa use milling plants to process most of their raw ores. ESKOM, in particular, receives the coal for its power stations in up to 30mm sized pieces. Before the coal is burnt, it is pulverized into a powder, which has an average particle size of less than 75µm. This comminution process is both energy and capital intensive. ESKOM use ball mills that are filled with a charge of coal and steel balls. The rotary motion of the mill causes the charge to grind the coal to the required dimensions. During the grinding process, both the balls and the replaceable mill lining are destroyed due to wear. The balls are replaced continually at a cost of approximately R1000 per mill per week. The linings have an average lifetime of 35 - 40 thousand hours and are replaced at a cost of up to R120 000 per mill. On average, a power station has four boiler units and five milling plants per boiler. The cost of consumed balls and liners by the early 1990's is expected to be about R10 million per annum.

This prompted ESKOM to initiate an investigation into the charge motion and wear characteristics of balls and liners. Much work has been done on milling from an experimental point of view, with empirical results and conclusions being drawn. ESKOM approached the University of Cape Town to conduct research into charge motion from an applied mechanics approach. The objectives of the research program are to further the understanding of charge motion and from this, to study the nature of the wear of the liners and balls.

The research began with a literature review into milling and specifically charge behaviour within operating mills. The aim of the review was to highlight any areas of lesser expertise and to provide a logical starting point for the project as a whole. Some of the early milling models and formulations examine the motion of a single particle or ball and analyse its response to changes in milling conditions (eg mill speed). These early formulations neglect to specifically include the effects of friction on the particle's behaviour. Secondly, these models make few provisions for a particle slipping or sliding along the mill lining. Hence it was considered a viable starting point to develop a formulation that specifically includes the effects of friction and slipping on a particle's behavior.

The aim of this thesis is to develop and test a new model that includes the effects of friction and slip on the response of a single particle moving on the inside of a rotating smooth cylinder. The main thrust of the work will be to gain an understanding of why, when and how a particle slips along a liner. The slipping of particles along the lining is one of the main sources for the wear of both the balls and lining.

This thesis forms the initial stages of the entire project and so the following limitations were imposed. The first was to investigate the response of only a single particle. To attempt to examine the motion of more than one particle from the outset, without a full understanding of a single particle's motion would not have been feasible. Secondly, the liners that are examined are smooth and not corrugated as used in practise. This was done to simplify the model with a view to extending it at a later stage. Finally, the effects of the interactions between the coal and the balls was ignored. This was done because the implication of including the powdered coal would be to transform the system into a multi-particle situation, which would not have been suitable as a starting point.

To achieve these objectives, the thesis develops formulations for some of the possible motion patterns of a single particle on a smooth lining. The governing equations are solved numerically and the results presented and discussed. Experimental research was conducted to compare and test the theoretical predictions with the physical results. Conclusions have been drawn about the accuracy of the mathematical model to the modelled physical situation. Finally, recommendations have been included for possible areas of future research.

2 LITERATURE SURVEY

The literature surveys a broad spectrum of work on milling and the milling process and was not restricted to the specific topic of the thesis. The background information and understanding of the milling process gained was important for the project as a whole.

The literature survey is divided into four main sections. The first includes a brief description of the milling process and the terminology used to describe the behaviour of a mill charge. The second section covers ball paths and ball trajectories. The behaviour of the 'en Masse' region is discussed in the third section with particular emphasis placed on the inter related nature of charge slippage and charge surge. The final section discussed is the radial segregation of the 'en Masse' region.

2.1 General Milling Terminology.

Balls mills are used in many different industrial applications. They are used to mix pigments, to produce fine talcs and powders, to crush ores for further processing (Mining industry), and to crush coal (Power industry).

During the time that ball mills have been in use, various authors have adopted their own terminology in referring to the components and behaviour of mills. In this section the currently accepted terms will be defined.

Figure 2.1 shows a section through a ball mill. The liner size has been exaggerated to show how it interacts with the charge. A milling charge consists of both the coal and the balls. The amount of charge in a mill is defined by the Percentage Filling (J). Percentage Fill is defined as the ratio of the volume of the charge to the volume of the empty mill, expressed as a percentage. The charge has been divided into two regions by the line AB in Figure 2.1. Below the line is the portion of the charge that is lying against the mill lining, it is termed the 'en Masse' region. The angle of line AB to the horizontal is defined as "The Angle of Repose" of the charge.

Two terms, Cataracting and Cascading, are used to describe the motion of the balls. The portion of the charge above the line AB is in flight. These balls have been detached from the main body of the charge and are defined

as Cataracting. The balls rolling down the face of the charge are in contact with the charge body and are defined as Cascading. The density of the cascading region is much higher than the cataracting region.

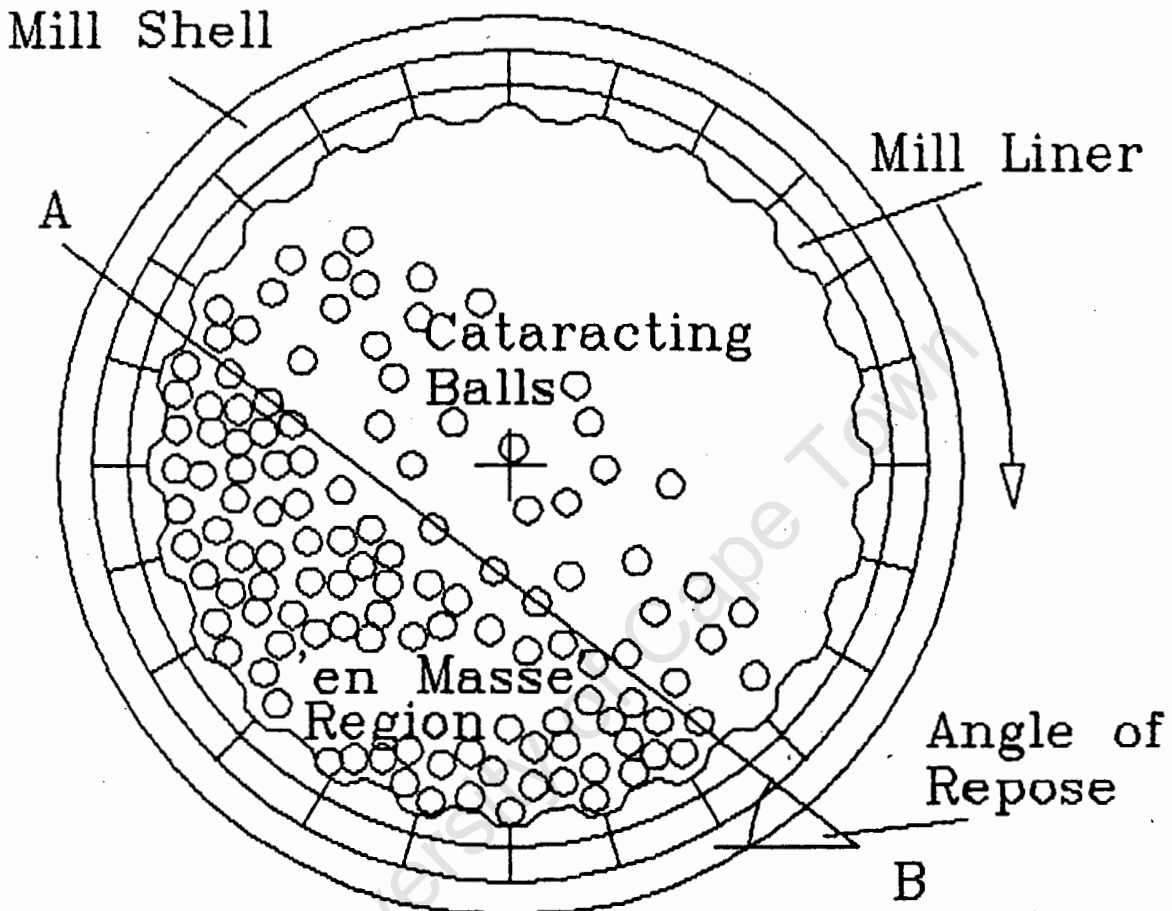


Figure 2.1: Section through a Ball Mill

As seen in Figure 2.1 the mill's rotation causes the balls to move up the mill wall, and then to either Cataract or Cascade down till they reach the charge Toe, where they are re-absorbed into the 'en masse' region. The point on the wall where the balls leave the charge is defined as the "Point of Departure" (POD), the angle of this point above the horizontal measured from the mill centre, is defined as the "Angle of Departure", (AOD). The faster the rotational speed the larger the AOD. If the charge never leaves the wall, then it is defined to be Centrifuging to the liner. The theoretical velocity at which this begins is defined as the "Critical Velocity" (N_c) of the mill.

The balls lying next to the liner are regarded as being "keyed in" to the liners if they move with the same velocity as the liner. This results in the relative velocity, between the balls and the liner, being equal to zero. When the relative velocity is non-zero, then slipping of the charge takes place and the charge rotates slower than the liner.

The grinding process is executed by two distinct actions within the mill. The initially large pieces of coal ($\pm 30\text{mm}$) are broken up by crushing. This is achieved by the cataracting balls impacting on the coal. The larger balls in the mill, $\pm 50\text{mm}$ diameter, are responsible for this action as the smaller balls are not large enough to produce the impacts required. The mill speed is controlled so that the majority of the impacts occur on or near the toe of the charge. If the operating speed is too high then the balls tend to impact against the exposed liner and undesirable excessive wear of the liner occurs.

The second process in the mill is the grinding of the chips of coal to a fine powder. This is accomplished by attrition and abrasion. The smaller balls do the fine grinding in two ways, firstly; by rubbing the coal between balls and secondly; between the balls and the liner. This procedure requires a large surface area, which the many small balls provide. The powdering of the coal is carried out in the 'en Masse' region, where the pressures are high and the relative velocities are small. The coal that is fine enough, is entrained into the air circulation in the mill, and removed to the boilers for combustion.

2.2 Ball Paths and Trajectories in a Tube Mill

White [1], in 1905, presented the first mathematical predictions for the paths of balls in a mill. Davis [2], in 1922, published an extensive report that incorporated and extended Whites' work. Both authors assumed that the only forces acting on a ball are due to the acceleration of gravity and the radial acceleration of the ball, due to the rotation of the mill. The ball will depart from the lining when the gravitational force exceeds the radial outward acting inertia force, this occurs at the Point of Departure. Both authors ignore the possibility of a ball slipping along the liner as well as any forces of cohesion and adhesion due to the coal. Figure 2.2 illustrates the acceleration and forces and their relative orientation, as predicted by White and Davis.

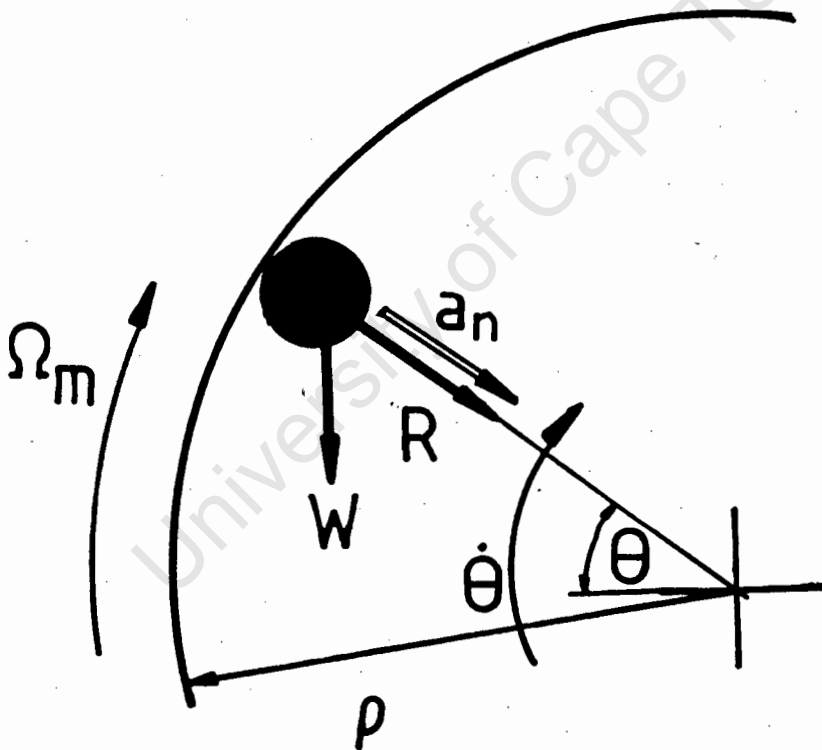


Figure 2.2: Formulation of the Forces acting on a Ball.

The mathematical analysis of White and Davis is as follows. It describes the motion of a single ball, moving without slip, on the inside of a rotating mill. The forces involved are: R , the reaction of the liner on the ball and W , the weight of ball due to gravity.

Summing forces in the radial direction (from Fig. 2.2):

By Newtons Second Law: $\Sigma F = ma$

$$\therefore mgsine + R = ma_{rn} \quad \dots(2.1)$$

$$\text{But } a_{rn} = \dot{e}^2(\rho - a) \quad \dots(2.2)$$

where: ρ = Radius of the mill
 a = Radius of the ball
 e = Angle of the ball above the horizontal
 \dot{e} = Rotational velocity of the ball
 Ω_m = Rotational Speed of the mill

Assuming $\rho \gg a$ then $(\rho - a) \approx \rho$ and $\dot{e} = \Omega_m$

$$\therefore R = m\Omega_m^2 \rho - mgsine \quad \dots(2.3)$$

Some authors use d'Lambert's principle and replace the radial acceleration with an equivalent outward acting inertia force. This force is then defined as a Centrifugal force acting on the ball and a_{rn} is set to zero.

The Point of Departure (POD) of the ball from the mill is defined as $R=0$. Therefore substituting $R=0$ into equation 2.3 yields:

$$\sin\alpha = \Omega_m^2 \rho / g \quad \dots(2.4)$$

where $e=\alpha$, and α is defined as the Davis Angle of Departure (AOD)

If the ball is still in contact with the liner when it reaches the top of the mill, then it has been Centrifuged to the liner. The mill rotational velocity for this condition is the Critical Velocity (N_c).

Substitution of $e=90^\circ$, $R=0$ and $\rho - a \approx \rho$ into (2.3) yields:

$$\dot{e}_c^2 = g/\rho \quad \text{rad/s} \quad \dots(2.5)$$

$$\text{or } N_c = \frac{29.9}{\sqrt{\rho}} \text{ rpm} \quad \dots(2.6)$$

After experimental observations, Davis assumed that the balls lie in distinct layers against the mill lining. From this assumption the effective radius of rotation is defined as $\rho' = \rho - a$, where ρ is the radius of the mill and "a" is the radius of a ball. A ball in the second layer will have an effective radius of $\rho' = \rho - 3a$. The inclusion of ρ' into equation 2.6 results in the AOD decreasing as the effective radius decreases. This predicts that the balls in different layers will have different points of departure. A ball in an inner layer will depart before a ball against the liner, as illustrated in Fig. 2.3

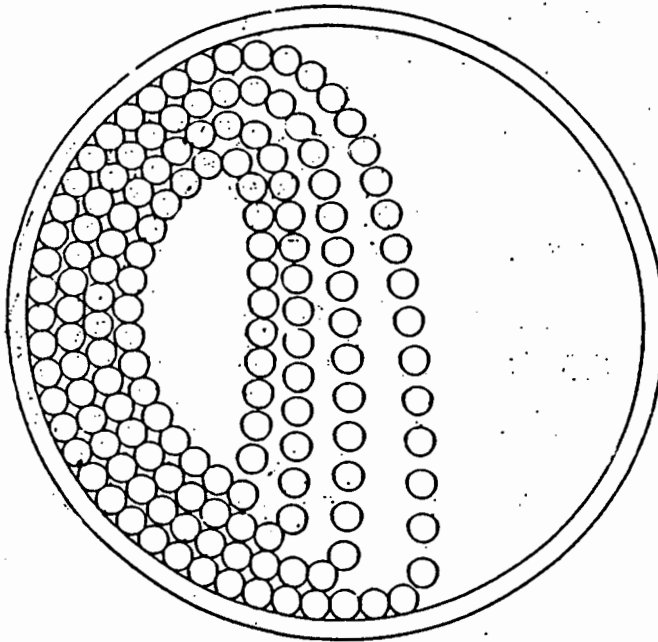


Figure 2.3: Distinct Ball paths according to White [1].

Extending the assumption, that each ball will leave the 'en masse' region at a particular point, a locus of all the POD's can be constructed, as shown by the line 'a'-'b' in Fig. 2.4. The balls lying against the liner, have the largest A.O.D. and hence travel furthest, to the extreme of toe of the charge. Assuming perfect packing after impact on the liner, then these balls will form a layer on to which the subsequent balls will impact. The points of impact or return can be joined to form a locus, as illustrated by line 'c'-'d'. By assuming perfect packing the radius at which a ball leaves and returns to the 'en Masse' region is the same. This is illustrated in Fig. 2.4 as the POD 'a' is at the same radius as the POR of 'c'. The same occurs for POD 'b' and POR 'd'.

The Points of Return, line 'c'-'d', are calculated by simultaneously solving the equation of the circle (with radius = ρ of that layer), and the equation that defines the trajectory of the ball. All particles are falling under the action of gravity only, so it is assumed that they follow parabolic trajectories.

The equation of the parabola trajectory is:

$$y = x \tan(\alpha) - \frac{gx^2}{2V^2 \cos^2(\alpha)} \quad \dots(2.7)$$

Hence the Point of Impact (or the Point of Return) will have coordinates

$$x = 4\rho \cos\alpha \cdot \sin^2\alpha \quad \dots(2.8)$$

$$y = -4\rho \cos^2\alpha \cdot \sin\alpha \quad \dots(2.9)$$

In 1929, Gow, Campbell and Coghill [4] challenged Davis' formulation and proposed a different interpretation as to the actual mechanics in a ball mill. They argued that at the point of departure, a ball is not able to follow a distinct path as there is bunching and crowding taking place between all the other balls. The net effect of the bunching is to push a ball further across the mill and to destroy its parabolic trajectory. The authors state that this effect is only noticeable for sufficiently filled mills. Below a certain percentage fill ($J \approx 20\%$) and $\Omega_m < N_c$, the charge does not cataract, as the slip against the liner is too high.

Gow et al present a mathematical formulation that includes the effect of the "extra push" due to the bunching effect, as presented in appendix 2.1 Figure 2.5 shows the trajectories due to Davis (dashed lines) and the Gow formulation (solid lines). The diagram illustrates that the new formulation throws the balls further across the mill.

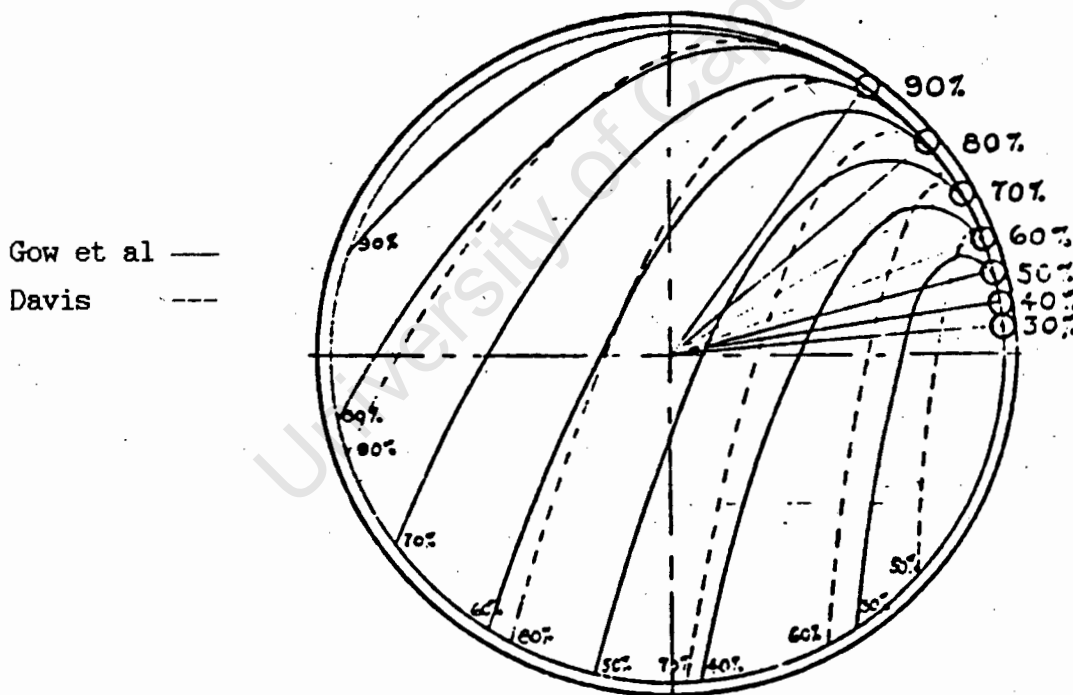


Figure 2.5: Ball Paths at Various Speeds (as a percentage of critical velocity) according to the Davis and the Gow et al [4] Formulations.

Gow et al used a test mill of 3ft ($\emptyset.91\text{m}$) diameter and 6" ($\emptyset.15\text{m}$) long, covered on both sides by a 1" (25.4mm) mesh screen. The anomalies in their results, the extra push, have been attributed to the interaction of the charge with the end screens. An interaction between a charge and a window

of a test mill is called an End Effect. Fahrenwald and Lee [5], in 1931, discuss Gow et al's results and state that Gow et al's formulation "exaggerates conditions somewhat." Fahrenwald and Lee conclude firstly; that the possible cause of Gow et al's observations was a jamming up of the charge in the narrow test mill and secondly that the parabolic formulation presents a better likeness to real charge motion. Two methods of avoiding end effects is to use rods [9,10] or use an open ended mill [5].

Fahrenwald and Lee derive an expression for the AOD that includes the effects of friction on ball motion. The authors assume that due to insufficient friction in a mill a charge is allowed to slip over the liner. The slip causes the balls to rotate and this rotation influences the AOD. No attempt was made by the authors to solve the resulting equations. Fahrenwald and Lee stated that when solved, the equations would provide a measure of the slip between the charge and the mill lining. The paper is concluded with a discussion of experimental results obtained by varying specific milling parameters. The parameters varied (power, percentage fill and ball size) fall outside of the scope of this thesis.

Rose and Sullivan [6], in 1957, re-derived Davis' results using a different approach. They question Davis' underlying assumptions, where he ignores the frictional characteristics of the charge and also any interaction between balls in adjacent trajectories. As an alternative they quote von Steiger whose work they included into their book. von Steiger developed a similar formulation to that of Gow et al. The similarity is that in both models, the balls are assumed to rise to their highest point with a constant velocity. There is no deceleration due to gravity, because the deceleration is counter acted by the extra push provided by the remainder of the charge. The end result is a trajectory of similar shape to that of Gow et al's. It is important to note that both formulations assume that there is no slipping between the charge and the liner.

Rose and Sullivan extended the work, by deriving an expression to predict the shape of the charge as the percentage fill and mill speed are altered. They incorporate into their formulation the concept of a locus of departure and arrive at a Davis like model. They are able to predict when a ball will leave the 'en masse' region and start to cascade or cataract. The difference with this formulation is that the effects of a coefficient of friction are incorporated, but again a non-slip charge is assumed

McIvor [7], in 1983, derived an expression for the flight of a single ball which included the effects of friction and the angle of the lifter bar face (see Appendix 2.1 for the formulation). McIvor stated that the outer layer of balls forms the key link for the transmission of energy from the rotating mill to the churned charge. Hence the amount of slipping or keying in of the charge greatly effects the efficiency of energy use of a specific mill. McIvor comments on the inaccuracies of previous investigator's [3,5,6] experimental results because of the small size of their test mills used and the resulting interlocking (or wedging) of the charge between the end walls. McIvor's observation is similar to that made by Fahrenwald and Lee [5].

McIvor draws numerous conclusions, two of the conclusions are particularly significant to this thesis. The first is that particle trajectories are independent of mill diameter. This implies that optimal grinding conditions are only influenced by the other variable condition, which is a mill operating speed. At present, the common practice is to quote mill operating conditions as a percentage of the critical velocity and not some other variable. This practise will be used in this thesis, all mill speeds will be quoted as a percentage.

The second conclusion is that ball trajectories are highly sensitive to the angle of the lifter face. This has significant implications on grinding conditions, as after a liner has begun to wear, the trajectories will not remain constant and the milling conditions will change. McIvor was one of the first investigators to state that though empirical milling relations are useful, they do not allow for a basic understanding of the milling process. He advocates that further elementary applied mechanical analysis, can provide the basic understanding still required to improve design and operating performance of mills.

Vermeulen et al [8], in 1984, in experimental testing, placed a piezoelectric sensor in a the liner bolt of an operating mill. This enabled measurement of the angle at which the balls were departing from the liner and also where they impacted back on to the liner. The experimental results were compared with the departure and impact points as predicted by Davis' model. Figure 2.6a illustrates the paths predicted by Davis and the experimentally recorded impact points (points α to T). There is a significant difference between the two sets of data. Vermeulen et al, using the same assumptions as Davis (ie non-slip charge motion), derived a new

formulation that was extended to include the effects of the adhesive forces between the wet slurry and a ball. The force balance at the surface of the liner included another term, the adhesive force, as an added percentage of the outward acting inertia centrifugal force, as shown in equation 2.10.

$$\Sigma F_{\text{radial}} = m\Omega^2 R(1+\phi) - mg\sin\alpha = R \quad \dots(2.10)$$

ϕ = The adhesion force as a percentage of the inertia centrifugal force.

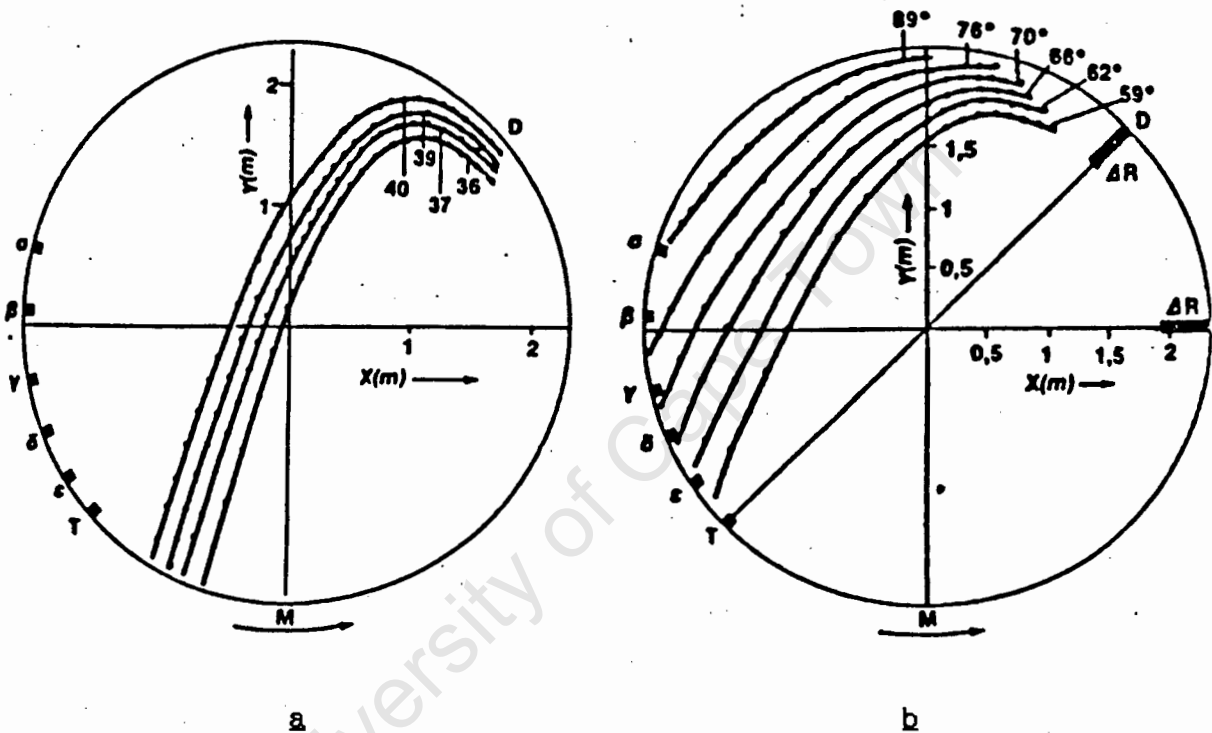


Figure 2.6: Ball paths before and after inclusion of the effects of adhesion, according to Vermeulen [8].

The effect is that the ball is held to the liner for a longer time and the AOD increases. Vermeulen et al heuristically chose a value for ϕ of 55%. The resulting trajectories are shown in Fig. 2.6b, where it can be seen that the experimental impact point (α to T) correspond to the theoretical impact points (the trajectories). Though the results show good convergence, it should be noted that the effects of slip of the charge and the ball interference at the POD have been neglected (The original simplifications used by Davis). The main import of this investigation was the experimental method that was successfully employed with an operating mill. Many investigators have tried, with varying success, to instrument an operating mill. Vermeulen et al were able to overcome many of the past problems.

Vermeulen [9], in 1985, in investigating the effects and interactions of lifter bars on rods in mills stated that the result would be applicable to both balls and pebbles. Included in the model is the effect of a rod either rolling or sliding down the face of the lifter bar, before it leaves the bar and starts to cataract. Appendix 2.1 contains a summary of the mathematical formulation.

Vermeulen concluded that the rod will not leave the lifter bar until it has reached the edge of the bar, i.e. the rod is further elevated while it is moving towards the edge of the bar. This overcomes the simplification of McIvor's, where the height of the lifter bar was ignored. Vermeulen shows that for the range of values of the coefficients of friction in a mill, the rod will tend to slide and not roll.

Figure 2.7 illustrates the effects of a lifter bar on a single rod. The circles are observed points from experimentation, the dashed line is the parabolic paths according to the new theory and the solid line is a parabolic path without the effects of the lifter (Davis). It can be seen that the new formulation models the liner-rod interaction effectively.

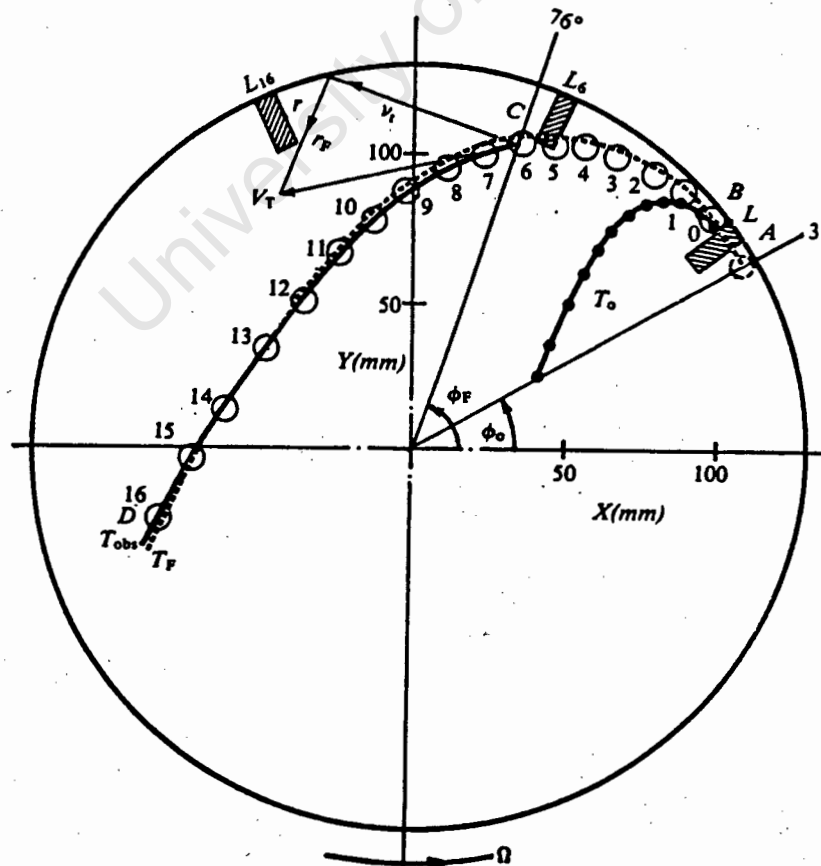


Figure 2.7: Ball paths in a Mill with the effects of Lifter Bars included, as per Vermeulen [9].

Von Steiger [6] and Gow et al [4], argued previously that the trajectory of a rod was only parabolic once it had started to descend. (Before the apex of travel is reached, the bunching of the other rods would disturb a particle's pure parabolic path). Vermeulen's experimental results (points 6 to 16) show that once a rod has departed from a lifter bar face, it follows a purely parabolic path. Vermeulen concluded that under the influence of lifter bars, rods and balls do travel in parabolic paths.

Furthermore, Vermeulen demonstrated that at the point of departure, a rod does not have a purely tangential velocity. The velocity has a radial component which is about 50% of the tangential component and acting inwards. This occurs because the rod has a velocity down the face of the lifter. This causes the rods to be flung further across the mill than previously predicted.

Powell [10], in 1988, extended Vermeulen's work to include lifter bars of varying face angle. (Vermeulen only used lifter bars which were perpendicular to the mill surface, ie 90°). An applied mechanics analysis is conducted on the rolling and sliding motion of a rod moving down a lifter bar. The analysis enabled the author to predict the time taken before a rod reached the edge of the lifter and hence the extra lift the rod received from the lifter. A parabolic trajectory is assumed for the rod's path after it leaves the lifter bar. An experimental investigation was conducted which yielded results that were in good agreement with the theoretical predictions.

Powell's main conclusions included the following:

- (i) To prevent slippage of the outer most layer of the charge, a lifter bar need not be larger than approximately one rod radius. The impact angle is not highly influenced as the lifter bar's height increases. The AOD is influenced, it increases as the lifter bar's height increases. Even so, the AOD increases only until a critical lifter height is reached, where upon it doesn't increase any further.
 - (ii) The lifter face angle has a significant influence on both the rod's lift and its impact point on the liner.
 - (iii) An increase in mill speed results in an increase in impact angle.
- Powell's work substantiates McIvor's comments about theoretical studies, and presents new information that allows for a deeper understanding of rod motion in a mill.

2.3 Charge Slippage in a Tube Mill

Various authors [3,4,7,11] have commented, on the slippage that takes place between the liner surface and a charge. The first were Haultain and Dyer [3], in 1922, when criticising Davis' model. They commented that the effects of slip ensured that the actual ball velocity, during departure from the lining, was less than the mill speed and this would affect the balls' trajectories. Haultain and Dyer observed that a corrugated lining prevented the outer layers from slipping as much, but even so the inner layers slipped relative to the outer layers. A quote from the paper highlights the uncertainties surrounding slippage in milling: "Of all the varying conditions existing in ball mills, slip is probably the least determinable, the most varying. The only sure thing about it is that it is always there."

Gow et al [4], conducted a series of experiments that showed that centrifuging of a charge can occur at velocities significantly different to the theoretical Davis critical velocity. (The critical velocity is determined for a non-slip situation) The degree of error in the experimental critical velocity was related to the percentage fill of the mill. Referring to Fig. 2.8, it is seen that for filling ratios (J) less than 20%, the charge has not begun to centrifuge at the critical velocity ($N=N_c$ or $N=100\%$). The balls are only able to cascade down the charge face, even at $N=N_c$. For $J=20\%$ minimal cataracting was visible, but no centrifuging occurred.

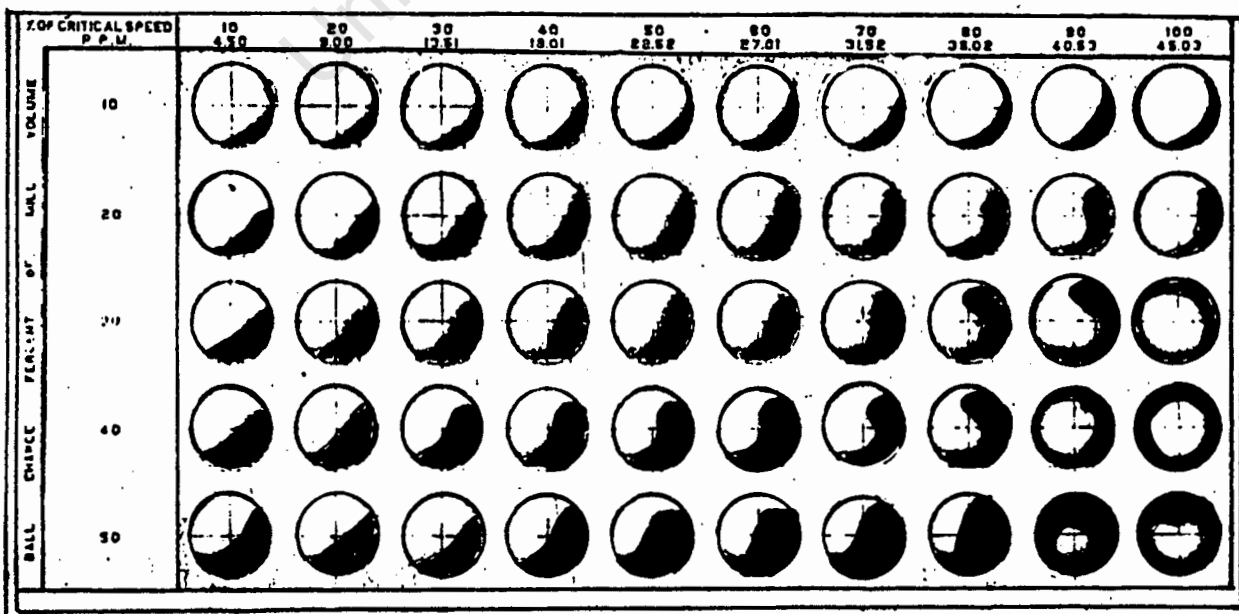


Figure 2.8: Charge Shapes at various Loads and Speeds as recorded by Gow et al [4].

For J between 30% and 40%, the critical velocity is approximately correct. At slow speeds, with $J=40\%$, no slipping was visible. It will be shown later that even though slippage may not be optically detectable, it is still taking place. While for $J > 50\%$, centrifuging occurs at less than the critical velocity. This is attributed to the crowding that occurs for large filling ratios. Gow et al do not account for these results, except for noting that slippage could be responsible for the discrepancies at the low filling ratios.

Gross [11], in 1938, presented results of an experimental investigation in which slip versus percentage fill and pulp density were plotted. The pulp density is a measure of the viscosity of the charge. Gross defines slip as the ratio of the actual centrifuge velocity to the theoretical centrifuge velocity. The experimental investigation yielded two main results. Firstly, that the magnitude of the slip decreases as the charge load increases. (This is a similar result to Gow et al's) The second result is that slip decreases as the charge pulp density increases. Hence as more fluid is added to a wet charge, and it becomes less viscous, one can expect more slipping to occur.

Hukki [12], in 1958, produced experimental results that are similar to Gow et al and Gross. He observes that the effect of an increased charge size is to reduce the slippage in a mill. Hukki explains the phenomena, by stating that the increase in charge mass will result in an increase in the frictional force between the liner and the charge. (Frictional Force = $\mu.R$ = $\mu.f(\text{mass})$). The increased friction will reduce slip. This is a concept that is extensively developed by Vermeulen and Howat [16].

The remainder of the paper concentrates on the idea of grinding at supercritical speeds (mill speeds exceeding Davis' critical speed). The author's idea is to take an underfilled mill and run it at supercritical speeds, such that the outer layer of the charge is centrifuged, while the inner layers cataract, or slip relative to the outer layer. This allows the outer layer of balls to act as the lining and so reduce liner wear.

The interesting point raised is that during this situation there is major slippage occurring, which Hukki maintains will grind the material by an enhanced abrasion zone. By this, Hukki recognises that some slippage is unavoidable and he employs the slippage in a positive way. Hukki derives a

mathematical model that includes friction and predicts the slip of a charge as a whole, see Appendix 2.2. Hukki concludes the paper by examining the initial results of an experimental investigation into the throughput capabilities of supercritical mills, without arriving at any definite conclusions.

In 1972, Manz [13], reported on an experimental procedure that measured slip in an operating mill. Instrumentation was developed to measure the velocity of the outer layer of balls, by inserting electrical probes into the rotating mill. The time that elapsed between recorded pulses from within the mill, was used to estimate the speed of a particle passing across the probe spacing. The experimental arrangement is illustrated in Fig. 2.9.

Manz defined slip as:

$$\text{Slip} = S = V_r/V_t \quad \dots(2.11)$$

$$\text{Pickup Ratio} = 1-S = V_k/V_t \quad \dots(2.12)$$

where: V_t = Speed of inner lining of mill

V_k = Absolute Speed of Grinding Medium

V_r = Relative Speed of Grinding Medium

and Filling Ratio (previously J) as ϕ_k , where:

$$\phi_k = \frac{\text{Pulp Volume of Charge of Grinding Medium}}{\text{Internal Volume of Mill}} \quad \dots(2.13)$$

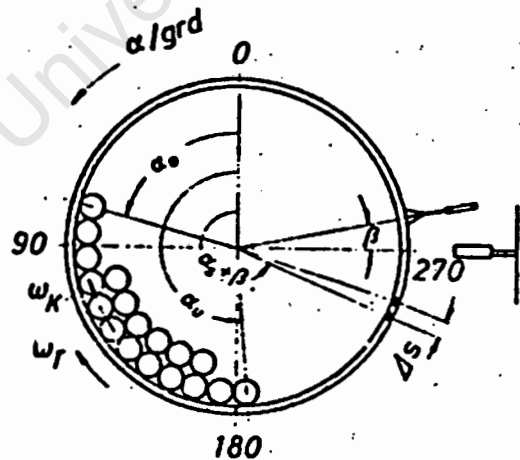


Figure 2.9: Arrangement of the Measuring Instruments, δ_s is the distance between the probes. (Manz [13])

Figure 2.10 illustrates the experimental observations of Manz that slip in a mill, is greatest at the toe of the charge and least at the shoulder. Hence as the charge starts to move up the mill liner, it initially travels

at about 10% of the mill velocity and is continually accelerated until it reaches mill velocity. Hereafter, the balls depart from the liner and cataract down to the toe. This explains why the major abrasion zone is found near the toe, where the charge slip is high. Secondly, some grinding also takes place at the shoulder due to slip occurring in the region.

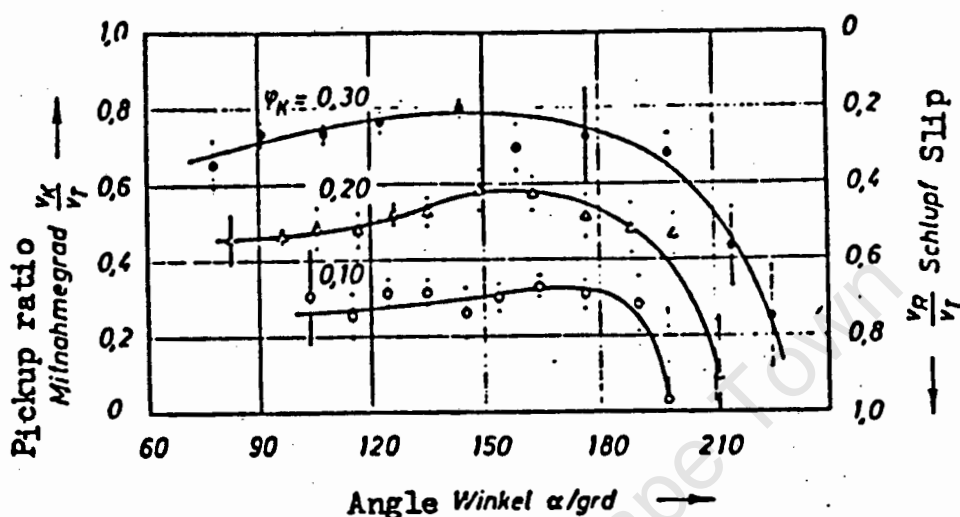


Figure 2.10: Pickup Ratio and Slip plotted against angle for a smooth Mill. (Manz [13])

Previous theory predicted that slip decreases as the filling ratio (J or ϕ_k) is increased. This is again validated by the results depicted graphically in Fig. 2.11. It is noted that the slip is fairly constant for a particular filling ratio, but varies greatly as the mill speed changes.

Manz included a plot of slip, for various charge ratios, against the number of lifters in the mill, as shown in Fig. 2.12. The effect of the lifters is to decrease the slip of the first layer of balls. As previously defined the charge becomes "keyed in". The mill was run at the Davis critical velocity in this series of tests. Comparing the slip of a 20% filled mill, run at the same speed (in Fig. 2.10), with the result in Fig. 2.12, for the same filling ratio but with 12 lifters. One observes that the slip has been reduced, from 60% to 30%. This reduction in slip is due to the interaction of the lifters with the charge and is in accordance with other investigators [9,10].

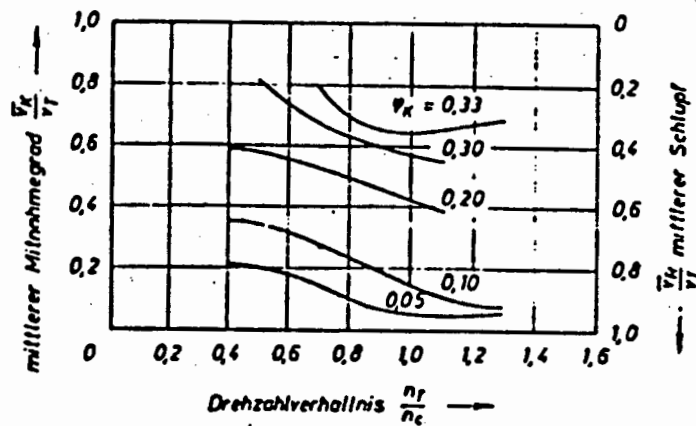


Figure 2.11: Average Pickup and Slip Ratios plotted against Speed Ratio for a Smooth Mill with different Charge Ratios. (Manz [13])

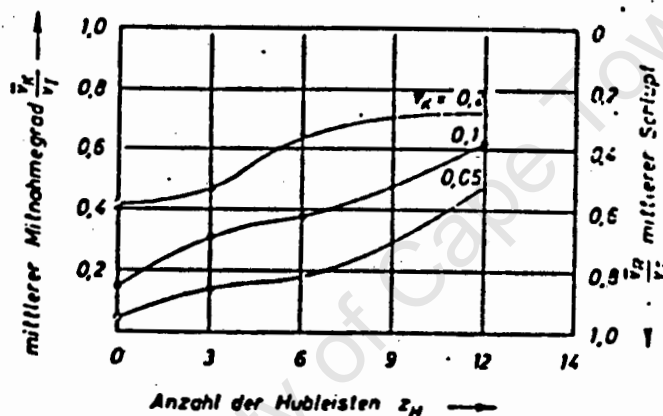


Figure 2.12: Average Pickup and Slip Ratio plotted against number of Lifters for various Charge Ratios. (Manz [13])

Manz's main conclusions from the experimentation include the following:

- (i) Slip increases as rotational speed increases.
- (ii) Slip increases as the power delivered to the mill increases.
- (iii) Slippage can be reduced by using cylinders (Cylpebs) or small balls as the small balls would "key in" more easily than the large balls.

The main contribution of the investigation, is that these results are consistent with other investigators results, but were obtained from the inside of an operating mill.

Henein et al [14], 1983, conducted experimentation on the nature of the motion of the charge in a rotary kiln. The major difference between kilns and mills is that the particle size in kilns is generally smaller than 10 mm, while balls in mills can be as large as 60 mm. The applicability of this study to milling is not stated, but the general trends seem to be appropriate.

Henein et al describe six types of bed motion namely; slumping, rolling, slipping, cascading, cataracting and centrifuging. Each motion type will be illustrated descriptively. The mathematical models developed by the authors, predict the onset and nature of each motion type. A summary of the models is contained in Appendix 2.2.

Slumping occurs at low rotational speeds, typically less than 2 rpm. At these low speeds, the inertia centrifugal forces are minimal, and so the effects of gravity and friction dominate. As the charge rotates with the cylinder so the angle of repose of the charge increases. A wedge is formed by the material contained above the static angle of repose and below the dynamic angle of repose. A shear plane, due to gravity, forms along the static angle of repose and hence the system can be modelled as a wedge sliding down a rotating inclined plane. The "slump" occurs when the gravitational force, down the plane, exceeds the shear stress along the plane. The wedge slides down the charge face and comes to rest at the toe.

This bed behaviour continues until the rotational speed has increased such that the motion pattern changes to Rolling. During the time that it takes the slumping wedge to reach the charge toe, more material has been transported to the charge shoulder to start forming the next wedge. Once a complete new wedge is formed it will in turn begin to slide. If this occurs before the old wedge has reached the toe, then the bed motion occurring is defined as Rolling. Rolling can be described as continuous charge slumping. It can also be seen as a less severe or diluted form of cascading.

The percentage fill or charge mass of a mill determines the magnitude of the pressure between the liner and the charge. As the percentage fill increases, so the dynamic pressure increases between the charge and the lining. The type of charge motion defined as Slipping occurs when the frictional force at the charge-liner interface is exceeded and the charge slides as a whole and comes to rest at a lower angle of repose. During Slumping the dynamic pressure is too high for slipping to occur. Hence slipping occurs at percentage fills smaller than required for slumping. Henein et al note that slipping is influenced by the type of mill lining and the percentage fill, but is not significantly influenced by the mill speed.

Cascading is similar to Rolling but occurs in mills that have a higher percentage fill. As mill speeds are increased, so the bed takes on a crescent shape due to the increased inertia centrifugal forces. The crescent shape forces the balls to leave the charge, and fly through the air. Cataracting occurs when a major portion of the charge is in flight above the 'en masse' region. These two definitions, cascading and cataracting, are the same as previously defined. The final motion type defined by Henein et al is Centrifuging. Centrifuging takes place when the charge is forced against the liner throughout its rotation.

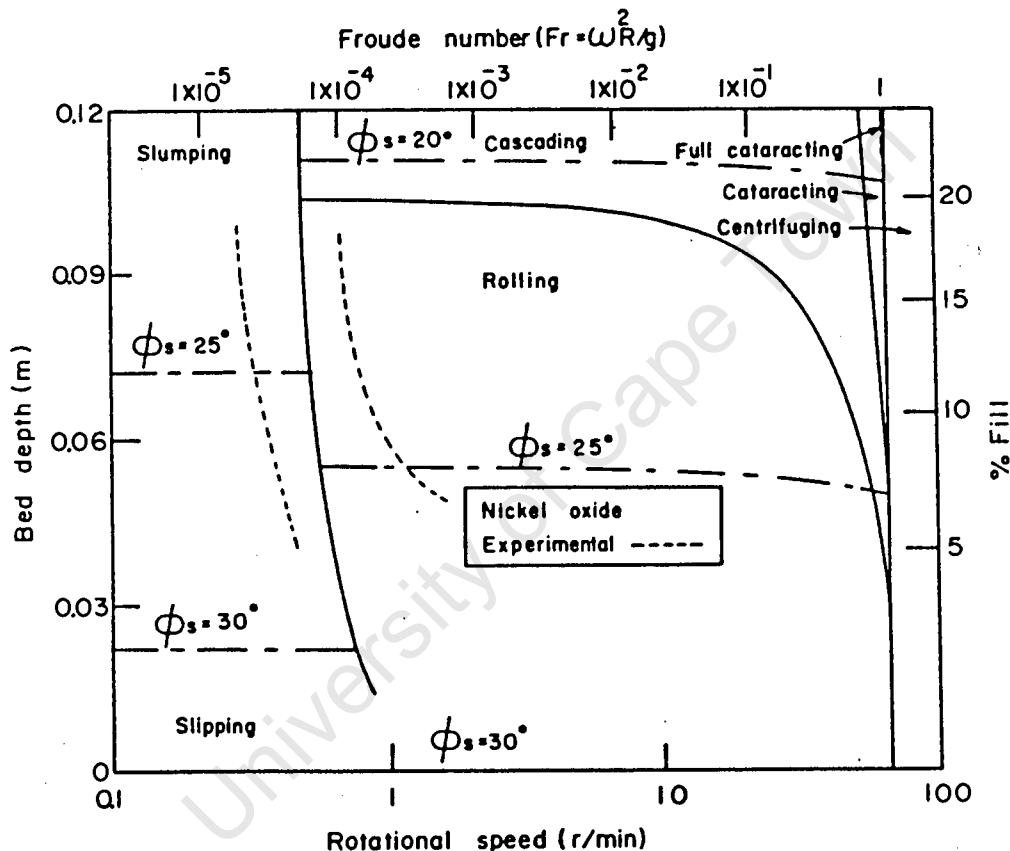


Figure 2.14: Bed Behaviour Diagram of Nickel Oxide [14] (Cylinder dimensions: $\emptyset,4m$ ID x $\emptyset,46m$)

Henein et al present all the experimental results with the aid of a single diagram, called a Bed Behaviour Diagram. A Bed Behaviour diagram is similar to a phase diagram that describes a solidification process. Rotational speed is plotted against percentage fill. The diagram highlights the interactions of the different motions with respect to changes in these two milling parameters. Figure 2.14 is a Bed Behaviour Diagram for spherical nickel oxide of less than 5mm diameter. The solid lines represent the transition criteria as predicted by theory and the dashed lines the transition zones recorded experimentally.

An analysis of a bed behaviour diagram, gives one an understanding of how the 'en masse' region might respond to fluctuations in milling conditions. In this way a mill operator would gain an appreciation of charge behaviour at start up and shut down, when a mill's rotational speed is fluctuating.

Vermeulen and Howat [15], in 1983, conducted experiments using rods instead of balls. It was argued that the rods would not be effected by the end effects of the glass window, as is the case with a charge made up of balls. Fig. 2.15 contains three photographs taken through the end of the test mill used by Vermeulen and Howat. In Fig. 2.15a a smooth lining was used, while the mills in Fig. 2.15b and Fig. 2.15c have lifter bars. (The bars in Fig. 2.15c are higher than those in Fig. 2.15b). The line TD approximately delineates the 'en Masse' region from the cataracting rods and is at the Dynamic Angle of Repose of the charge.

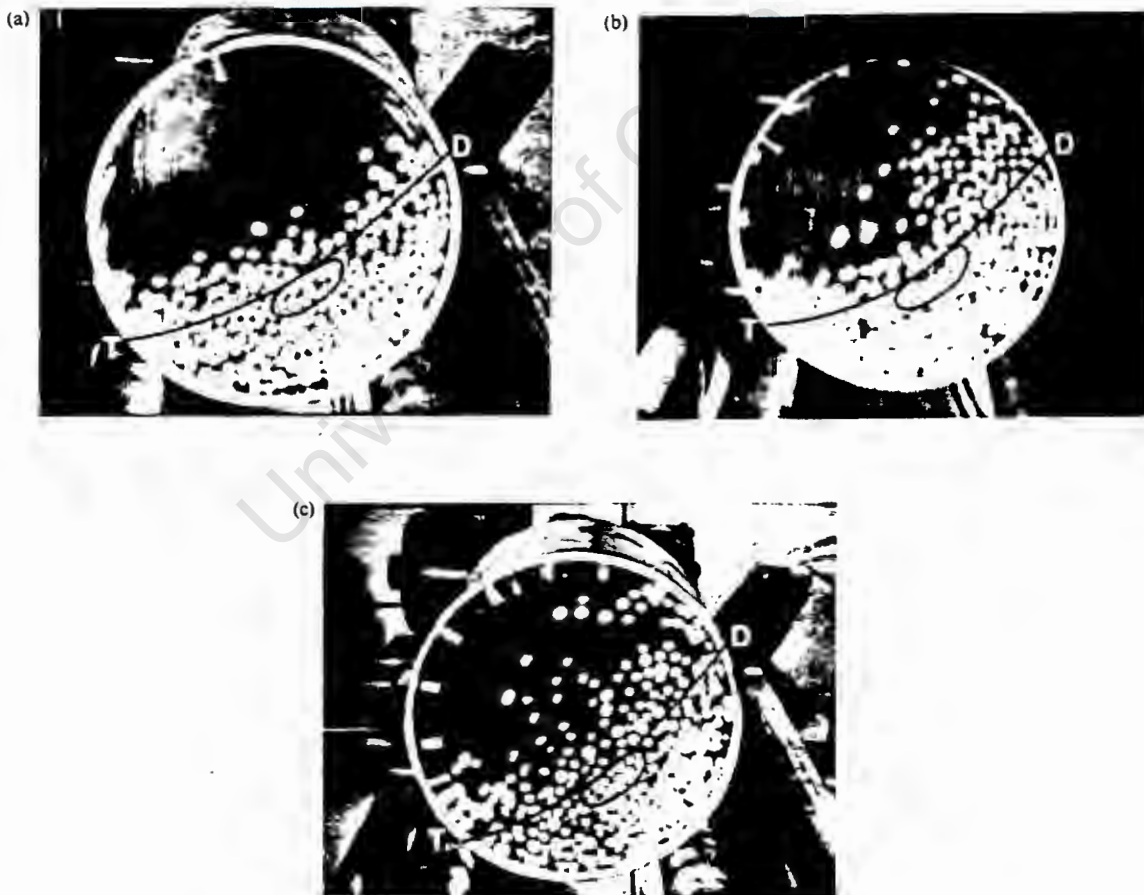


Figure 2.15: Reproduction of experimental results from Vermeulen and Howat [15].

The most noticeable consequence of including lifter bars is to increase the amount of cataracting that takes place. In Figures 2.15b and 2.15c, the outer layers of rods, are keyed in to the lifters. This allows more rods to reach the POD without excessive slipping, and hence to cataract down to the charge toe. There is no significant effect on the 'en masse' region due to the increase in the lifter bar height. (Fig. 2.15b to 2.15c). This result agrees with Powell [10].

Vermeulen and Howat derive a mathematical expression that models the variation of the dynamic pressure (p) in the 'en masse' region. The formulation makes possible the calculation of the dynamic pressure between two adjacent layers of rods. The authors state that the pressure between two adjacent layers must exceed a certain limit before the top layer will become keyed onto the lower layer. When this occurs the slip between the two layers is much reduced and the two layers move at approximately the same speed.

When the formulation is applied to the interface of a charge and a smooth lining, it becomes apparent that the dynamic pressure will never exceed the required limit for no slipping to occur. This explains the large slip associated with smooth liners. Similarly the slip that is noticed between the inner layers of a lined mill occurs because the dynamic pressure at the inner layer, is less than the required pressure, and so no keying occurs. An explanation is provided for the limited effect of an increase in lifter height beyond a rod radius. It is due to the fact that beyond the second layer away from the liner, the dynamic pressure is not sufficient and so the rods begin to slip in spite of the lifters.

2.4 Charge Surging in a Tube Mill

The phenomena of surge is one which is comparatively unresearched. Charge surge incorporates the entire 'en masse' region. Its occurrence is difficult to predict and can seriously damage a mill and its drive mechanism. A brief overview has been included in the literature review to highlight the complexities and uncertainties involved in trying to quantify charge motion.

Rose and Sullivan [6] developed a surge model in terms of the centre of gravity of the charge and the distance of the centre of gravity from the centre of the mill. The centre of gravity of the charge was estimated by approximating the charge surface to a straight line, similar to line AB in Fig. 2.1. The forces acting on the centre of gravity are split into components, with the tangential component being used in a balance of rotational forces. The balance of forces is similar to that used by Henein et al [14] to describe the Slipping class of motion. By observing the angle of repose of the charge just before slip, estimating the dynamic and static coefficients of friction and assuming that when the charge rises, it rises without any slip, it was possible to predict the frequency of surging.

Rose and Sullivan conducted a dimensionless analysis (Pi Theorem) on the factors that would effect the angle through which a charge surges. The result was:

$$\beta = \phi\{ (D/d), (\mu), (J) \} \quad \dots(2.14)$$

where: β = Angle through which the Charge Surges
 μ = Coefficient of Friction
 D = Mill Diameter
 d = Ball Diameter
 J = Filling Ratio

The fluidity of the charge is dependent on both J and μ , so the authors plotted the product $J\mu$ against the ratio of D/d as shown in Figure 2.16. From the analysis of experimental data it was determined that a line could be drawn that approximately separated a region of surge from a region of non-surge. The absolute accuracy of the graph is not as important as the trends that are illustrated.

Referring to Fig. 2.16, it is seen that as the ratio of D/d increases so the likelihood of surge decreases. This is in accordance with Manz [13], and is because the smaller balls get keyed in to the lining easier than

the larger balls. The other noticeable feature is that as J or μ increases so surge decreases. From this analysis an important conclusion can be drawn that the surge and slippage of a charge are very closely inter-linked and the one influences the other.

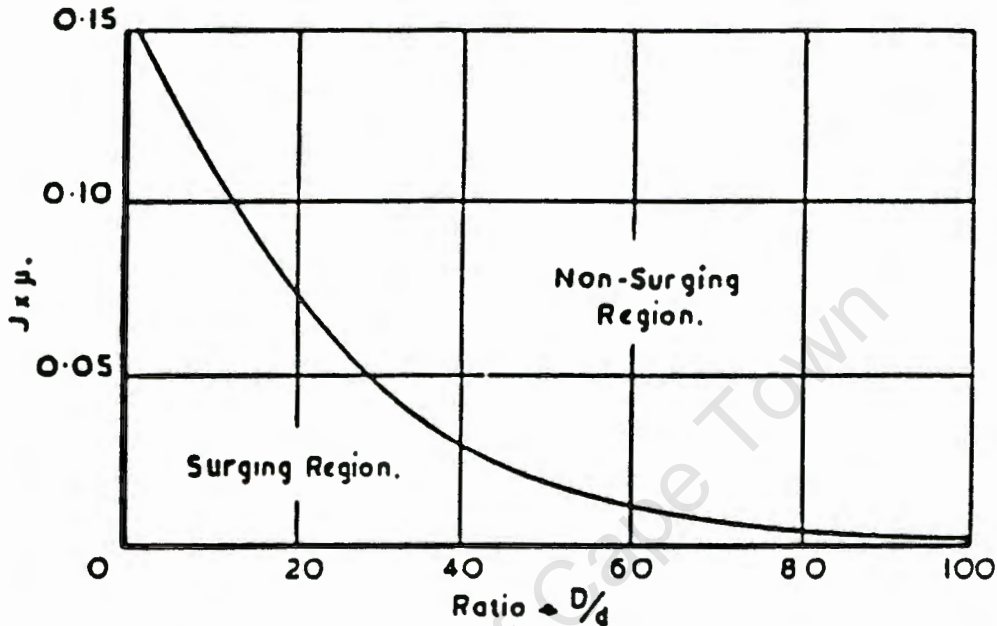


Figure 2.16: Graphical depiction of the dependence of Surge on the Milling Parameters [6].

Rose and Sullivan stated that: "The phenomena known as surging consists of a pendulum-like oscillation of the whole charge of the mill, within the mill shell. Thus for one part of the cyclical motion the charge is moving around the centre of the mill in the same direction as the mill shell, and during the second part of the motion, in the opposite direction." By this the authors predict that a charge is capable of moving in the opposite direction to the mill lining. This could account for the excessive liner wear experienced in some situations.

Vermeulen and Howat [16], in 1986, conducted an experimental investigation into charge surge using high speed photography of a rod mill. The individual film frames were analysed by projecting, each one onto a wall covered with graph paper. Each frame was analysed, and the paths and velocities of individual rods were recorded, as well as the angle of repose and density of the 'en masse' region. This provided the investigators with information over a definite time period.

The experimentally observed surge of the test mill, was not periodic. The time between each surge and the duration of each surge were not constant. So for this condition the surging can not be described as "pendulum like". Secondly, during each surge, it was observed that none of the rods moved in the opposite direction to the mill liner, this is contrary to Rose and Sullivan. The rods were observed to experience varying degrees of slipping. Vermeulen and Howat comment, (although without elaborating) that for mill fillings of less than 30%, the charge motion did look pendulum like. It will be shown later that an experimental observer can not decide conclusively, whether a charge is slipping or not, from visual evidence alone. The reason being, that an observer can only truly comprehend relative displacement and not relative velocity or slip.

Vermeulen and Howat present a visual description of the characteristics of a surging charge (Figure 2.17). The sequence begins with the 'en masse' region lying at a large angle of repose ($\sigma=33^\circ$) with 35 rods in the cataracting mode. The following pictures, with $\sigma=33^\circ, 30^\circ, 26^\circ$ respectively, show the 'en masse' region slipping back down the liner wall. During this period the number of rods cataracting decreases from 35 to 14 and the motion is dominated by rods cascading. The density of the 'en masse' region is a maximum when the minimum number of rods are in flight, as shown in Fig. 2.17d. After this maximum density, σ starts to increase and the number of rods cataracting has risen again, as shown by Fig. 2.17e. After this the cycle repeats itself.

Vermeulen and Howat explain the cycle in terms of dynamic pressure within the charge. The dynamic pressure between the charge and the lining is highest when the 'en masse' region is most dense. This allows the charge to rise up the mill wall and force some rods to cataract. When these rods cataract, they reduce the density of the region and so the dynamic angle of repose decreases, causing the rods to start to cascade and not to cataract. The cascading rods increase the 'en masse' density and hence the dynamic pressure increases, which results in the dynamic angle of repose increasing. This process is self perpetuating and forms a cycle. The authors presented a mathematical model which described the velocity of the rods in terms of the dynamic pressure fluctuations. The governing equations are summarised in Appendix 2.3.

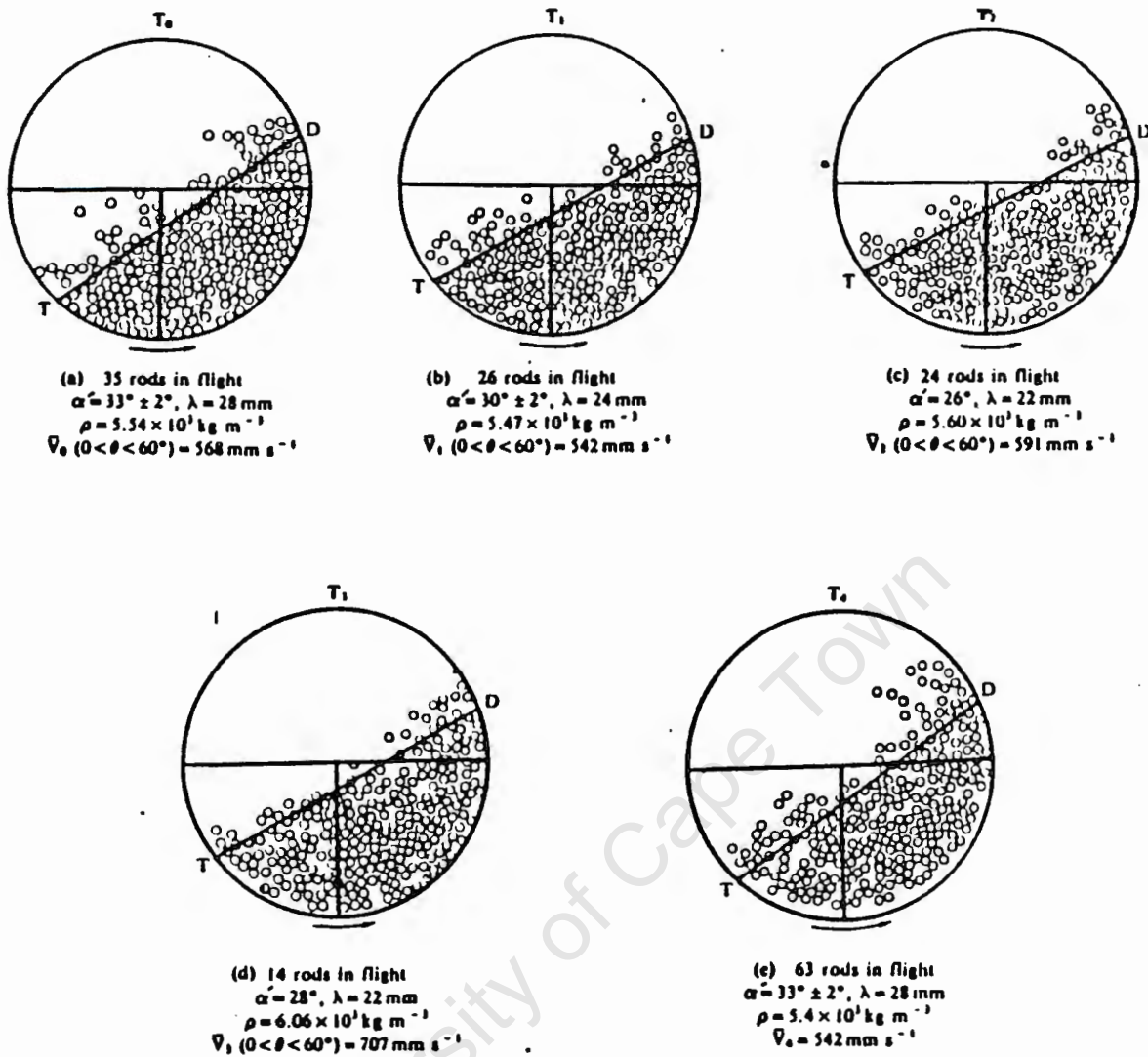


Figure 2.17: Tracings from the film strip of the rod configurations during a cascading phase of the charge motion. The inclination of the load profile (line TD) is at the angle of repose, α . ρ is the 'en masse' density, V is mean rod velocity and λ is the distance from the mill centre to the load profile [16]

The results of Vermeulen and Howat's investigation resolved some of the anomalies presented in Rose and Sullivan's treatise. Secondly, Vermeulen and Howat's surge model presents a relatively simple description of the dynamic nature of the 'en masse' region and shows how fundamentally friction and slip are interrelated.

2.5 Radial Segregation in a Tube Mill.

The occurrence of Radial Segregation of a charge has been mentioned by various authors [2,3,7,11]. Radial Segregation is defined as the division of the charge into separate zones. These zones differ according to element size and occur radially in a mill. They can be considered to be continuous throughout the length of the mill, like a cylinder within a cylinder.

Haultain and Dyer [3] were the first to comment that during experimental work, they observed radial segregation of their charge. The authors experimented with a mixture of black rape seed and white peas. The smaller seeds were observed to migrate to the mill centre at low speeds. While at high speeds, the peas moved to the centre and the seeds to the periphery of the mill. The aforementioned authors [2,7,11] comment about similar observations, though none give a detailed explanation for the effect.

Henein et al [17], in 1985, conducted an experimental investigation into the radial segregation of rotary kilns. They define three methods by which segregation occurs in kilns namely percolation, flow and vibration. Percolation segregation occurs when the size of the voids between the larger particles are large enough to permit the smaller particles to trickle or percolate through the voids. Bed packing, particle size and particle shape all effect the speed and extent of the resulting percolation segregation. Flow segregation occurs when a charge made up of granular solids is set in motion down an inclined slope. The charge is segregated by two different mechanisms. Firstly, the larger particles travel further down the surface than do the small particles and secondly the spherical shaped particles travel further than the irregular shaped particles. The two actions combine and segregate the 'en masse' region as it flows over the charge face. Segregation due to vibration occurs over a longer time duration. The result is the smaller particles rises to the top of the charge, while the larger particles sink to the bottom of the container.

Nityanand et al [18], in 1986, repeated some of the previous authors' work and extended the modelling of the radial segregation. The main difference between Henein et al and Nityanand et al's research is the size of particle observed. Henein et al used sand particles smaller than 1 mm, while Nityanand et al used beads ranging in size from 4 to 9,5 mm.

Nityanand et al studied the radial segregation of the charge at various rotational speeds. Only the effects of percolation segregation and flow segregation were analysed, as the effects of vibrational segregation were not considered significant in the case of a rotating cylinder. The speed range used allowed the charge to Roll, Cascade, Cataract and Centrifuge. The types of bed motion are the same as defined by Henein et al [14] in section 2.4. Figure 2.18 contains a reproduction of some of Nityanand's results.



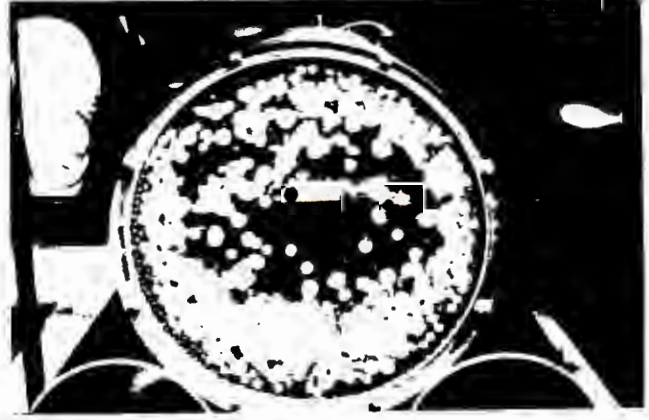
a: Rolling Central Segregation



b: Cascading Well Mixed Bed



c: Cataracting Onset of Reverse Segregation



d: Centrifuging Reverse Segregation

Figure 2.18: Radial Segregation for different types of bed motion [18]. $J = 34\%$, Ball sizes: 9.5, 6.4 & 4.0 mm. Mill Dimensions: $\emptyset.2m$ ID x $\emptyset.2m$ L

Nityanand et al define two types of segregation. The first is normal segregation and takes place when the smaller particles form a core in the centre of the charge. The second type is defined as Reverse segregation,

where the opposite occurs, with the smaller particles diffusing to the cylinder wall and the larger particles forming a central core. These actions are the same as those observed by Davis, Haultain and Dyer, McIvor and Gross.

Nityanand et al explain the mechanics of reverse segregation as being due to a function of the ratio of the inertia centrifugal and the gravitational forces. These two forces can be combined to form the Froude number (Fr). The Froude Number, which is dimensionless, is defined as the ratio of an inertia force to a gravitational force, i.e. $Fr = u^2/lg$. The value of the critical velocity of the mill is used for u . The critical velocity for each particle is calculated by taking into account the effective radius for that particle. Hence as a particle's size decreases so its effective radius increases and hence the critical velocity is increased. This results in an increase in the ratio of the inertia centrifugal to gravitational forces. Thus as the particles size decreases so its Froude number increases.

At high rotational speeds the velocities of the different sized particle's are nearer to critical and the differences between the Froude numbers of the various sized particles becomes significant (because of the u^2 term). A particle with a high Froude number, a smaller one, is more effected by the inertia forces and hence segregates towards the wall. This results in the larger particles being pushed into a central core. This is shown in Figs. 2.16c and 2.16d, where Reverse Segregation is plainly visible.

The inertia forces at lower rotational speeds are not as significant and so the Froude number becomes less dominant. When a bed is spinning slowly, the balls roll or cascade very slowly down the charge face. Due to the effects of flow segregation the larger balls travel further and stop closer to the charge toe. The smaller balls do not travel that far and come to rest near or just above the central core. The 'en masse' region is not as dense, at its surface as at its core, hence the void size on the surface is significantly larger. The larger voids between the big particles allows the smaller particles to percolate through the surface of the charge face, and down into the central core.

The larger balls that reach the toe are keyed into the liner motion. They travel underneath the core and back up the wall where they re-roll down the charge face again. The small particles that get entrained in this

flow, are re-percolated down into the centre, as they flow over the charge face. Hence there is a slow continual drift of small particles to and from the central core, with the body of the core remaining intact. This can be seen in the first picture of Fig. 2.16. The second picture shows a well mixed bed, formed by the two types of segregation actions occurring simultaneously, which hinders the formation of a central core.

Nityanand et al experimentally observe that the speed or rate at which the segregation occurs was independent of the depth of the bed, but dependent on the rotational speed. So at startup, irrespective of the filling ratio, segregation will occur that depends only on the startup velocity. Furthermore the size ratio of smallest to biggest particle effected the rate of segregation. The larger the particle size ratio, the faster the segregation occurred.

2.6 General Discussion of Reviewed Literature

A resume of all the reviewed literature is contained in Appendix 1. A point form summary of the reviewed literature is presented below. It is intended to highlight the major trends and advances made by the various authors.

(i) Vermeulen and Howat's [16] modelling of the dynamic pressure in a mill presents an explanation for the causes of the inter-related actions of slip and surge. The model assumes perfect packing which could be possible for a rod mill, but less likely for a ball mill. Even so, the concepts are very applicable to milling as a whole. Further investigations and the application of this theory to ball mills would impart a greater understanding of the slipping and surging in a ball mill.

(ii) Indications [11,12,18] are that radial segregation could play an important role in ball wear by isolating different sized balls to different areas within the mill. Segregation could also have an effect on determining the degree of slip that occurs at the liner interface, which in turn determines liner wear. The growth and effectiveness of the abrasion zone could also be dependent on the degree of the radial segregation. Hence the development of a model for segregation in a ball mill could provide new insight into charge motion and wear characteristics.

(iii) The milling process has so many independent variables (Rotational velocity, percentage fill, liner configuration, ball size distribution etc.) that isolating any one and analysing another leads to incorporating significant assumptions. At present the best that researchers can do is to try and minimise any assumptions made while conducting experimental investigations or developing numerical models.

(iv) While examining mill internal interactions, the most difficult step is to be able to determine what is a first order and what is a second order effect. Slippage, with the associated frictional forces, of the charge seems to be a first order affect. The secondary concepts of dynamic pressure, 'keying in' of the charge and the actual effects of lining configuration must be investigated more fully before slippage can be completely modelled.

(v) Finally, the realm of ball paths has been extensively investigated [1-10]. All the theories developed significant initial assumptions about friction and the effects of friction on ball paths. Of all the papers reviewed, only McIvor [7], Vermeulen [9] and Powell [10] have explicitly included friction. To date, no reference was found that included friction for a *single* ball on a smooth or slightly corrugated lining. This is the new direction that this investigation will follow with the effects of friction being incorporated into the existing models.

University of Cape Town

3. DERIVATION AND DISCUSSION OF THEORETICAL MODELS

An analysis of single particle motion yielded 3 distinct motion types. A particle can either slide along the liner or roll over the liner or move with a combination of sliding and rolling. Each motion type will be presented and discussed in a separate section of this chapter.

3.1 The Sliding Model

An arbitrary particle moving in space has 6 degrees of freedom, 3 translational and 3 rotational. An initial assumption that is made by many investigators [2,7,9,10], is to limit the particles' motion to a vertical plane. In this way horizontal travel is ignored and the system reduces to 2 dimensions. This results in the particles' motion being reduced by 3 degrees of freedom. The remaining 3 degrees of freedom are made up of 2 translational (Cartesian Coordinates: x & y or Polar Coordinates: θ & r) and 1 rotational (spin about an axis parallel to the mill axis).

A further degree of freedom can be restricted by specifying that the particle can move off the liner. By this it is meant that the particles motion is along the liner, either rolling or sliding. Another degree of freedom can be removed by assuming that the particle can not rotate or spin about its own centre. The end result is a particle that has only one degree of freedom. Practically, this is equivalent to a block shaped particle sliding (but not rolling) along a mill lining. As the system has only one degree of freedom, it is relatively easy to model mathematically.

Balls that are retrieved from a mill before they are completely consumed exhibit two characteristics. Most of the balls have flat faces that have been ground away, during the comminution process. The second characteristic is that the balls that have more than one flat face, tend to lose their spherical shape and take on a cubic shape. These two points, a single degree of freedom system and the cubic shaped particle, justify the use of a block shaped particle as the starting point in the analysis of single particle motion on the inside of a rotating cylinder.

3.1.1 Derivation of Sliding Equations

The orientation of the forces acting on a single block are depicted in Figure 3.1. The block is moving up with the liner and a frictional force has been inserted between the block and the liner. The force is assumed to act tangential to the liner. Assuming that the block is moving slower than the mill, then the direction that friction acts is to prevent the block from sliding, so it acts up the liner.

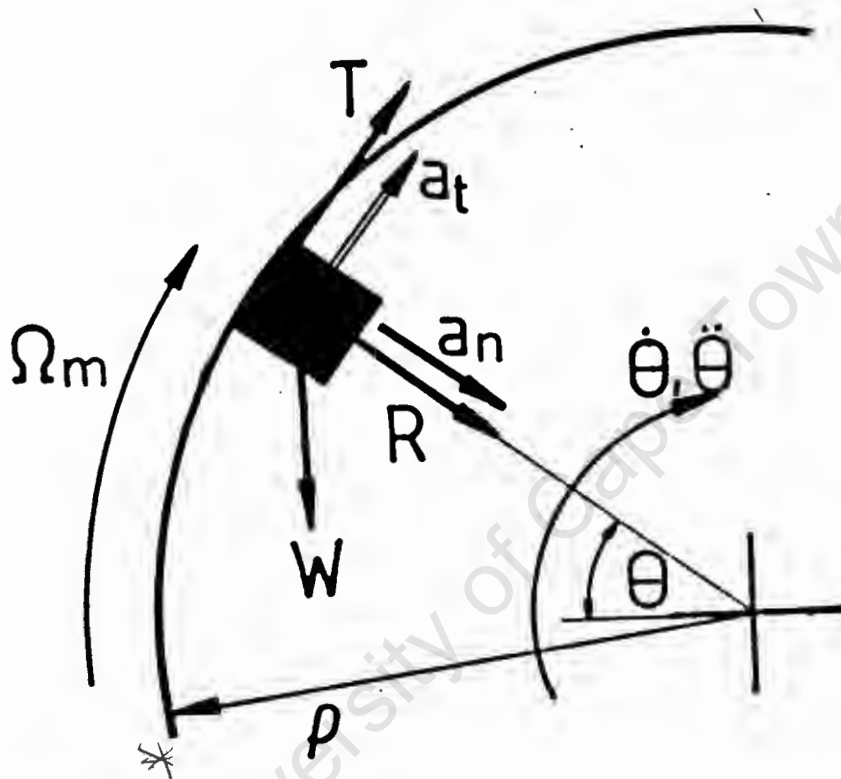


Figure 3.1: Orientation of the forces acting on a Block.

Summing forces radially:

$$\Sigma F_r: ma_n = R + W_r \quad \dots(3.1)$$

$$\text{But } a_n = \dot{\theta}^2(\rho - \frac{1}{2}l_r)$$

$$\text{Assuming that } \rho \gg l_r \therefore \rho - \frac{1}{2}l_r \approx \rho$$

$$\therefore R = m\dot{\theta}^2\rho - mg\sin\theta \quad \dots(3.2)$$

Summing forces tangentially:

$$\Sigma F_t: ma_t = T - W_t$$

$$\text{But } a_t = \ddot{\rho} \quad \dots(3.3)$$

$$\therefore T = m\ddot{\rho} + mg\cos\theta \quad \dots(3.4)$$

where: T = Tangential Frictional Force (N)
 R = Normal Reaction on liner (N)

W_r = Weight Component in the Radial Direction (N)
 W_t = Tangential Weight Component (N)
 a_t = Tangential acceleration (m/s^2)
 a_n = Normal acceleration (inwards is positive) (m/s^2)
 θ = Angular position of the block, from the mill centre ($^\circ$)
 $\dot{\theta}$ = Angular Velocity (rad/s) (clock-wise = positive)
 $\ddot{\theta}$ = Angular Acceleration (rad/s^2)
 Ω_m = Rotational velocity of the mill
 ρ = Radius of the mill (m)
 l_r = Width of block perpendicular to the liner surface (m)
 m = mass of the block (kg)

Equations (3.2) and (3.4) are 2 equations in 3 unknowns (θ, R, T). A third equation is required to solve the system. One simple condition is that $\dot{\theta} = \Omega_m$, ie the block is rotating at the same velocity as the mill. It is a case of simple rotational dynamics with no acceleration in the tangential direction. It is the same as Davis' formulation [2], as there is no slip between the block and the liner. The governing equations can be derived as follows:

$$\text{Putting} \quad \dot{\theta} = \Omega_m \quad \dots(3.5)$$

$$\text{Integrating (3.5)} \quad \therefore \theta = \Omega_m \cdot t + \beta \quad \dots(3.6)$$

where β = constant

$$\text{Differentiating (3.5)} \quad \therefore \ddot{\theta} = 0 \quad \dots(3.7)$$

Hence equations (3.8) and (3.9) can be derived:

$$R = m\Omega_m^2 \rho - mg \sin(\Omega_m \cdot t + \beta) \quad \dots(3.8)$$

$$T = mg \cos(\Omega_m \cdot t + \beta) \quad \dots(3.9)$$

The block will continue to rotate with Ω_m until friction is exceeded, at this point the model is no longer valid. Once friction is exceeded, then the block will start to slide relative to the liner. Assuming that the frictional force between the block and the liner is proportional to the normal reaction, then:

$$\text{Frictional Force} \equiv T = \mu_k R \quad \dots(3.10)$$

The static coefficient of friction (μ_s) is used before slipping has begun. After slipping has started the kinetic coefficient of friction (μ_k) is used. The difference between μ_s and μ_k is not significant and hereafter a single value (μ) will be used when required.

Hence substituting (3.10) into (3.4) and combining the result with (3.2) yields:

$$\ddot{\theta} \rho - \mu_k \dot{\theta}^2 \rho + g(\mu_k \sin \theta + \cos \theta) = 0 \quad \dots(3.11)$$

Examining equation (3.11) it is apparent that it is only in terms of θ , the single degree of freedom. Once solved, R and T will be determinable for any θ . Furthermore it is noticeable from equation (3.11) that the mo-

tion of the block is independent of the mass. The only effect the mass has on the system is on the magnitudes of both R and T (equations 3.8 and 3.9).

3.1.2 Numerical Solution of Sliding Equations

Equation (3.11), is a second order, non-linear, homogeneous, ordinary, differential equation. Due to its highly non linear nature (the cosine and sine terms), a numerical solution was sought.

One possible method of solving a second order differential equation is to decompose it into a system of first order differential equations. These equations are then solved simultaneously. An Euler Numerical Approximation [19] was found to be most suited for the solution technique. Hence an Euler Forward Step was employed; the complete procedure is contained in Appendix 3. Here follows the results of the Euler Forward Step Numerical Solution procedure.

$$\theta_{n+1} = \theta_n + h\dot{\theta}_n \quad \dots(3.12)$$

$$\dot{\theta}_{n+1} = \dot{\theta}_n + h\left\{\frac{\mu_k(\dot{\theta}_n)^2 - g\mu_k \sin\theta_n - g\cos\theta_n}{\rho}\right\} \quad \dots(3.13)$$

$$R_{n+1} = m(\dot{\theta}_{n+1})^2 \rho - mg \sin\theta_{n+1} \quad \dots(3.14)$$

$$T_{n+1} = m(\ddot{\theta}_{n+1})\rho + mg \cos\theta_{n+1} \quad \dots(3.15)$$

where h = the time step increment

n = the value at the present (nth) increment

n+1 = the value at the next (n+1th) increment

From equations (3.12 to 3.15) the magnitudes of θ , $\dot{\theta}$, R and T are determinable at any time after the start of the block's motion.

The final elements required to complete the solution of the differential equations are the initial and final conditions, ie the boundary conditions. The initial conditions required are the block's position, $\theta(0)$, and its angular velocity, $\dot{\theta}(0)$ at the start of the motion period when $t=0$. These could be arbitrarily specified and the resulting solution found by "stepping forward in time" with a sufficiently small time increment that satisfies convergence.

For the case of a block on a mill liner, two initial conditions are known. The first is that as sliding is about to begin, the block's velocity is the same as the mill velocity ie $\dot{\theta}(0)=\Omega_m$. Secondly as the block is

moving with a constant velocity, the angular acceleration is zero. So equating the forces, in the tangential direction, acting at the Point of slipping:

$$\therefore W_t = T$$

But friction is such that $T = \mu_s R$

$$\therefore W_t = \mu_s R \quad \dots(3.16)$$

$$\therefore mg \cos \theta = \mu_s (m \dot{\theta}^2 \rho - mg \sin \theta)$$

$$\text{But } \dot{\theta} = \Omega_m, \quad \therefore \cos \theta + \mu_s \sin \theta = (\mu_s \Omega_m)^2 \rho / g \quad \dots(3.17)$$

Equation (3.17) defines θ_{slip} , the angular position when the block will start to slip. The equation can be solved numerically using a Newton-Cotes Method. The value obtained will be $\theta(0)$. A sample problem illustrating the complete numerical solution procedure is contained in Appendix 4.

3.1.3 Examination of the various End Conditions of a Sliding Block

The initial boundary conditions start the solution, but as this is not a self terminating problem, end conditions must be imposed. A block moving up a liner has four possible outcomes (excluding rolling). They are:

1. Sliding back down the liner.
2. Leaving the liner and following a parabolic trajectory.
3. Becoming centrifuged and never leaving the liner.
4. Toppling down the liner, either before or after sliding has begun.

The first case that will be examined will be that of a block sliding back down the rising liner. Once the block has begun to slide, the forces acting on it are gravity, down the liner, and friction up the liner. The net resultant angular acceleration of the block is always down the liner (at slipping $W_t=T$, thereafter $W_t>T$) and hence the block is continually decelerating. The block continues to decelerate until it comes to rest, that is $\dot{\theta}=0$. Thereafter, the block will move back down the liner ($\dot{\theta}<0$), in a similar way to a parcel sliding down a rising conveyor belt. On reaching the mill bottom, the block will continue rising up the other side of the mill until it, once again, comes to rest ($\dot{\theta}=0$). The oscillation of the block will restart as once more it starts to move with $\dot{\theta}>0$, ie travelling in the same direction as the liner.

The oscillations will continue until the block travels above the horizontal of the mill and leaves the liner. When $R \leq 0$, it is assumed that the block has departed from the liner. A block is not able to leave the liner

before the horizontal has been passed, as the reaction force (R) is always positive for $\epsilon < 0^\circ$ (See equation 3.2). As the block slows down, the likelihood of departure increases. This is because R is dependent on $\dot{\epsilon}^2$.

Examining the energy transfer from the rotating liner to the block, the path is via the frictional force between the block and the liner. As the coefficient of kinetic friction increases, so the energy transfer rate increases and so the block's energy input increases. The larger the block's energy (kinetic and potential), the sooner it is able to rise above the horizontal and start to cataract. Hence the magnitude of the coefficient of friction should play a significant role in determining how long a particle takes before cataracting.

The departure velocity of the block is assumed to be purely tangential ($V = \dot{\epsilon} \rho$). From the POD a parabolic trajectory is easily calculated; it ends when the ball impacts on the liner. The POD is easily recognisable, as at the end of each time increment the magnitude of R is checked. When $R < 0$ the approximate AOD has been reached and flight is initiated. No provision has been made for any "bunching or crowding" effects of the charge at POD, as there are none with a single particle

When a block reaches the top of the mill, $\epsilon \approx 90^\circ$ and $\dot{\epsilon} > 0$, then it is defined that Centrifuging has occurred. A block can be centrifuged even if $\dot{\epsilon} < \Omega_m$. This occurs when the block is slipping, but $\dot{\epsilon}$ is still large enough for the inequality $\dot{\epsilon}^2 \rho > g$ to be valid. The inequality is derived by putting $\epsilon = 90^\circ$ and $R \geq 0$ in equation 3.2. This type of centrifuging will be referred to as Slipping Centrifuging. A second type of centrifuging occurs if $\dot{\epsilon} = \Omega_m$. This occurs if either μ or Ω_m are very large. The situation results in the block never slipping relative to the liner. It will be defined as Totally Centrifuged and it is the same as Davis' formulation.

On descending back down the liner a centrifuged block will either continue moving with $\dot{\epsilon} = \Omega_m$ or accelerate until it reaches the mill velocity. Upon reaching mill velocity, the block can either continue at Ω_m or continue accelerating till $\dot{\epsilon} > \Omega_m$. Any of the situations will lead to the block re-ascending the liner and the process repeating itself.

The fourth ending condition, the toppling over of the block occurs for higher values of μ_s and lower Ω_m . The problem is one of elementary applied mechanics ie determining whether the block will slide or topple down the

plane as the angle of inclination increases. Once toppling has occurred, the block does not move along the liner surface, but rolls or bounces over the liner face. The motion characteristics of a tumbling block have not been analysed beyond being able to predict when toppling will occur. The onset of toppling can occur either before or after the block has begun to slide. The equations that predict both cases have been derived and discussed in Appendix 5.

3.1.4 Computer Implementation of the Numerical Solution to the Sliding Equations

The Euler Forward Step numerical solution process lends itself to rapid computer implementation. Only one previous value is required to calculate the value of ϵ , $W R$ and T at the next time increment. Other numerical solution methods require two or three previous values to calculate the prediction for the next time increment (e.g. Milne or Adams-Moulton Methods). With the initial conditions known, the Euler method has the advantage of being a self-starting system.

A computer program was written in Fortran that would implement the required algorithms and allowed for the block's motion to be animated. Figure 3.2 contains a simplified flow diagram of the program structure. A listing of the program is contained in Appendix 8. A computer disk containing the relevant executable files has been included with the thesis.

The program can be divided into 5 main parts. The first is the initialisation and processing of the input variables. All the input variables are adjustable from within the program by using the user interactive data handling subroutines. At startup three types of output files are specifiable and they will be discussed later. The final step in the first part of the program is to solve for the theoretical Angle of Sliding (equation 3.17) and the Angle of Toppling. The two values allow one to determine whether the block will slide before toppling or vice versa.

Flow chart for Computer Implementation

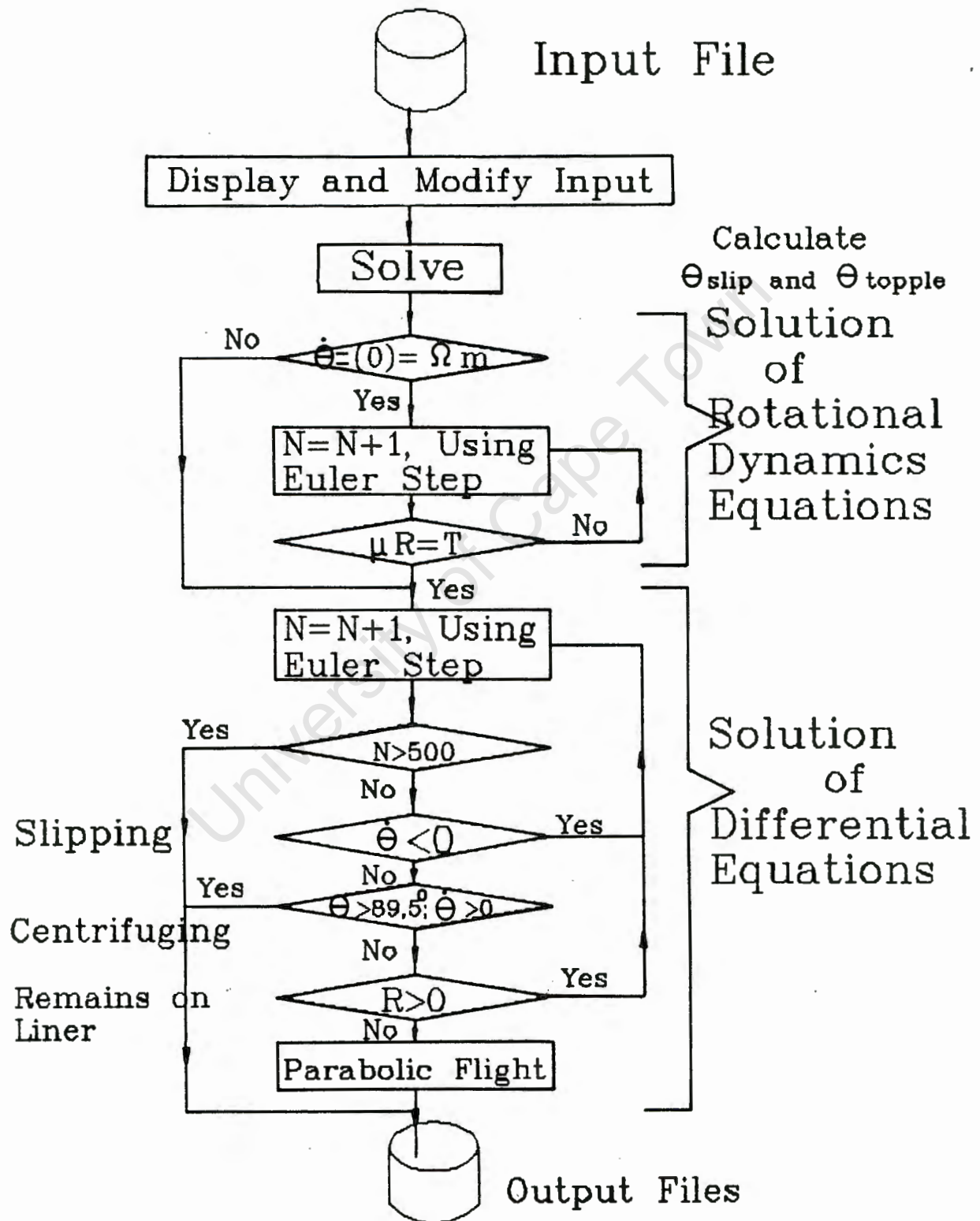


Figure 3.2: Flow Chart of Computer Program.

The next phase of the solution is for a block moving with $\dot{\theta} = \Omega_m$. the governing equations are the simple rotational dynamics equations (3.5 to 3.9). The entire solution sequences is bypassed if $\dot{\theta}(0) \neq \Omega_m$, as this implies that right from time zero the block is sliding. This second stage of the program is terminated in one of two ways. The first is if the block never slips and it becomes Totally Centrifuged ($\dot{\theta} = \Omega_m$) or the second is if the maximum frictional force is exceeded.

The third stage of the program starts when the block begins to slide, that is, when $T \geq \mu_s R$. From here on the program implements the Euler solution to the governing differential equation (equations 3.12 to 3.15). At the end of each time increment, the program checks if any of the four end conditions have been reached. When a sliding condition is encountered the ball is permitted to slide down the liner and re-ascend. The process of sliding would be terminated after a pre-determined number of increments, if flight has not begun. If toppling occurs, the program signals the event to the user, but does not terminate the implementation of the sliding equations. The program was written in this way so that, if required, the toppling condition could be ignored.

The centrifuge condition is realized if the ball has not left the liner, but $\theta \geq 89.5^\circ$ and $\dot{\theta} \geq 0$. The program is terminated at that point with the ball not being permitted to travel beyond the mill apex. When the ball leaves the liner it causes the program to branch into its fourth stage, the step-wise solution of the block's parabolic path. The parabolic flight is terminated when the block's centre reaches the mill liner.

The final stage is the writing of the numerical results from the computers memory to the initially specified output files. The first type is a full output file that contains some of the variables' incremental values at all the time increments. The second file type is a summary file. This file only contains the significant time increments' values. By "significant time increment" is meant, for example, when the block first begins to slide or when the block leaves the liner. This file is particularly useful when observing the effects of changing the various input parameters.

The final type of output file contains the coordinates of the block's centre at each time increment. This file allows the block's path to be plotted and is also used as the interface to a computer animation procedure. The program drives a graphics subroutine that displays the block's and mill's movement at the end of each time increment. The animation is

fast enough to provide a realistic visual interpretation of the block's response to variations in the operating parameters.

3.1.5 Discussion of the Results from the Numerical Solution of the Sliding Equations

The analysis on computer was begun by initially running the program with varied input values. After the initial trial period, 3 parameters, δt , μ and Ω_m , were selected as having significant effects on the block's motion. The time increment was chosen so that an optimum value could be found that gave satisfactory convergence. The other two parameters were chosen because they are the only two input parameters that are alterable within an existing milling situation. The reason for the remaining parameters being omitted is briefly outlined below.

Mass: The motion of the block is independent of m (see Eqn. 3.11)

Ball Radius: This was assumed negligible for realistic mill sizes.

Gravity: Changing g wouldn't provide much new relevant information.

Mill Radius: The mill radius was varied between $1m$ and $2m$, and the program re-run. The numerical results indicated that more information could be obtained by concentrating on the variation of μ and Ω_m . Secondly, in practice, the radius of an existing mill cannot be significantly altered.

$e(0)$ and $\dot{e}(0)$: These were kept at $e(0)=-90^\circ$ and $\dot{e}(0)=\Omega_m$. ($e=-90^\circ$ is equivalent to the mill bottom, with e and \dot{e} increasing in a clock-wise direction.) It was the intention to observe the response of a block placed at the bottom of a mill and moving with the mill, thus these two parameters were not changed. The experimental investigation was designed to be able to produce these same initial conditions.

The first parameter that was varied was h , the size of the time increment. The increment was varied from $0,01$ to $0,0001$ seconds. The objective was to determine a value for h that allowed accurate results, yet did not increase computational time significantly. A value of $\delta t=0,001$ seconds was found to be most suitable, and was used throughout the remainder of the investigation. An examination of the convergence of the numerical solution to a theoretically known value is contained in Appendix 4.

The second independently varied parameter was the coefficient of friction. To simplify the investigation it was assumed that the difference between μ_s and μ_k was not significant. Therefore the value of coefficient of friction used was $\mu = \mu_s = \mu_k$. The first group results examined were with respect to the effect on the angle at which slip begins (θ_{s11p}) and secondly on the general motion of block.

Equation 3.17 can be re-written as $\mu = f(\theta, \Omega_m, \rho, g)$ ie

$$\mu = \frac{g \cos \theta}{\rho \Omega_m^2 - g \sin \theta} \quad \dots(3.17a)$$

A descriptive interpretation of the equation is that the value of μ calculated is the minimum to just allow the block to reach the angle θ , at that specific Ω_m , without slipping. (Implied is that at $\theta < \theta_{s11p}$ then $\dot{\theta} = \Omega_m$) Thus the value of θ can be seen as the angle at which slipping just begins. Mathematically $\mu_{min} = f(\theta_{s11p}, \Omega_m)$ or $\theta_{s11p} = f(\mu_{min}, \Omega_m)$.

Trends were generated of μ_{min} versus θ_{s11p} for three different mill speeds. Two views of the results are contained in Figure 3.3. The magnitude of μ was permitted to exceed 1, while θ has been restricted such that $90^\circ \geq \theta_{s11p} \geq -90^\circ$ (the top and bottom of the mill)

Using Davis' equations [2.6], $N_c = 24.4$ rpm for a mill with $\rho = 1.5m$.

with	Ω_m	20 rpm	25 rpm	30 rpm	
	% Critical	82%	102%	123%	
then	$\sin \alpha$	0.671	1.048	1.510	($\alpha = AOD$)
hence	α	42,12°	—	—	

Davis' model predicts that the last two speeds exceed the critical velocity for a 1.5m mill and hence the block will become centrifuged for $\Omega_m \geq 24.4$ rpm

Examining Figure 3.3 (the top graph) with $\Omega_m = 82\%$, it is observable that as θ_{s11p} tends to the Davis predicted Angle of Departure ($\alpha = 42.1^\circ$), μ tends to infinity. Hence there is a singularity in μ 's trend at $\theta = \alpha$, which implies that for the block to reach the Davis predicted POD, μ must be very large indeed. This in turn implies that friction between the block and liner must be near infinite. Davis assumes that the block leaves the liner with $\dot{\theta} = \Omega_m$. For this non-slip condition to occur, friction would have to be large. The conclusion that can be drawn is that by Davis ignoring

friction, the implied assumption is that friction is assumed infinite. This is a less obvious by-product of Davis' formulation and is an unreasonable assumption.

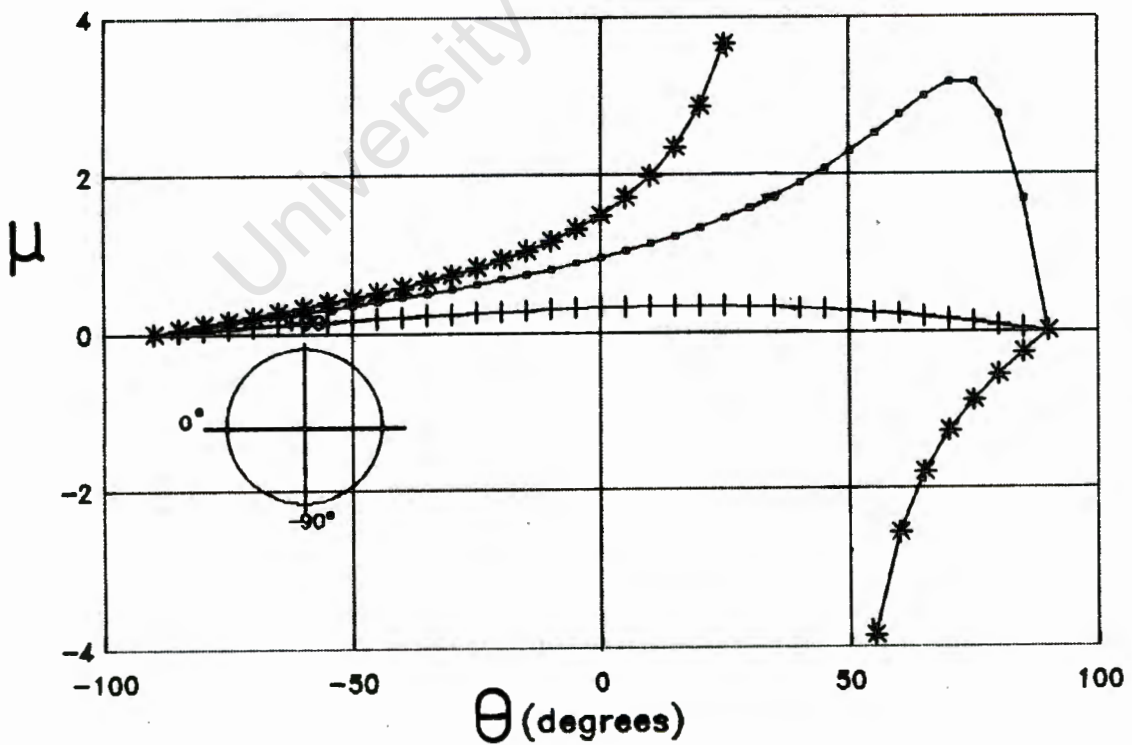
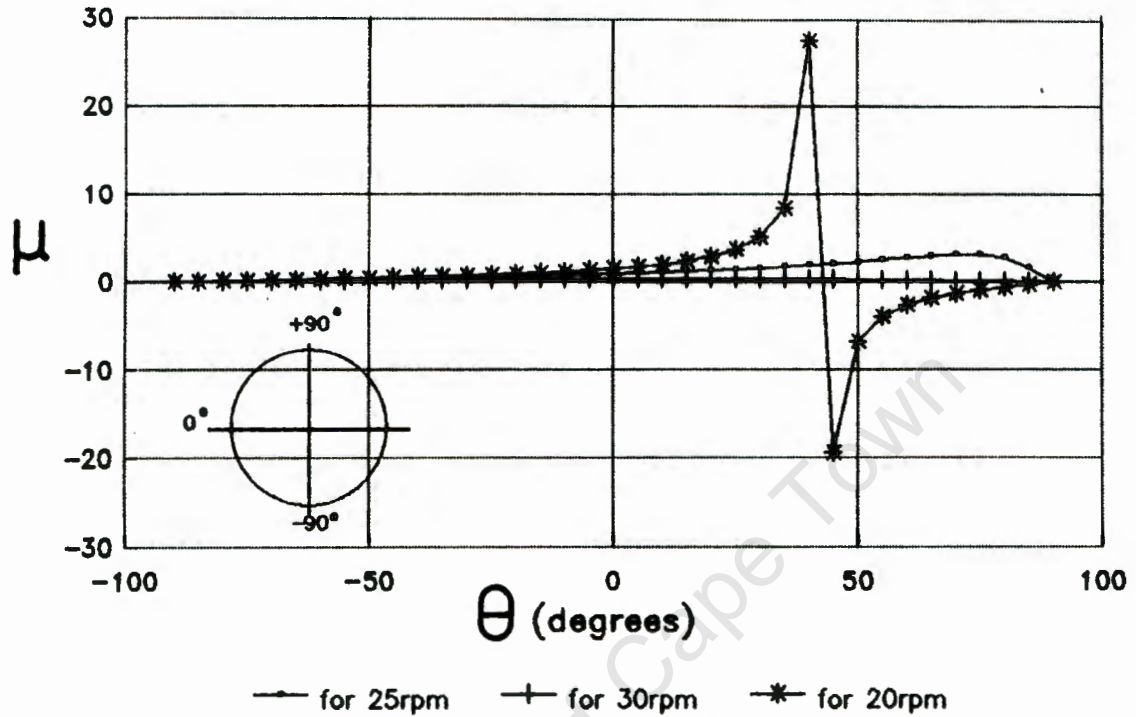


Figure 3.3: Two Graphs of μ versus θ , for various Ω_m

The trends at the other mill speeds ($\Omega_m=102\%$ and 123%) each exhibit a distinct peak or maximum. The maximum can be interpreted as the value of μ required for the ball to become Totally Centrifuged to the liner. For example: $\mu=2$ & $\Omega_m=25\text{rpm}$ (which is greater than Davis' critical speed), the block will still not centrifuge, because friction is not sufficiently large. A minimum value of $\mu=3,2$ (the peak of the trend) is required for a single block to be totally centrifuged at $\Omega_m=102\%$. With $\Omega_m=123\%$, the minimum μ required is $\mu=0.89$. The pattern that becomes apparent is that as Ω_m increases, so the minimum μ required for total centrifuging decreases.

The observations made by Haultain and Dyer [3] about slipping can be further understood in the light of the aforementioned observations. The values of μ encountered in practice are generally $\mu < 1$, yet full charges are observed to centrifuge. Vermeulen and Howat [16] derive an expression for the Dynamic Pressure in a mill. The reaction of the liner, R , is directly proportional to the dynamic pressure. The magnitude of R in a full mill, as stated by Vermeulen and Howat, is significantly larger than that for a single block. The magnitude of a frictional force is determined from the product of μ and R . So for smaller values of μ , the larger values of R would produce the same magnitudes of friction and allow a charge to centrifuge.

The next set of tests done were to vary μ , with emphasis being given to the effects on the block's ending condition. A set of computer runs were completed for with constant values of $\Omega_m=102\%$, $\rho=1.5\text{m}$ and $m=0.5\text{kg}$. The coefficient of friction was varied between $\mu=0.2$ and $\mu=3.0$. All three end conditions (ignoring the occurrence of toppling) were obtained from this range Figure 3.4 contains the three cases with $\dot{\epsilon}$ plotted against ϵ . Figure 3.5 contains the variation of R and T under the same conditions. (Figures 3.4a, 3.4b and 3.4c correspond to Figures 3.5a, 3.5b and 3.5c respectively.)

Figure 3.4a illustrates the case where the block slides back down the liner, called the Sliding case. It occurs when μ is relatively small. The block has initially the same velocity as the mill, but soon after it has started to rise, it slips relative to the liner. It continues to rise until $\dot{\epsilon}=0$, after which it will slide back down the liner with $\dot{\epsilon} < 0$. It is interesting to note that ϵ is never larger than zero, and hence the block does not even reach the horizontal. Figure 3.5a has the Point of Sliding ($\mu_5 R=T$) labelled. From Figures 3.4a and 3.5a it can be seen that R is

never less than zero, and so the ball never leaves the liner.

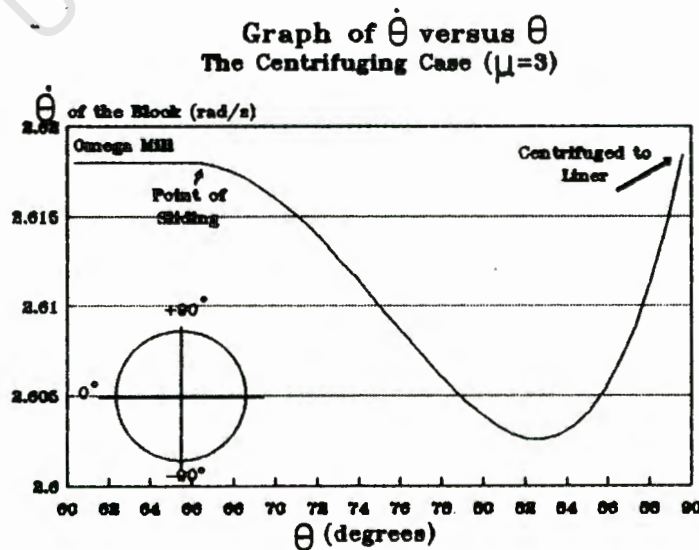
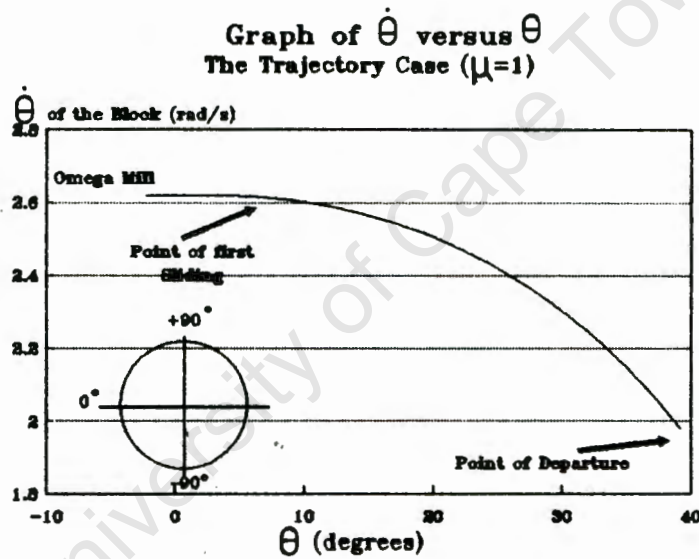
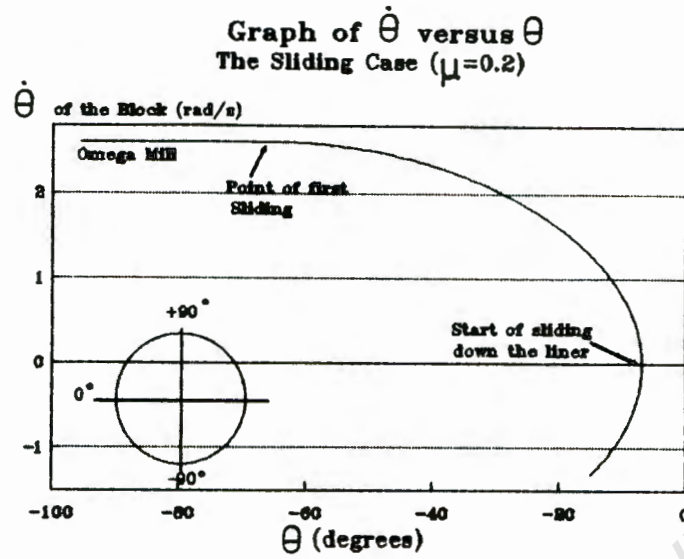
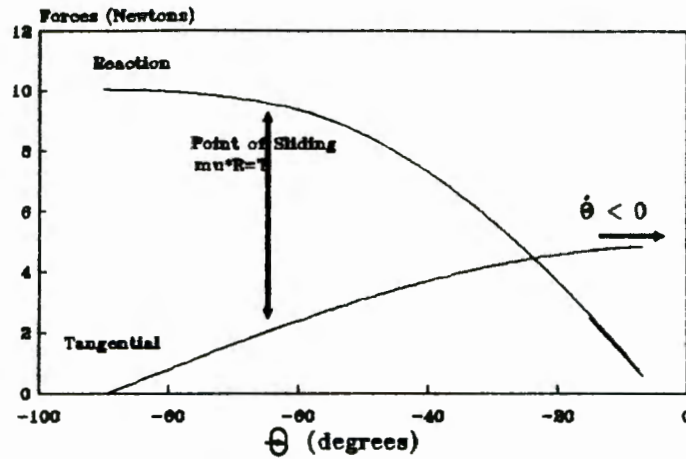
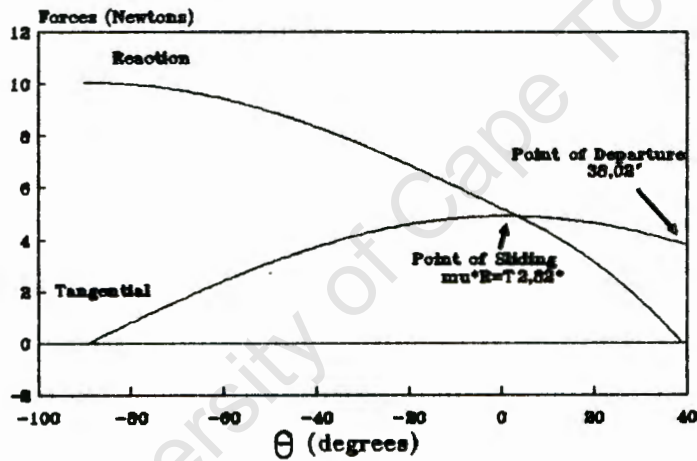


Figure 3.4: Graphs illustrating the possible End Conditions of a Block on a Smooth Liner.

Graph of R and T versus θ
The Sliding Case ($\mu=0.2$)



Graph of R and T versus θ
The Trajectory Case ($\mu=1$)



Graph of R and T versus θ
The Centrifuging Case ($\mu=3$)

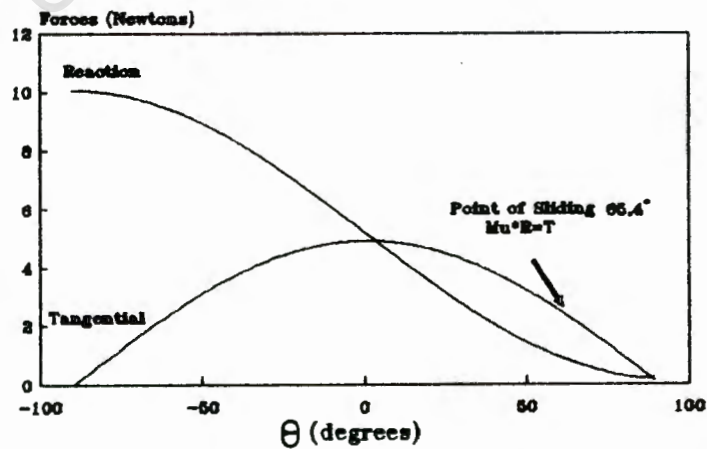


Figure 3.5: Graphs illustrating the trends of R and T versus θ for a Block on a Smooth Liner.

Figures 3.4b and 3.5b depict the case when the block is able to leave the liner and become a body moving with free fall. The block starts to slip at a larger e , than that for the sliding case, and consequently has $\dot{e} > 0$ when $R = 0$. This condition allows the block to start cataracting with an initial tangential velocity of $V = \dot{e} \rho$. The reason for the plot of R ending abruptly is that the block is no longer on the liner after the POD, and so R and T have no meaningful values.

For values of $\mu \geq 3.2$ the Totally Centrifuging situation is reached. It has not been illustrated, as the plot of \dot{e} versus e would be a straight line ($\dot{e} = \Omega_m$). Figure 3.4c illustrates that the fact that even during centrifuging, the block does slip, but the magnitude of the slip is significantly less than that which occurs during the other two situations. Consequently this is a depiction of the Slipping Centrifuge situation. Figure 3.5c shows that R is never less than zero.

The final analysis undertaken was to look at the effects on the block's trajectory, by firstly keeping Ω_m constant and varying μ , and then holding μ constant and varying Ω_m . The two investigations were done concurrently as similar results were expected. Figure 3.6 contains the outcome of keeping Ω_m constant ($\Omega_m = 82\%$). The circle represents the mill liner.

The general effect of increasing friction is to make the block ascend higher, before starting to slide i.e. increase e_{slip} . As the block has slipped less, its \dot{e} is greater and once it leaves the liner, its tangential velocity is comparatively higher. The higher tangential velocity causes the block to be flung further across the mill. This is visible by the different paths taken by a block when $\mu = 1$ or $\mu = 2.5$. The second block travels beyond the mill's vertical centre, while the block which has $\mu = 1$ has little lateral travel. With a full mill the lower μ would result in the block cascading down the charge face and the other block cataracting.

The limit to the increase in friction is the Davis Model, where the ball rises as high as possible ($AOD = \alpha$) and leaves the liner with $\dot{e} = \Omega_m$. The Davis model is illustrated by the dashed line in Figure 3.6. When $\mu = 15$ the block's path is almost as predicted by Davis. Once again the Davis predictions are only reproducible for very large or near infinite values of friction.

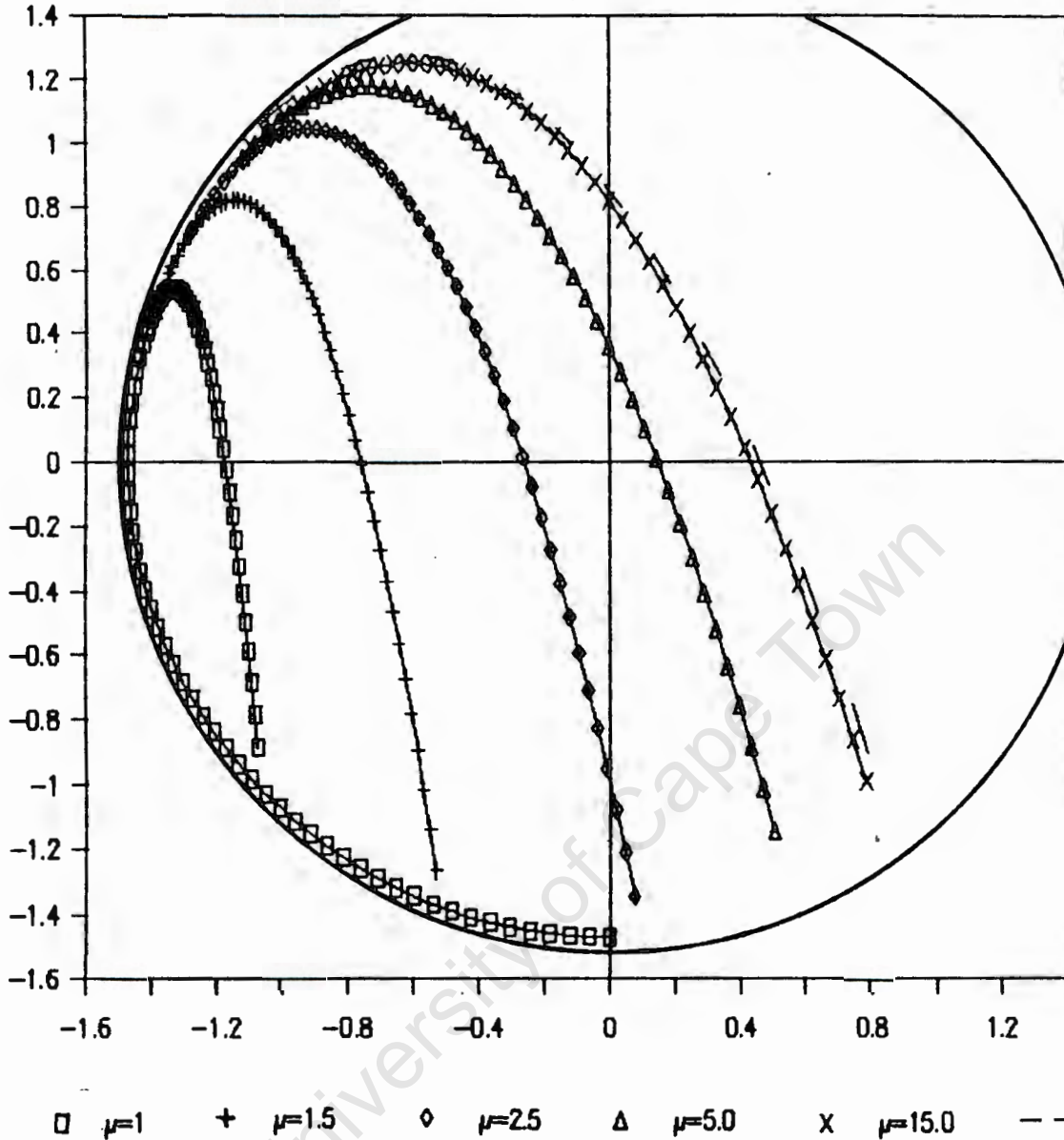


Figure 3.6: The Parabolic Trajectories of a Block for varying μ and constant Ω_m ($\Omega_m=82\%$).

The results of varying Ω_m while holding μ constant, are presented in Figure 3.7. A value of $\mu=1$ was chosen, because all the ending conditions were reproducible at suitable chosen speeds. When $\Omega_m < 74\%$, the block slides down the liner before it travels back up again and only then does it manage to achieve a state of free fall. With a full mill this condition would be similar to cascading. The path the block would trace is on the inside of the 74% trajectory and has not been included in Figure 3.7.

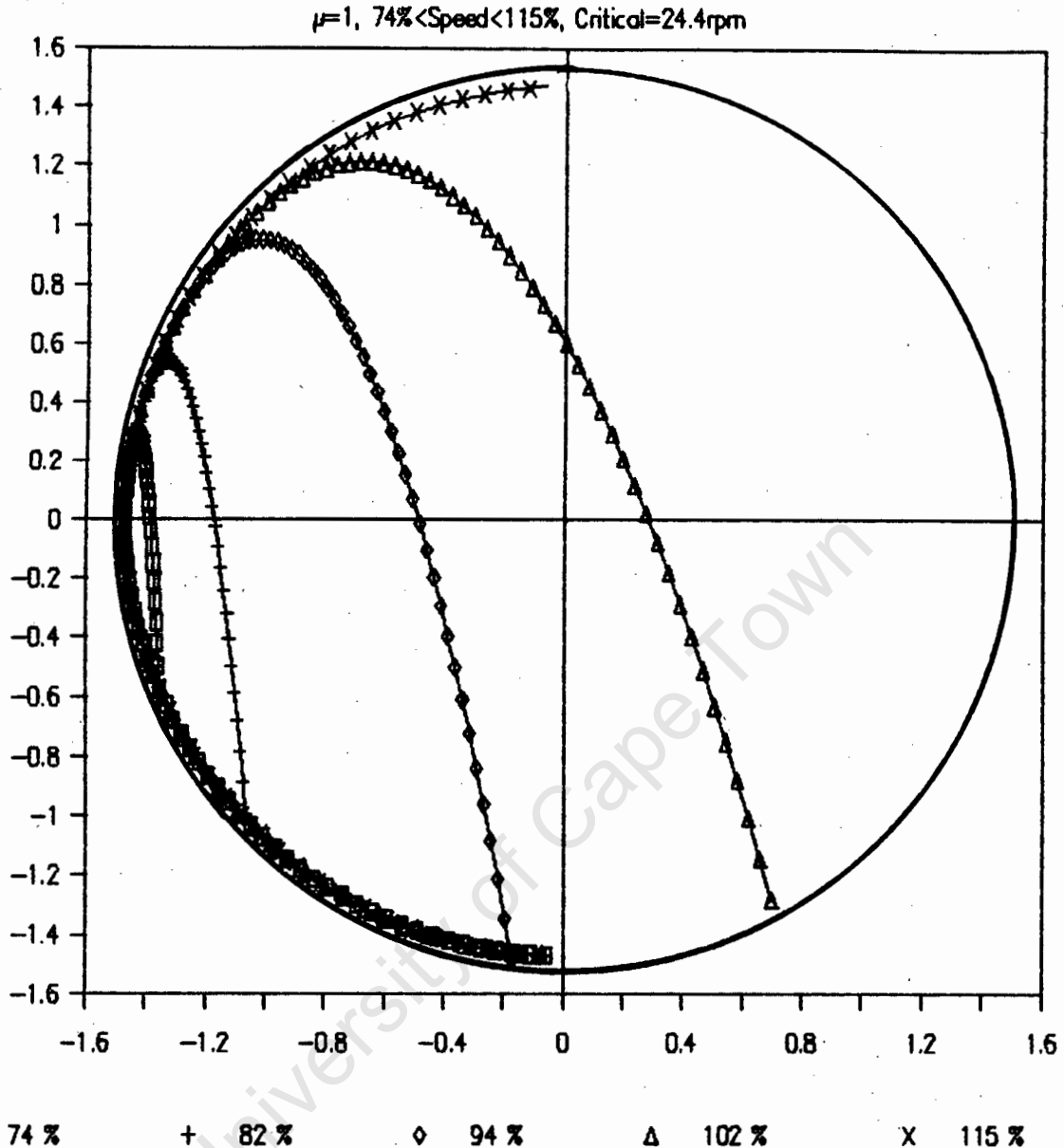


Figure 3.7: The Parabolic Trajectories of a Block for varying Ω_m and constant μ ($\mu=1.0$).

For mill speeds from $\approx 74\%$ to $\approx 102\%$, the block rotates with the liner (with varying degrees of slip) and then follows a parabolic flight path. As the speed is increased, so the block's departure velocity increases, (equivalent to increasing friction at constant Ω_m) and it is flung further across the mill. Above 102% , the block does not slip sufficiently to prevent centrifuging from occurring. The uppermost path depicts a ball centrifuging at 115% . At 123% equation (3.17) has no solution and so it is inferred that the ball never slips and is Totally Centrifuged to the liner. Hence for Ω_m between 102% and 123% , the block is only being Slip Centrifuged and not fully centrifuged.

In conclusion, the movement of a block is directly dependent on its angular or tangential acceleration. The only variables that can be varied to increase a_t are μ , ρ or $\dot{\theta}$. To keep slipping to a minimum, a_t must be as large as possible, and by maximizing μ , ρ and $\dot{\theta}$ this would be possible. In the milling process some slipping is desirable, (to form the abrasion zone), while too much is not (no cascading or cataracting). The variation of the specific parameters is controllable to achieve the desired milling situation.

University of Cape Town

3.2 Rolling Model

A second mode a particle can move with is Pure Rolling. Pure rolling assumes that the point of contact between the ball and the liner does not slide. So the point of contact is assumed to move at the same velocity as the liner.

The situation of a block on a liner has 1 degree of freedom, ie e . A ball rolling on a liner has two degrees of freedom, namely the rotation of the ball about the mill centre (e), and the rotation (spin) of the ball about its own centre (ω). When a rolling ball leaves the liner, its motion has 3 degrees of freedom, 2 in the x and y directions and the third is its spin about its own centre. The case presented below is that of a ball on a liner, and therefore has only 2 degrees of freedom. Once the ball leaves the liner it is assumed that the interaction of the ball's spin on the parabolic trajectory is insignificant. Therefore after departure the ball is assumed to still move with only 2 degrees of freedom.

3.2.1 Derivation of the Equations for a Ball moving with Pure Rolling

The governing equations for rolling will be derived in a similar way to that used for the sliding case. The orientation of the forces on a ball has been illustrated in Figure 3.8. Point A is the point of contact between the ball and the liner, P is the centre of the ball and O is the centre of the mill. e and ω are both positive in a clockwise sense and 'a' is the radius of the ball.

Referring to Figure 3.8, summing forces in the tangential and normal directions yields:

$$\begin{aligned} \Sigma F_t: \quad ma_t &= T - mg \cos e \\ \text{But} \quad a_t &= \ddot{\theta}(R-a) \\ \text{Assuming that } R \gg a \quad \therefore R-a &\approx R \\ \therefore m\ddot{\theta}R &= T - mg \cos e \end{aligned} \quad \dots(3.18)$$

$$\begin{aligned} \Sigma F_n: \quad ma_n &= R + mg \sin e \\ \text{But} \quad a_n &= \dot{\theta}^2 R \\ \therefore R &= R\dot{\theta}^2 - mg \sin e \end{aligned} \quad \dots(3.19)$$

Summing moments about the ball centre, P:

$$\Sigma M_{tSP}: \quad I\dot{\omega} = Ta \quad \dots (3.20)$$

$$\text{But} \quad I_{ball} = 2ma^2/5 \quad \dots (3.21)$$

Combining equations 3.18 to 3.21 yields:

$$2\dot{\omega}a = 5\dot{\theta}\rho + 5g\cos\theta \quad \dots (3.22)$$

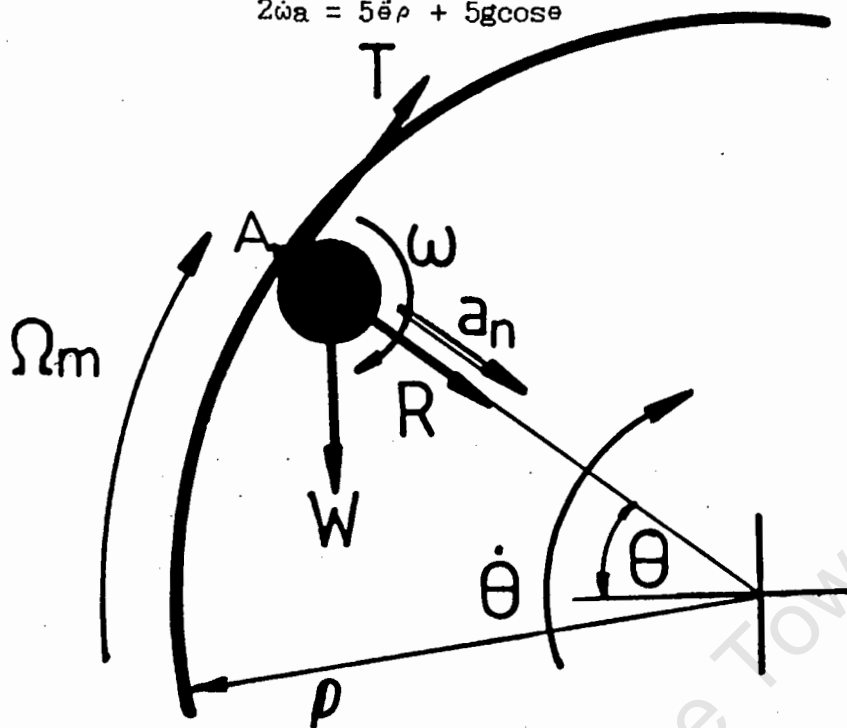


Figure 3.8: Orientation of the forces acting on a Ball.

It is required that the ball rolls with pure rolling, ie Point A moves with at the same speed as the liner $\therefore V_A = \Omega_m \rho$

Summing Velocity vectors at A: $\Omega_m \rho = \dot{\theta}(\rho - a) + \omega a$

Assuming $\rho \gg a \therefore (\rho - a) \approx \rho \therefore \Omega_m \rho = \dot{\theta}\rho + \omega a \quad \dots(3.23)$

Differentiating (3.23) with respect to time ($\Omega_m = \text{constant}$) yields:

$$\ddot{\theta}\rho = -\dot{\omega}a \quad \dots(3.24)$$

Substituting (3.24) into (3.22) yields:

$$\therefore 7a\dot{\omega} = 5g\cos\theta \quad \dots(3.25)$$

Equations (3.18, 3.19, 3.23 and 3.25) are 4 equations in 4 unknowns, R, T, θ and ω . Equation (3.18) and (3.19) are dependent on θ only (ie $R = f\{\theta, \dot{\theta}\}$ and $T = f(\theta, \dot{\theta})$). Equations (3.23) and (3.25) are a pair of coupled equations, ($\dot{\theta} = f\{\omega\}$ and $\omega = f\{\theta\}$), this leads to the equations being solved simultaneously. The solution for the block had 1 degree of freedom and hence 1 governing equation. This scenario has 2 degrees of freedom and hence 2 equations in 2 unknowns. It is notable that in deriving these equations, even though a frictional force (T) was included, no explicit need occurred for the inequality $T \leq \mu_s R$. Secondly μ is not contained in any of the governing equations.

With the one sliding equation two initial conditions were required, hence with two rolling equations three initial conditions are required. They are $\theta(0)$, $\dot{\theta}(0)$ and $\omega(0)$. Equation (3.23) couples the variables, $\dot{\theta}$ and ω and so

once either is specified, the other becomes a dependent variable. Assuming that the ball is initially moving with $\dot{e} = -\Omega_m$, then $\omega(0) = 0$. The specification of $e(0)$ will be kept the same as that used for the block i.e. $e(0) = -90^\circ$, the bottom of the mill.

3.2.2 Numerical Solution of the Rolling Equations

An Euler Forward Approximation Method will be used to numerically solve the two simultaneous equations. The full procedure can be found in Appendix 6. The final equations are:

$$\omega_{n+1} = \omega_n + \frac{h5g \cos e_n}{7a} \quad \dots(3.26)$$

$$e_{n+1} = e_n + h\dot{e}_n \quad \theta_{n+1} = \theta_n + h \left(\frac{\dot{\theta}_n \rho - a\omega_n}{\rho - a} \right) \quad \dots(3.27)$$

$$\dot{e}_{n+1} = \dot{e}_n + \frac{h(\Omega_m \rho - a\omega_n)}{\rho} \quad \dots(3.28)$$

$$\ddot{e}_{n+1} = \frac{-a(\omega_{n+1} - \omega_n)}{(\rho - a)h} \quad \dots(3.29)$$

Hence at the end of the step:

$$R_{n+1} = m\rho \dot{e}_{n+1}^2 - mg \sin(e_{n+1}) \quad \dots(3.30)$$

$$\text{and } T_{n+1} = -m\rho \ddot{e}_{n+1} - mg \cos(e_{n+1}) \quad \dots(3.31)$$

The initial conditions used modelled a non-spinning ball, moving at the same speed as the liner and being placed at the bottom of the mill. The numerical values of the initial conditions are: $\omega(0) = 0$

$$e(0) = -90^\circ$$

$$\dot{e}(0) = \Omega_m$$

$$\ddot{e}(0) = 0$$

3.2.3 Discussion of the Results from the Numerical Solution of the Rolling Equations

The numerical solution was performed by a computer program, similar to that used for the block. The major difference between the two programs was the algorithm used to implement the respective Euler Approximations. The data handling aspects of two programs were generally similar. After the program had been executed for various initial parameters, it became apparent that the ending conditions for the ball were different to those for the block.

The possibility of centrifuging did not occur, even though provisions had been included in the computer program. The ball was observed to run up one side of the mill and then roll down and continue up the other side. Each successive oscillation was larger than the preceding one. Once the ball came to rest above the horizontal it did not return down the liner, but fell away from the liner i.e. $R < 0$. It cannot be said that the balls were cataracting as the departure velocities were significantly smaller than those of the sliding block. The situation would be similar to a charge that has just started to cascade. An ending condition of a specifiable maximum number of iterations was included in the program.

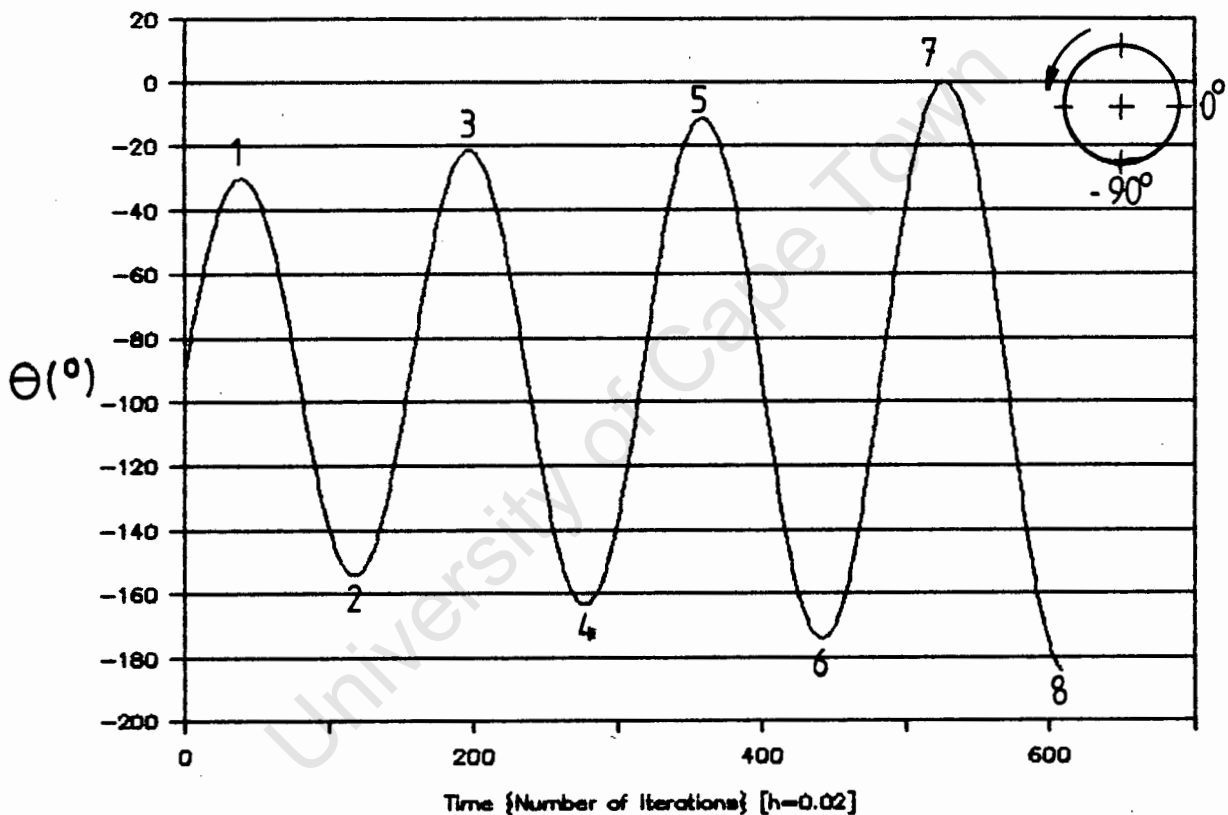


Figure 3.9: Graph of θ versus time for a Ball moving with Pure Rolling on a smooth liner with $\mu = \infty$.

Figure 3.9 contains a plot of θ versus time. At the start of each computer run, a value of μ is required as an input parameter. Even though μ is not explicitly contained in the governing equations, the magnitude of the limiting friction is an implied boundary condition. The pure rolling formulation assumes that there is no skidding of the ball and this implies that $T \leq \mu R$ ($\mu = T/R$). Hence the model breaks down (and is forced to terminate) if $\mu_{\text{input}} \leq \mu_{\text{required}} = T_n/R_n$. This occurs if the frictional

force required to stop skidding is less than that available i.e. μ_{input} . So by setting $\mu=\infty$, as in Figure 3.9, implies that the ball is never allowed to skid as friction can not be exceeded. This will be re-examined in Figure 3.12

With the mill rotating clockwise, $e=-180^\circ$ is the horizontal axis to right of the mill centre, while $e=0^\circ$ corresponds to the horizontal on the left side. As before $e=-90^\circ$ is the mill bottom. Examining Figure 3.9 it is noticeable that the ball's movement seems to be a divergent system, where the size of each successive oscillation is ever increasing. A description of the ball's behaviour is, once it has ascended up one side of the mill, on its return past the neutral position (mill bottom), it has a significantly larger spin than during the previous pass, and is therefore able to rise higher up the other side. The trends and relative phases of \dot{e} and ω are illustrated in Figure 3.10.

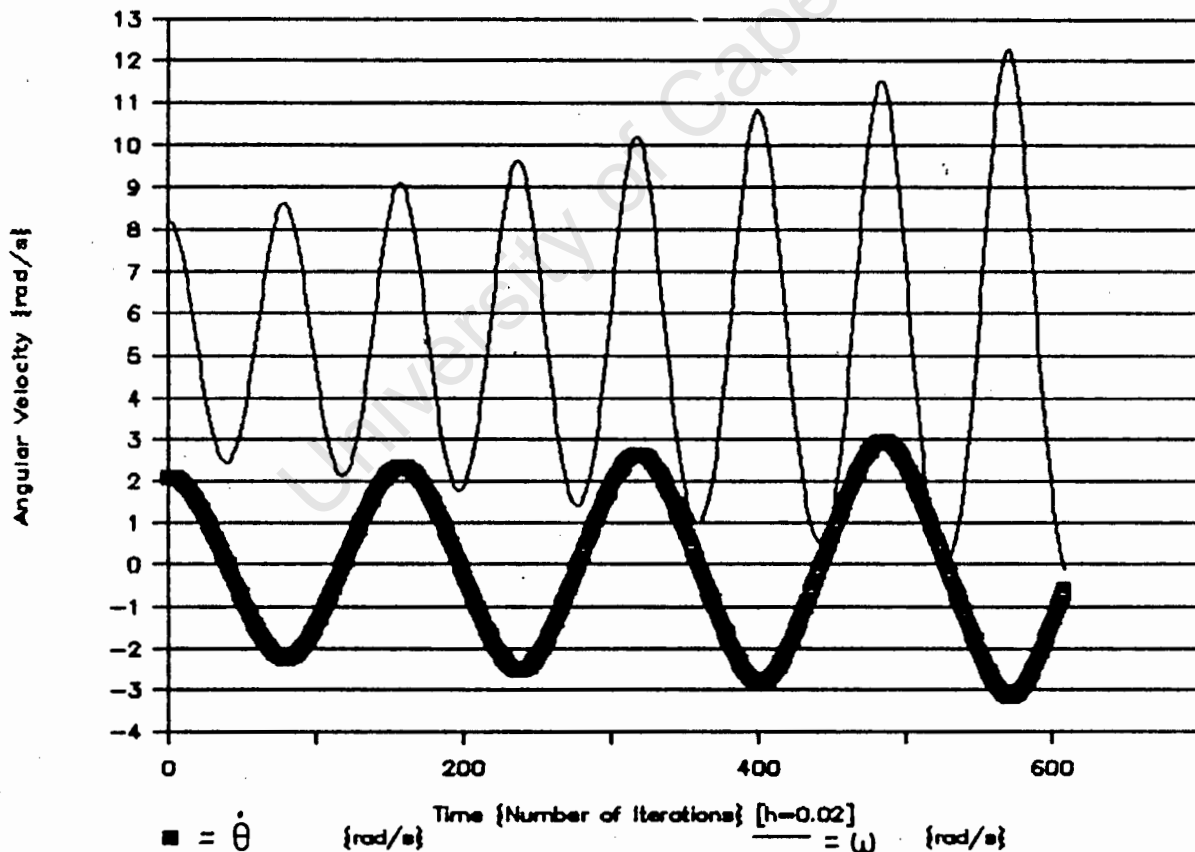


Figure 3.10: Graph of \dot{e} and ω versus time for a Ball moving with pure Rolling on a smooth liner.

Another explanation for the response, from an energy point of view, is that the mill continually increases the ball's energy. The energy is transferred via the frictional force acting at the point of contact, A,

between the ball and liner. There is no provision in the model for energy dissipation, as the block is not permitted to skid ($\mu=\infty$). Energy is only dissipated if a force acts through a distance. With a non skid condition there is no distance moved between the two surfaces and so the energy dissipated is zero. Each time the ball returns to the mill bottom, the increased energy is contained in two modes of kinetic energy, ie the ball's spin (ω) and its angular velocity ($\dot{\theta}$). When it reaches its highest point on the liner the energy is transformed into potential energy due to the height of the ball and the kinetic energy due to the spin (At the highest point $\dot{\theta}=\emptyset$). As the ball's energy increases on each pass, the additional energy is converted to an increase in both the potential and kinetic energy. This explains why the ball rises higher and spins faster after each oscillation.

The boundary condition of a ball departing from the liner is illustrated in Figure 3.11. The radial reaction, R, of the ball against the liner has been plotted against time. The graph is for the same initial conditions as used in Figures 3.9 and 3.10. The ball's first oscillation (Figure 3.9) results in a rise of only 50° ($\theta_{\text{highest}} \approx -30^\circ$). A further 8 oscillations are needed, before the ball has enough energy to rise above the horizontal. At the end of each successive oscillation, the magnitude of the reaction reaches a new minimum. (The reaction is a maximum when the ball passes the mill bottom) After the 8th oscillation, the reaction becomes negative and the ball leaves the liner. The solution was terminated at this point, hence the abrupt end of the graph.

The other condition that was used as an end condition (besides number of iterations) was whether friction had been exceeded and the ball had begun to skid. At the end of each iteration, the value of $T/R=\mu$ was calculated. Figure 3.12 contains a plot of the T/R produced from the same conditions used to generate the other graphs. At each of the highest points of oscillation, the value of T/R is a maximum. This is because at the extremities of each oscillation $\dot{\theta}=\emptyset$ and hence the ball's spin is a new maximum. From equation (2.23), if $\dot{\theta}=\emptyset$ then $\omega=Q_{mp}/a$. This means that μ must be large enough for the ball to move and spin without skidding. (A tyre skids if it can not get good traction on the road. The traction is directly proportional to the coefficient of friction between the two surfaces.) As the ball's energy increases so the magnitude of the frictional force required to eliminate skidding increases.

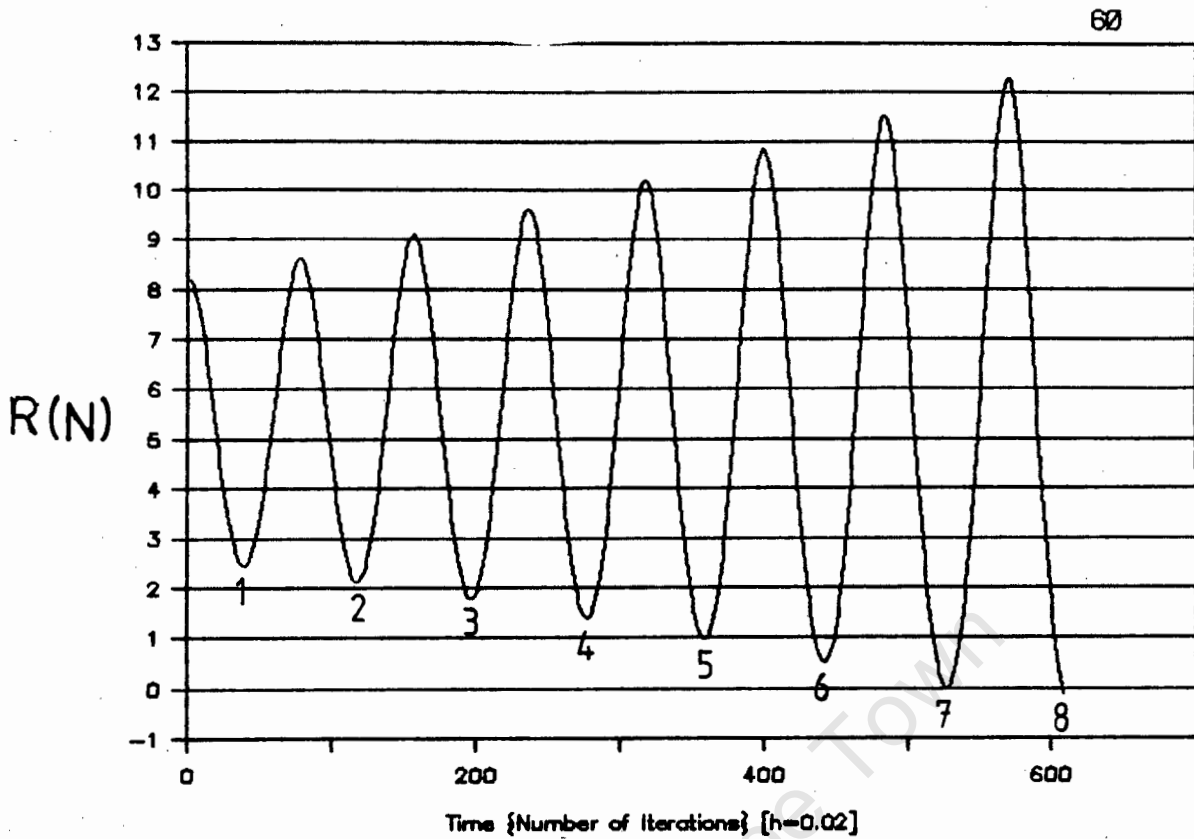


Figure 3.11: Graph of R versus time for a Ball moving with pure Rolling on a smooth liner.

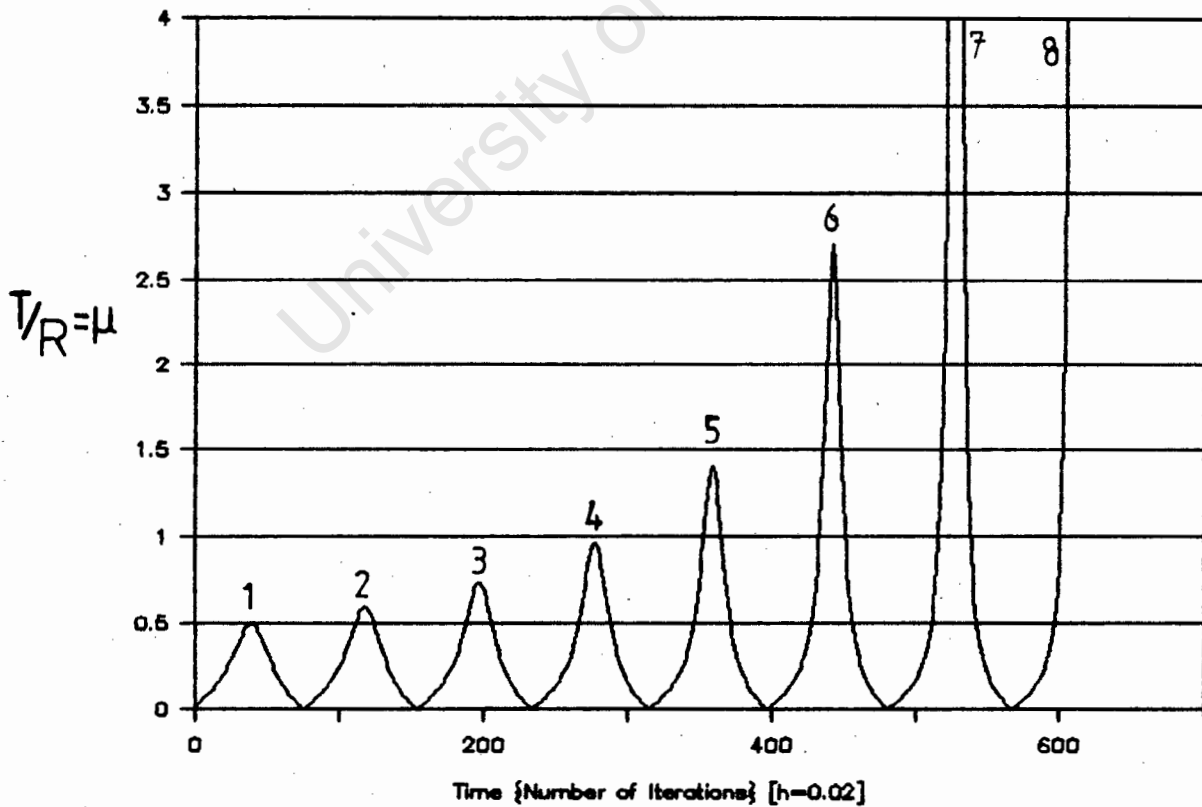


Figure 3.12: Graph of T/R versus time for a Ball moving with pure Rolling on a smooth liner.

Figure 3.11 illustrates the case where the ball departed from the liner. For this to have occurred, then $\mu \geq 162$ as this is the ratio of T/R at the extremity of the 7th oscillation. A value of this magnitude is not feasible and so the ball would have skidded before departure would occur. In reality, $\mu \leq 1$, and so the pure rolling model would have broken down after only the 4th oscillation or approximately $5\frac{1}{2}$ seconds. The coefficient of friction between two steel surfaces, is approximately $\mu = 0.35$. If the ball and liner were both made of steel, then the pure rolling model would have failed sooner, after only 29 iterations or 0.58 seconds.

The mill's speed was varied in order to observe the ball's general response. The trend that became apparent was that the higher the value of Ω_m , the sooner (both in time and θ travelled) the ball started to skid. Therefore, in conclusion, the pure rolling model holds only for the initial motion of the ball. Soon after the motion is initiated, friction would be exceeded and the ball would start to skid. The time duration for which the model holds decreases as the mill speed increases. At realistic mill speeds and coefficients of friction, the time taken before skidding occurs is generally less than a second.

3.3 Combination of the Rolling and Sliding Models

The two previous sections looked at the cases of pure sliding and pure rolling. Both had inherent assumptions that in practice would not have been permissible. The block model excluded the possibility of rolling, while the rolling model excluded the possibility of sliding or skidding. In reality, a particle would move with a combination of the two models.

Using the same derivation as for sliding (see Figure 3.1), the resulting equations after summing forces in the radial and tangential directions, are:

$$R = \rho m \dot{\theta}^2 - mg \sin \theta \quad \dots(3.2)$$

$$T = \rho m \ddot{\theta} + mg \cos \theta \quad \dots(3.4)$$

Referring to Figure 3.1, if the particle is permitted to spin or tumble clockwise, then taking moments about the centre yields:

$$I \dot{\omega} = T a \quad \dots(3.32)$$

Substituting (3.4) into (3.32) yields:

$$\dot{\omega} = \frac{ma(\ddot{\theta} \rho + g \cos \theta)}{I} \quad \dots(3.33)$$

As with sliding, the assumption used is $\mu_k R = T$ and hence combining (3.2) and (3.4) yields equation (3.11):

$$\ddot{\theta} \rho - \mu_k \rho \dot{\theta}^2 + g(\mu_k \sin \theta + \cos \theta) = 0 \quad \dots(3.11)$$

Equation (3.11) can be solved using an Euler Approximation and would yield equations (3.12) and (3.13). Solving equation (3.33) with an Euler Approximation yields:

$$\omega_{n+1} = \omega_n + \frac{hma\{\rho \ddot{\theta}_n + g \cos \theta_n\}}{I} \quad \dots(3.34)$$

The 2 governing equations, before numerical approximation, are equations (3.11) and (3.33). These equations model a particle moving with a combination of spinning and sliding. The equations for rolling were coupled and had to be solved simultaneously. Those resulted in both $\dot{\theta}$ and ω influencing the ball's motion. The equations for this model are uncoupled. Equation (3.11) is of the form $\ddot{\theta} = f(\theta, \dot{\theta})$ and is independent of equation (3.33), which is of the form $\dot{\omega} = f(\theta, \ddot{\theta})$.

The physical interpretation of the system of equations is that of a particle that is sliding and spinning along the rotating surface. The anomaly is that the particle's spin has *no* influence at all on its behaviour. In

other words, the frictional force is producing a torque that in turn causes the particle to spin, but the resulting spin has no influence on the particle's motion.

Therefore these equations are equally inadequate in their attempt to model the conditions occurring in practice and the analysis of this motion type will not be pursued any further. The ultimate model to be sought would need to include the effects of the spin on the motion of the ball. The solution would have the ball's motion made up partly by spin and partly by rotation about the mill centre.

University of Cape Town

4. EXPERIMENTAL RATIONALE AND PROCEDURE

This chapter has been divided into three parts. The aims and reasons for the experimentation are covered in the first part. The second part discusses the experimental apparatus used and the manner in which the theoretical situations were modelled in the experimental situation. The final part describes the data acquisition techniques employed for measuring the various operating parameters.

4.1 Experimental Rationale

All the preceding analysis and discussion has been based on purely theoretical predictions. An experimental investigation was initiated to compare the theoretical predictions with experimental results. The main advance in the new formulations were the inclusion of the frictional force between a particle and the liner. The derived model permitted a more accurate prediction of the particle's motion. With a block, the starting and ensuing magnitudes of slip are predictable, as well as the resulting slip's influence on the Angle of Departure and Centrifuge conditions. This resulted in most of the experimental investigation concentrated on the sliding equations. A brief experimental investigation was done on the pure rolling model. The rolling investigation was less extensive because the theory predicted that it would only be applicable for less than 1 second and hence more difficult to analyse experimentally.

In order to verify the sliding and rolling theories applicability, the aim of the experimentation was to observe a particle's response to specific variations in selected operating conditions. The operating conditions that were selected to be varied were: the mass of the particle, the coefficient of friction (μ) and the test mill velocity (Ω_m). The influences of Ω_m and μ were examined in the analysis of the theoretical predictions. The variation of m , was included to validate the postulation that a particle's motion is independent of its mass.

The specific sliding condition that was examined, was the response of a block initially at the bottom of the drum and moving without slipping. The initial conditions can be represented mathematically as: $\theta(0) = -90^\circ$ and $\dot{\theta}(0) = \Omega_m$. These conditions were chosen because they are the same conditions that were modelled in the theoretical analysis. Secondly, these conditions would allow various specific results to be easily gauged. These are θ_{slip} ,

the AOD and the onset of the two types of Centrifuging. As in the theoretical modelling, the shape of the particle's trajectories after departure was assumed to be parabolic. Various authors [2,4,6,9] have experimentally investigated particle trajectories and it was therefore decided to exclude the post departure behaviour from this investigation.

4.2 Experimental Apparatus

Past experience has shown that a test mill mounted on rollers, runs with large induced vibrations. The effect of the vibrations [10] is to reduce the coefficient of static friction (μ_s) to almost zero. This occurs because, a particle placed onto an even slightly inclined vibrating plane does not remain still. It will slide down the plane and so the apparent coefficient of friction tends to zero. This would not have been suitable as no provision is made in the theory for a surface that has $\mu_s = 0$. To eliminate mill vibration, an axially mounted mild steel drum ($\phi=404\text{mm}$, depth=~~100~~mm) was constructed. As no liquid was to be added to the charge, in this case a single particle, no front was constructed. The open drum made the positioning and retrieval of the particle simple. It also eliminated the problems encountered due to end effects of a glass window [2,5]. Figure 4.1 contains a photograph of the experimental apparatus. Clearly visible is the axially mounted drum, and below it, a motor and variac.

The drum was powered by a $\frac{1}{4}$ Hp DC motor attached to a variac. This allowed the drum's rotational speed to be variable, across a fixed speed range. The Critical Velocity as predicted by Davis is 66.7 rpm (Equation 2.5). The motor was able to rotate the drum at speeds well exceeding 300% of critical. This speed range was required because the new formulation predicts that a single particle will not centrifuge at the Davis predicted speed.

An electronic speed transducer was incorporated to measure the drum velocity. It consisted of a slotted disc mounted directly on the mill shaft. When attached to an ordinary frequency counter, the rotational velocity of the shaft is measurable. The disk has 60 slots cut into its edge, so the displayed frequency is equivalent to the shaft speed in rpm. The speed transducer is visible at the back of the shaft in Figure 4.1.

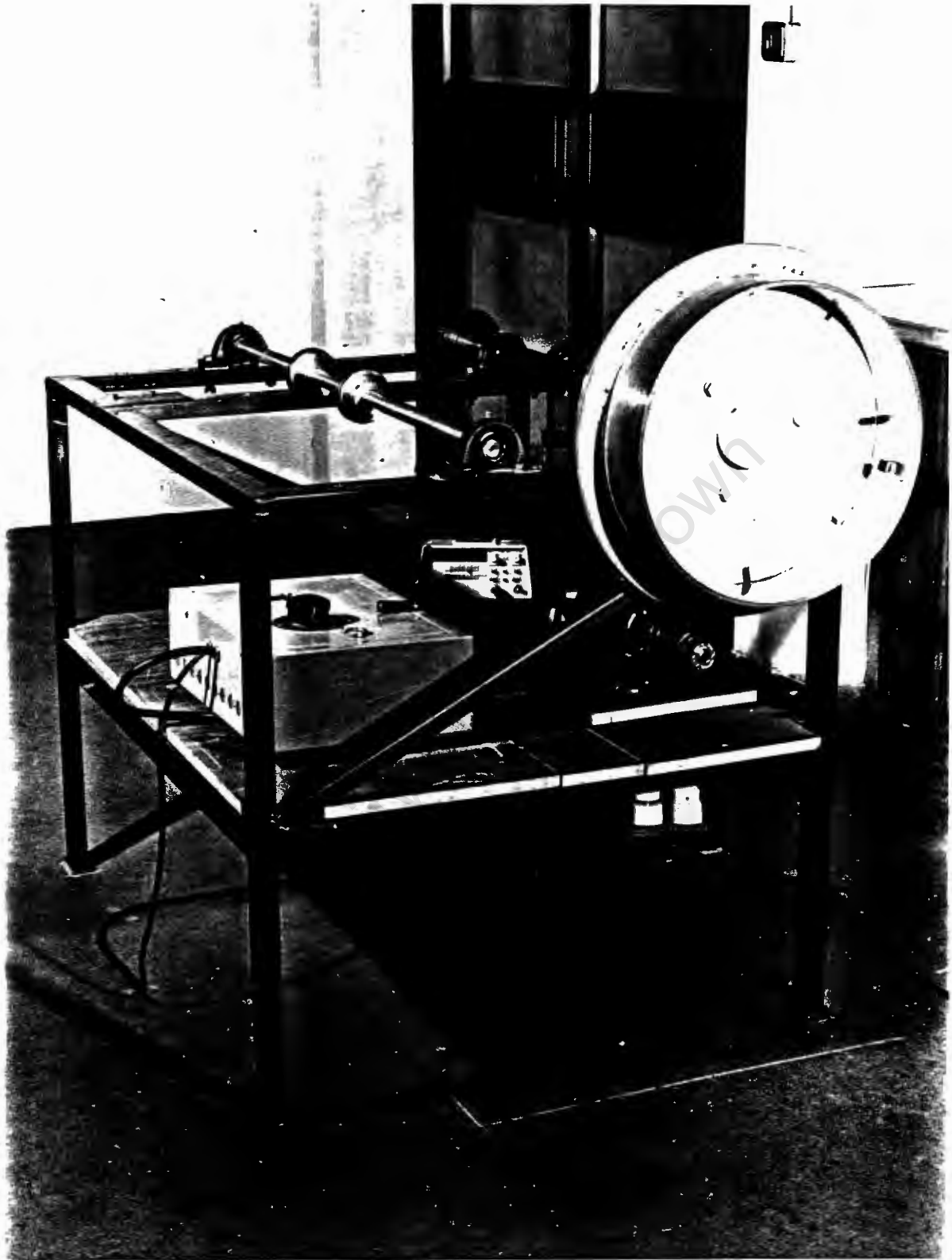


Figure 4.1: Photograph of Experimental Apparatus

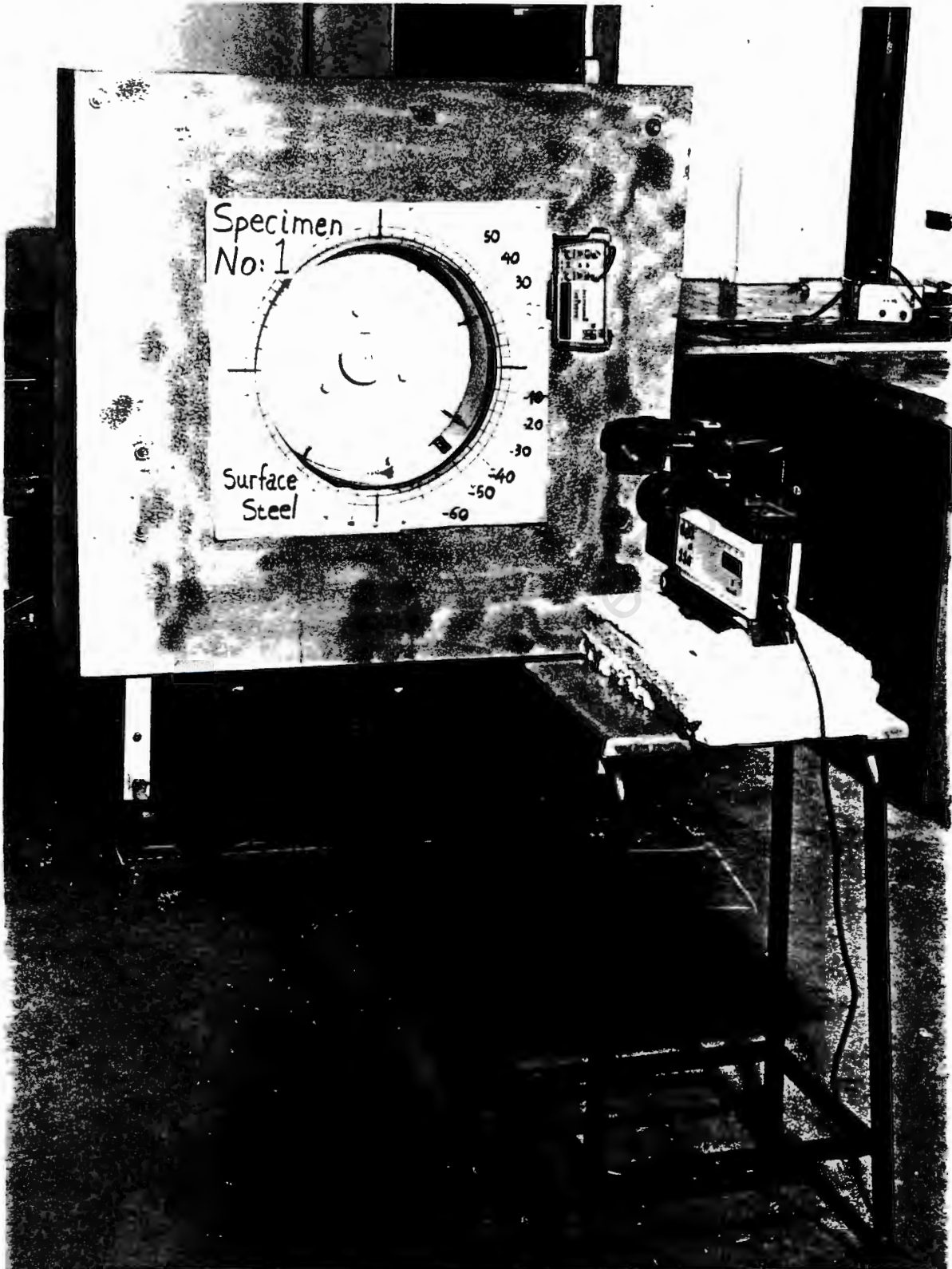


Figure 4.2: Photograph of Information Panel and Camera position.

Figures 4.1 and 4.2 contain photographs of the experimental layout out. A vertical panel was built that fitted around the drum. A circular hole was cut in the panel. The panel was positioned so the hole and drum centres were concentric. To allow the block's angular displacement to be easily measurable, the perimeter of the cavity was marked at 5° intervals. In accordance with the notation used in the theoretical discussion, the drum bottom was labelled $\theta = -90^\circ$, but the angular displacement and velocity increased in an *anti-clockwise* direction. Included in the panel were areas onto which test information could be mounted and a position for the mounting of the frequency counter.

A video camera and recorder were used to record the block's motion. The positioning of the camera is illustrated in Figure 4.2. The camera's image included the drum and particle, the information panel and the mill rotational speed (the frequency counter) as shown in Figure 4.3. A video camera was selected instead of a high speed camera for the following reasons. High speed photography requires expert knowledge for successful operation and film processing. In comparison, a video camera is relatively simple to use and has the advantages of automatic focussing and lighting control. Secondly a video camera does not need any time for film processing and developing. This permits the experimenter to recognise and correct faults immediately.

The video images were analysed using a video recorder that had a single frame advance facility. This enabled the motion to be easily quantified, while still using relatively unsophisticated equipment. The video camera operated at 25 frames/second, which was predicted to be fast enough for the experimental speed range.

The developed theory for the sliding model assumes that there is no rotation of the particle. A rectangular shaped particle made from steel square bar was most suited. Furthermore, the theory requires that the particle size (l_r and l_t) must be small compared to the mill radius (ρ). A standard bar size of cross section 15x15 mm, results in the $\frac{1}{2}l_r/\rho$ ratio of 0.037, which is within an acceptable range. To test the theoretical prediction that a particle's motion is independent of its mass, 3 blocks of varying length were fashioned. The respective lengths and masses used were; 21mm, 29mm, 37mm long and 26g, 36g and 46g of mass. To observe and test the validity of the pure rolling model a cylinder ($\phi=30\text{mm}, l=29\text{mm}$) was fashioned.

The second parameter that was to be varied was the coefficient of friction between the particle and the drum surface. After an initial trial period, the two surfaces selected were the bare steel drum and a lining of cloth. The cloth lining was stuck to the drum using latex. Initially bare latex was also used, but its "stickiness" resulted in $\mu > 1.3$ and the block tended to topple before sliding, so it was deemed unsuitable. The last parameter that was varied was Ω_m . This was done with the aid of the variac.

4.3 Experimental Procedure

The investigation used the initial conditions described $\{\theta(0) = -90^\circ$ and $\dot{\theta}(0) = \Omega_m\}$ and evaluated the particles' responses when each of the three independent physical parameters were altered. The three parameters that were controlled were Ω_m , μ and m .

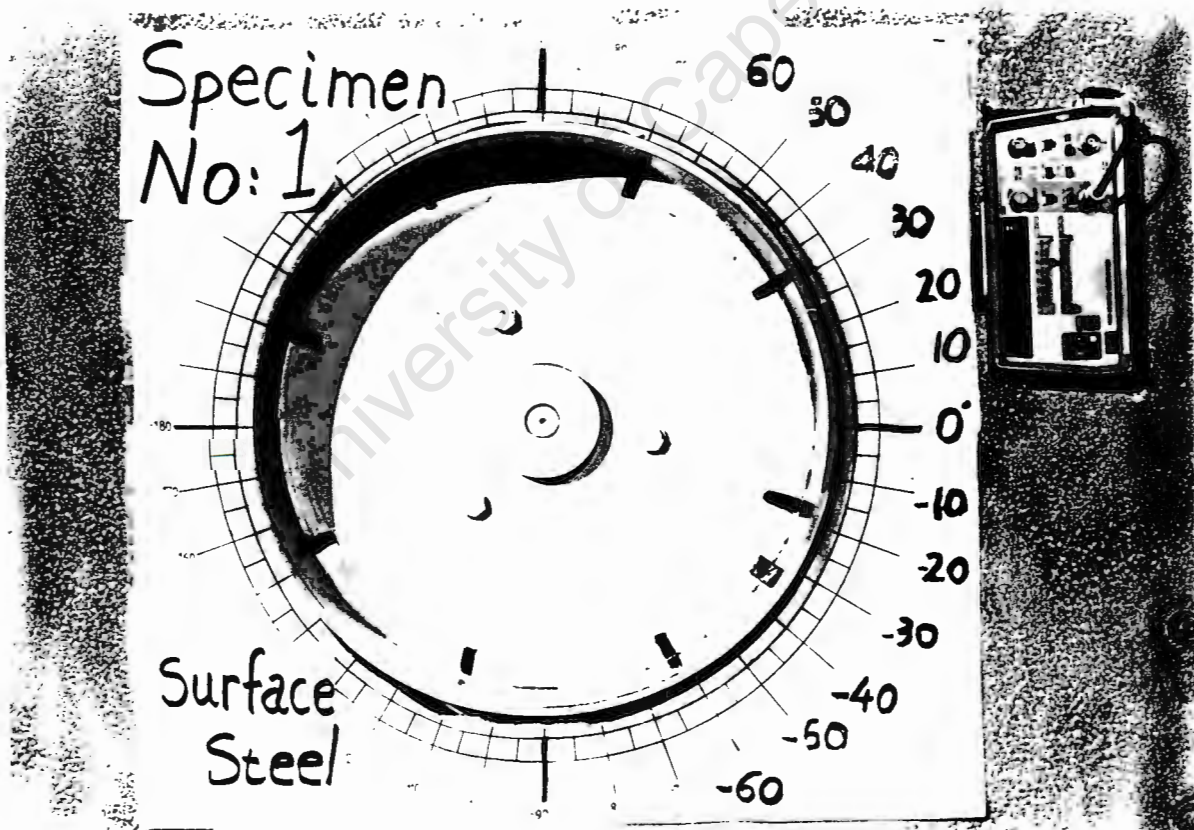


Figure 4.3: Photograph of a Sample Video Recorded Frame.

The determination of the Angle of Slip and Angle of Departure of each particle was done by analysing the recorded video. Figure 4.3 contains a sample frame from the video recordings. The block is visible at approximately $\theta = -33^\circ$. The Angle of Slip (θ_{slip}) was determined by observing when the block first started to move relative to the markings on the rear surface in the drum. When the block started to move away from the liner, it cast a shadow onto the liner. The angle at which the shadow was first visible was assumed to be the Angle of Departure.

Batches of tests were run on the two surfaces. Each batch consisted of varying the mill speed from 20 rpm (30% Critical) until the block became centrifuged. A number of visual recordings were made at each of the mill speeds. In this way a mean value was calculable for the θ_{slip} and the AOD at each speed. Each set of data was analysed statistically, using a Student or "T" Test, to determine an appropriate confidence range.

The last parameter that had to be quantified was the effective coefficient of friction between the block and the two linings. The static coefficient was measured by placing the block at the bottom of the mill and slowly rotating the mill. The process was filmed and by analysing the video, the angle at which the block just started to slip could be determined. A kinetic coefficient of friction was not measured, as the difference between μ_s and μ_k , on a steel surface, is not significant.

5.0 PRESENTATION AND DISCUSSION OF THE EXPERIMENTAL RESULTS

The presentation of the experimental results will be divided into five sections. Each section will present the relevant experimental data and thereafter compare these results to the theoretical predictions. The five sections will cover;

- (1) The measuring of the Coefficient of Friction for each surface,
- (2) The determination of the Angle of Departure for each surface,
- (3) The determination of the Angle of Slip,
- (4) The experimental Centrifuge speed required for a single block and
- (5) A brief discussion of the experimental observations for the Pure Rolling situation.

5.1 Determination of Coefficient of Friction (μ) for each Surface.

The coefficient of friction was determined while the mill was stationary. Examining equation 3.11 and setting $\dot{\theta}=\emptyset$ and $\ddot{\theta}=\emptyset$, the resulting expression is:

$$\mu = \cot(\theta) \quad \dots(5.1)$$

$$\text{If } \theta < \emptyset \text{ then } \mu = -\cot(\theta) \quad \dots(5.2)$$

The mill was rotated and the angle determined when the block started to slide. This is equivalent to placing the block on an increasing inclined plane and observing when the block starts to slide down the plane. The accuracy with which the angle could be established was $\pm 1-2^\circ$. Figure 4.3 illustrates that $1-2^\circ$ is not an excessive uncertainty. The block's width (15mm) is equivalent to an arc of 4.3° and the angular graduations are marked in 5° increments. The relative size of the block to the angular increments makes it unfeasible to quote angles with a confidence of more than 2° .

Surface	Angle	μ	Uncertainty in μ	Uncertainty Range
Steel	-77.0°	0.231	± 0.037 ($\pm 16\%$)	0.194 - 0.268
Cloth	-67.0°	0.424	± 0.042 ($\pm 10\%$)	0.382 - 0.466

Table 5.1: Tabulation of the Uncertainty in μ

Due to the nature of the cot function an uncertainty of $\pm 2^\circ$ can lead to a large uncertainty in the value of μ . Table 5.1 contains the medium of the values measured for each surface. An uncertainty of 2° in the measured

angle is equivalent to an uncertainty of $\pm 2.5\%$ for steel and $\pm 3\%$ for the cloth surface. When these results are used to calculate μ , the uncertainty in μ on steel rises to $\pm 16\%$ and on cloth $\pm 10\%$. The increase in the uncertainty range is unavoidable and the values of μ that will be used to evaluate the theoretical predictions, will be restricted to within these uncertainty limits.

5.2 Results of the Angle of Departure of a Single Block

During the examination of the filmed results, it became relatively simple to determine when a block had departed from the liner. Due to the lighting conditions, once the block had moved a significant distance away from the lining, a shadow was cast onto the lining. The Angle of Departure (AOD) was recorded when the shadow was just visible.

The theory predicts that if $\epsilon > 0^\circ$ and $R \leq 0$, then the block will leave the liner and start its parabolic trajectory. The block can not leave the liner if $\epsilon < 0^\circ$, as the normal component of the block's weight is always positive (Equation 3.2). When the situation arises where $\epsilon = 0$ but $\epsilon \leq 0^\circ$, then the block will just slide back down the mill.

Tests were run to determine the AOD of the block for the two surfaces and for three different masses on the steel surface. If a block did not rise above the horizontal ($\epsilon \geq 0^\circ$), then the highest angle reached after the first oscillation was recorded instead of the AOD.

Appendix 7 contains a listing of the experimental data. Each data sample was analysed statistically. The appendix contains the number of data points (N) and the mean of each sample. A Student test was applied to each sample and the 90% Confidence Range determined. The upper and lower limits of the ranges have been tabulated in the appendix. Included alongside the experimental results are the theoretical predictions. The theoretical results will be referred to as required and explained from within the text. Relevant data will be selected from Appendix 7 and plotted to emphasise specific trends and responses.

The aim of the first batch of tests was to confirm that a block's motion is independent of its mass as predicted by equation (3.11). Figure 5.1 contains a plot of the Angles of Highest Rise (or Departure) against Mill

Speed. The three blocks have masses of 25.9g, 36.05g and 46.0g. As the largest block is 1.8 times heavier than the smallest, it will be assumed that blocks of different masses were used. The data collected for the three blocks has been plotted at discrete points. The largest and smallest blocks have data for increments of 20rpm, while the 36.05g block has data at 10rpm increments.

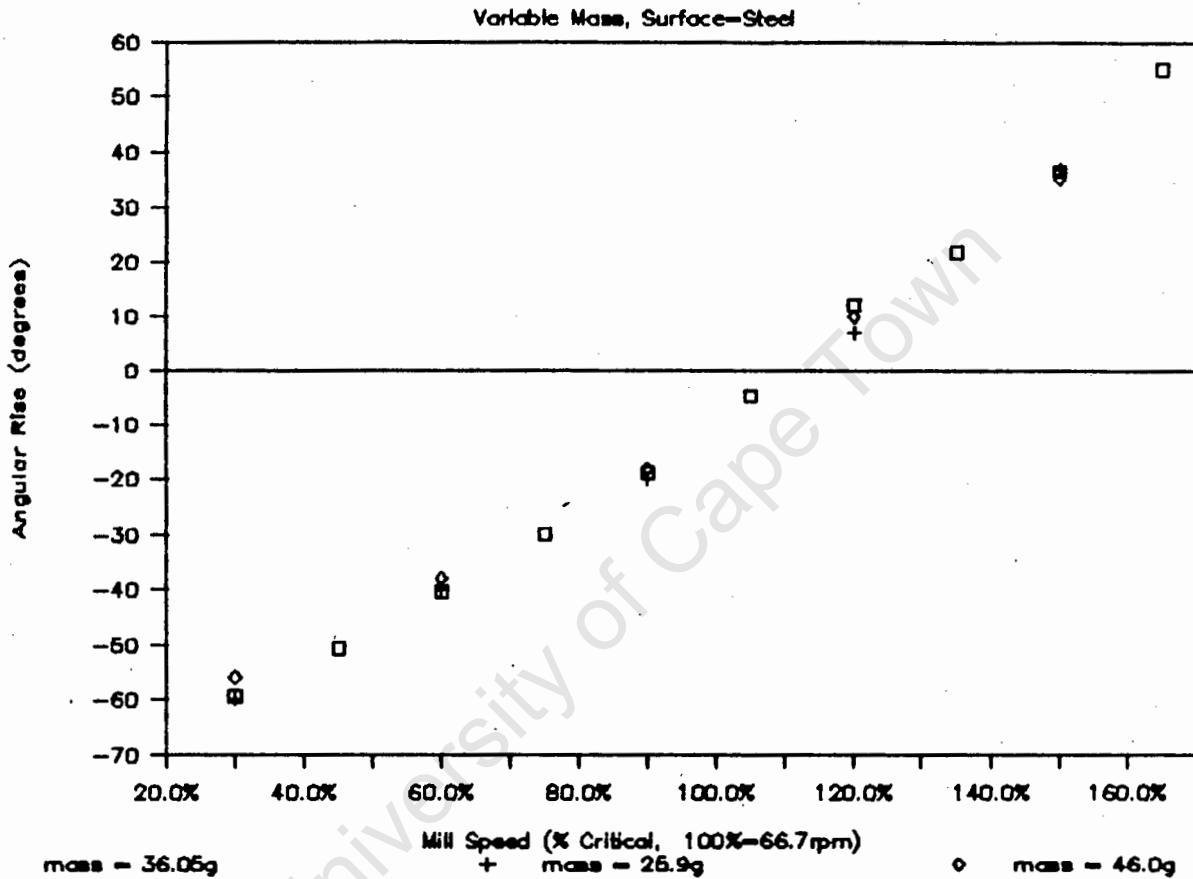


Figure 5.1: Graph of Angular Rise versus Mill Speed for three different blocks on a steel surface.

The experimentally determined Angles of Departure for the three blocks fall within a narrow band. Their values differ from each other by a maximum of 4° , this occurs at 30 % critical (20rpm). The uncertainty range, at 30%, as a percentage of the mean of the sample is only 6%. The magnitude of the differences, or errors, can be attributed to general experimental uncertainty.

Therefore it can be stated that the three blocks of different mass, exhibit a similar response on a liner of constant roughness. The conclusion that can be drawn is that the prediction by the theoretical model, that a particle's motion is independent of its mass, is confirmed. Furthermore it

is feasible to assume that for the other experimental investigations still to be presented, they need only be done with a block of arbitrary mass, and do not have to be re-run for particles of different masses. This was implemented and the remainder of the experimental investigation used only the 36,05g block.

The second batch of tests examined the change in the Angle of Departure as μ and Ω_m were varied. The two surfaces used were steel and cloth, the particle was the mild steel block. Figure 5.2 contains an a plot of the mean values of each sample and the 90% Confidence Intervals as determined from the T Tests.

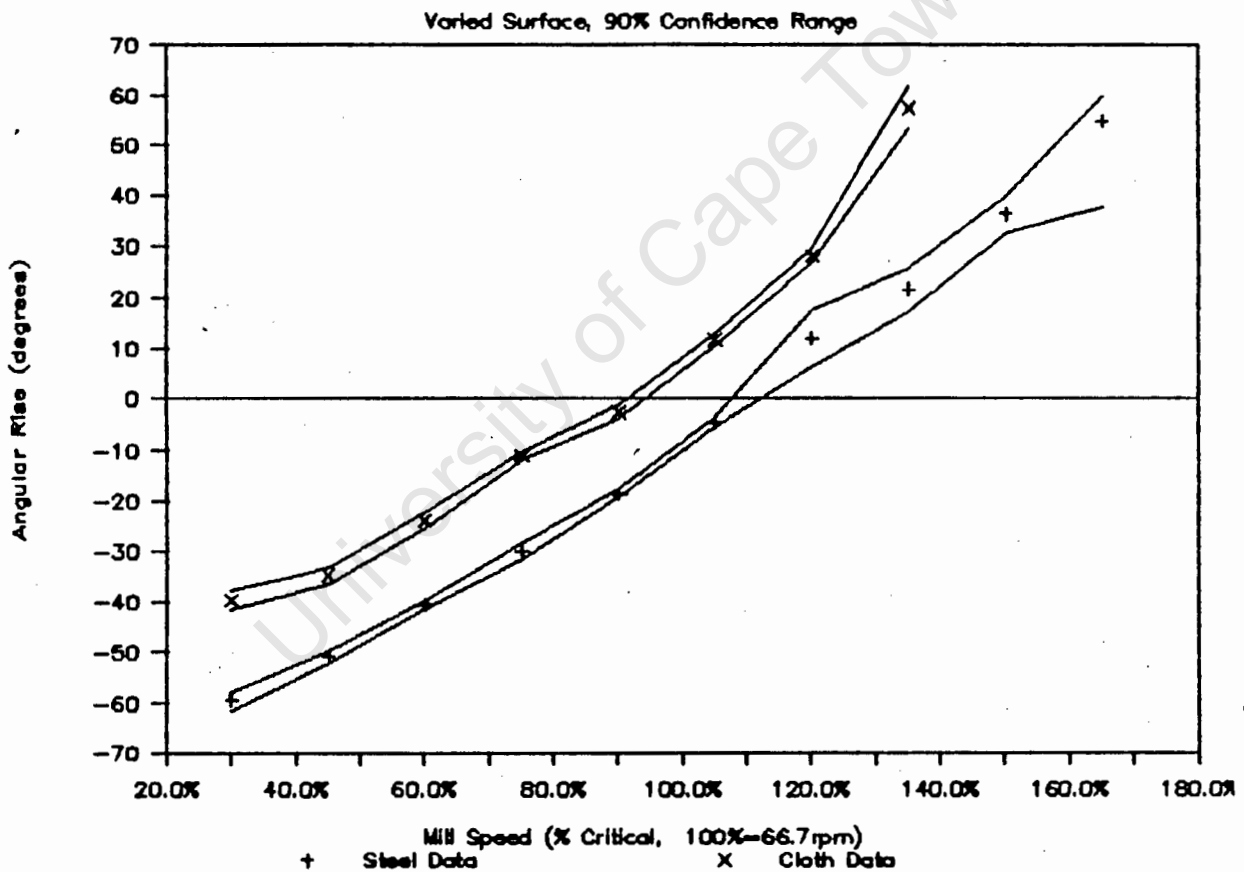


Figure 5.2: Graph of Angular Rise versus Mill Speed, with the 90% confidence range.

The confidence intervals are generally less than 4° . This indicates a high probability that a repeated experiment would yield similar results. The confidence interval increases at the higher mill speeds because the AOD could be determined less accurately because of the limits of the video camera's frame resolution. In practice a mill is generally run at speeds

around the 70-80% critical range. So the accuracy of the experimental results beyond the operating range is less important. They have been included to present the general trends at higher mill speeds.

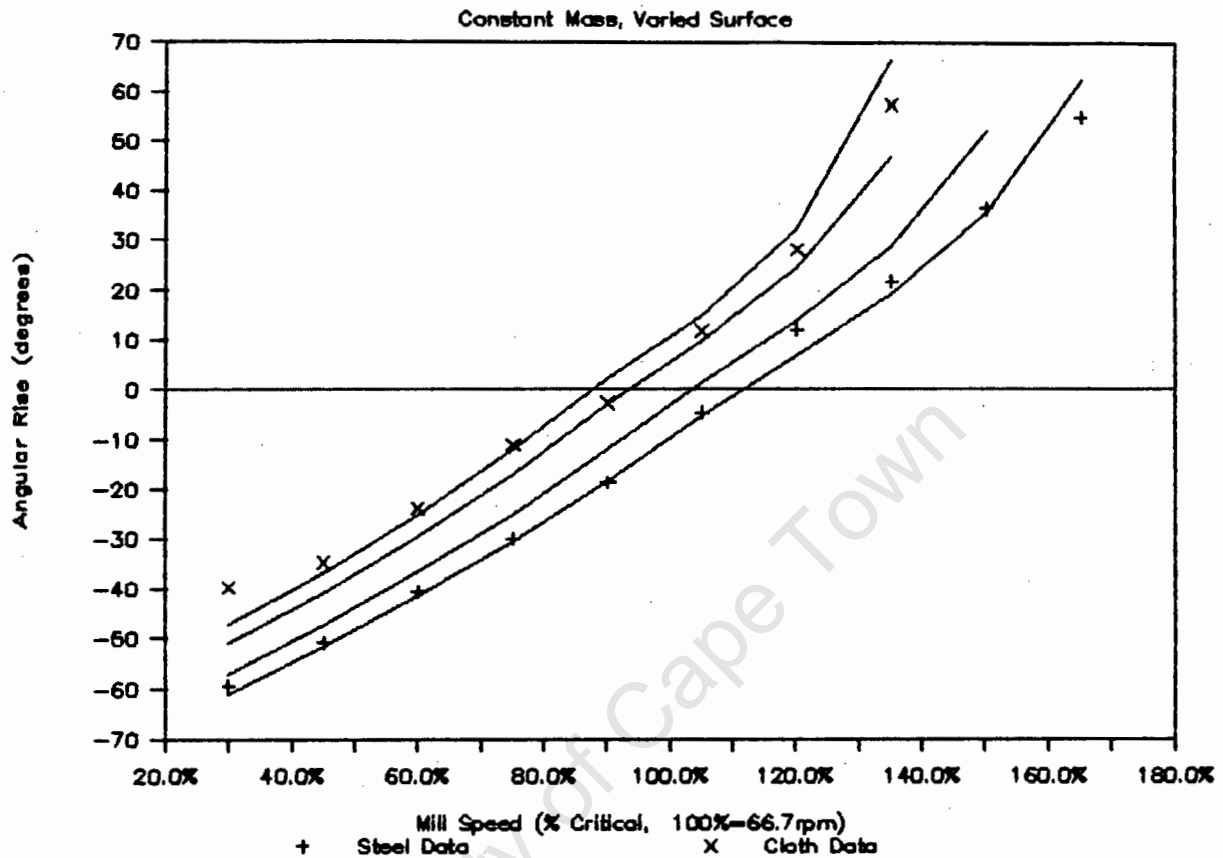


Figure 5.3: Graph of Angular Rise versus Mill Speed, with the mean sample values and the theoretical predictions.

Figure 5.3 contains a plot of experimental results and the theoretical predictions. The experimental results are the mean values contained in appendix 7. The theoretical curves were obtained from the numerical solution of the governing sliding equation and using a value of μ within the limits of experimental uncertainty. In each case the top curve corresponds to the upper limit in the experimentally determined μ and the bottom curve to the lower limit. There is good agreement between the theoretical predictions and the experimental results. Two points of note that fall well outside of the uncertainty band, are the $\Omega_m=150\%$ on the steel lining and the $\Omega_m=30\%$ on the cloth lining.

An explanation for the lower than predicted value of the $\Omega_m=150\%$, is that the block's initial velocity, $\dot{\theta}$ at $\theta=-90^\circ$, was less than the mill velocity. During the experimentation the blocks were released, from rest,

at angles less than -90° . This was done so that when they reached -90° , the block would have accelerated up to, and achieved, mill speed. As the mill speed was increased, the blocks had to accelerate for a longer time, or distance, before achieving mill velocity. If a block is not placed sufficiently distant from the mill bottom, then particularly on a smooth lining, it will never reach Ω_m and so passes $\theta = -90^\circ$ with $\dot{\theta} < \Omega_m$. For a value of $\dot{\theta} = 88\%$ of Ω_m at $\theta = -90^\circ$, then the theory predicts (with $\mu = 0.2$) that the AOD is 54° . This is a better correlation with the experimental data and explains the apparent anomaly. A similar explanation could be used for the inconsistency at 30% critical on the cloth lining. If the block is released from too high, then $\dot{\theta} > \Omega_m$ at $\theta = -90^\circ$ and the experimental angle of highest rise will exceed the theoretical prediction.

Finally, Figure 5.3 illustrates that the theory developed for a single particle on the inside of a rotating cylinder, does satisfactorily predict a block's departure point. As predicted by the theory and corroborated by the experimental results, the departure angle increases as the coefficient of friction increases. Secondly, the departure angle increases as the speed of rotation increases. It can therefore be concluded that the predicted trends generated by the numerical solution of the sliding equations, are valid.

5.3 Discussion of the Results of the Slip Angle of a Single Block

The results of the investigation into the Angle of Slip (θ_{slip} as defined by equation 3.17) are contained in Figure 5.4. The data is contained in Appendix 7. The two bands represent the 90% confidence interval as obtained from the "T" Tests. The two uncertainty bands increase at the larger mill speeds. This is because the exact slipping point is more difficult to detect as the mill speed increases. Again the increase in the uncertainty occurs outside of the operating range of most mills.

Two trends are illustrated in Figure 5.4. The first is that as the Ω_m increases, so there is an associated increase in θ_{slip} . The coefficient of friction between the cloth surface and the block is larger than between that for the steel surface. So the second noticeable trend is that, as μ increases so θ_{slip} increases. Both of these trends were predicted in the discussion of the theoretical predictions.

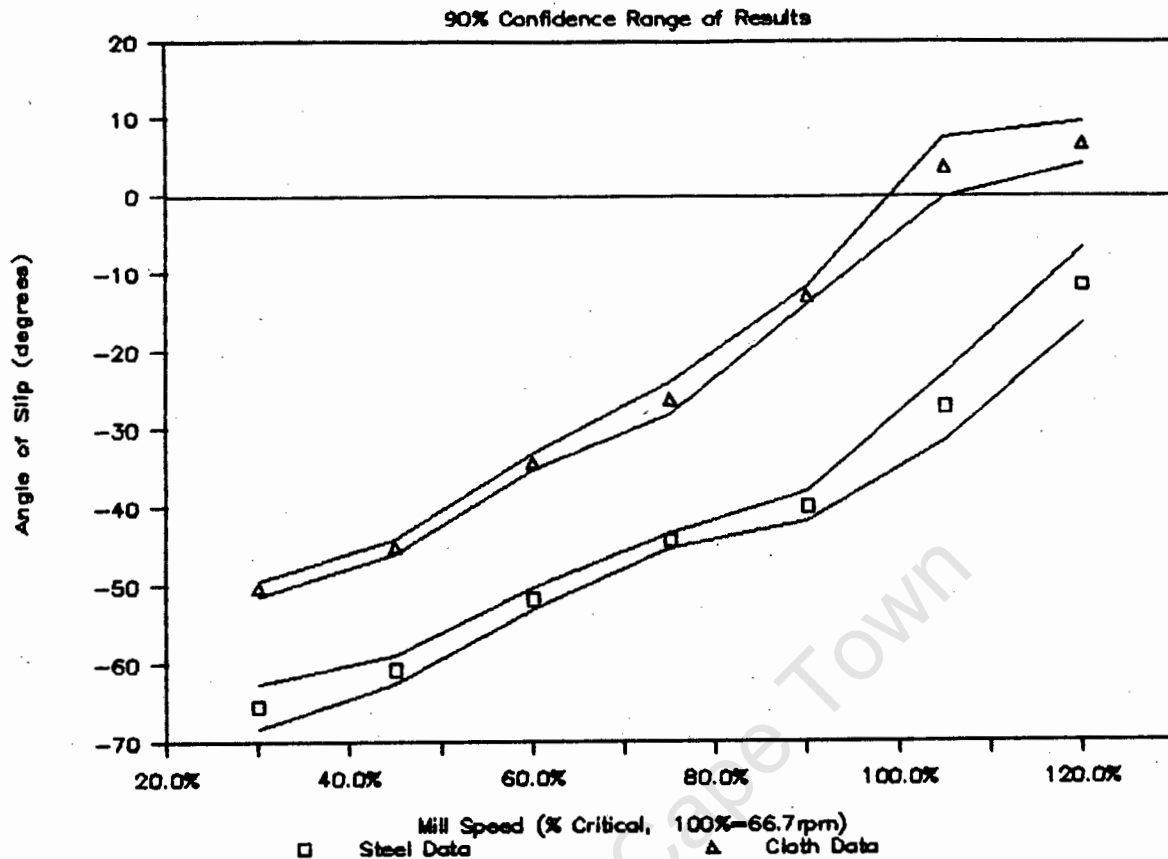


Figure 5.4: Graph of Slip Angle versus Mill Speed

An anomaly arose when the experimental results were compared to the theoretical predictions. The following discussion will explain the anomaly and present the relevant theoretical predictions and experimental results for comparison.

A block moving with the mill will only begin to slip relative to the mill when the limiting friction is exceeded, this occurs at $e = e_{slip}$. Before the block has begun to slip, $\dot{e} = \Omega_m$, while just after it has slipped $\dot{e} < \Omega_m$. After slipping has begun, the block's angular acceleration is negative (down the liner) and so its angular velocity decreases. The block continues to decelerate until one of the possible ending conditions is encountered.

An analysis of the block's displacement relative to the mill's displacement is presented in Figure 5.5. The horizontal axis represents time, with $t=0$ corresponding to the moment the block begins to slip. The particular case presented is that of a block on a steel surface ($\mu=0.2$), with the test drum rotating at 90% critical (60rpm). The data comes from the output

generated by the computerised numerical solution of the Sliding equation. Solving equation 3.17 yields $e_{slip} = -68.7^\circ$ and the numerical solution predicts that the block comes to rest ($\dot{e} = 0$) at $e = -17.9^\circ$.

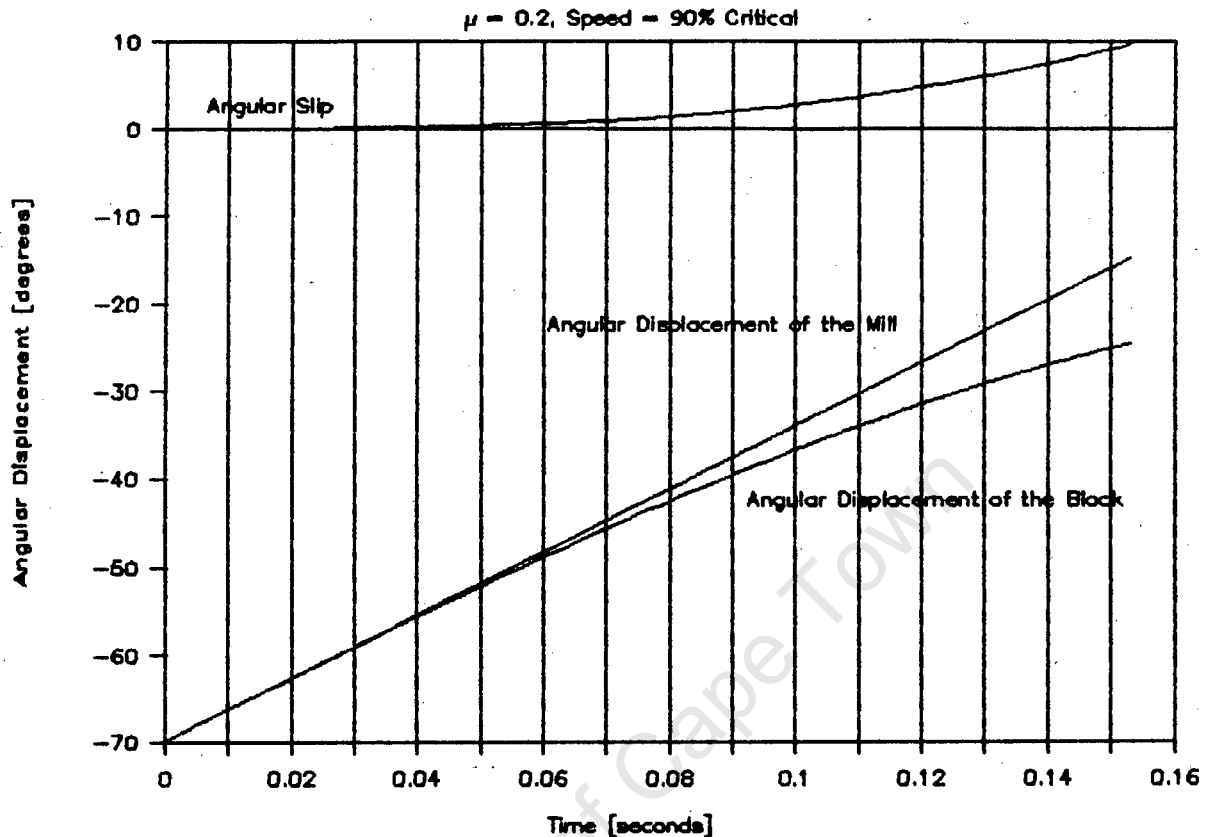


Figure 5.5: Graph of Angular Displacement of a Block and the Mill Liner versus Time

The plot contains three curves, the middle curve is the angular displacement of the mill (Ω_m is constant, hence the curve is a straight line), the bottom curve is the displacement of the block, $e(t)$, while the top line is the Slip of the block relative to the liner. The Slip has been defined as the angular displacement of the mill less the angular displacement of the block ie

$$\text{Slip} = e_{\text{mill}} - e_{\text{block}} \quad \dots(5.3)$$

The video camera used, operates at 25 frames per second, ie one frame corresponds to 0.04 seconds. The information contained in Figure 5.5 is therefore equivalent to approximately 4 frames. If 4 lines are drawn on the graph at times; $t=0.4$, $t=0.8$, $t=0.12$ and $t=0.16$ to represent the four frames, then the data presented in Table 5.2 is obtained.

Time	$\theta(t)$	θ_{slip}	Distance Slipped
0.04s	-55.6°	0.2°	0.5 mm
0.08s	-42.4°	1.4°	4.9 mm
0.12s	-31.4°	4.8°	16.8 mm
0.16s	-23.3°	11.1°	39.1 mm

Table 5.2: Tabulation of Data obtained from Figure 5.5

The tabulated information represents the data that would be obtained from a frame by frame analysis of the recorded video. During the analysis of the film, the Angle of Slip was only recorded when a detectable amount of slipping had occurred. A detectable amount of slip was at least 7.5mm or $\frac{1}{2}$ the width of the block. The slip at 0.04s, would therefore not be noticeable, while the slip at 0.08s might just be detectable. The slipping at 0.12s would certainly have been detected, but $\theta = -31.4^\circ$ would have been recorded as the angle of first slip. The difference between the actual Angle of Slip and the recorded angle is 37° . This illustrates the inherent difficulties incurred with the use of the video, and will explain the anomaly between the experimental data and theoretical predictions.

Tests were conducted on each of the two surfaces to determine the Angle of Slip of a block for varying μ . Figures 5.6 and 5.7 present the results. Figure 5.6 contains the data obtained on the steel lining, the 90% confidence interval has been plotted around the sample means. Figure 5.7 contains the results from the cloth surface. Both figures contain results generated by the numerical solution of the Sliding equation.

Values of $\mu = 0.2$ for the steel surface and $\mu = 0.44$ for the cloth surface were used in the theoretical models. These values were chosen as they are within the experimental uncertainty ranges for the two values and they yielded the best correlation to the experimental data. The three continuous curves denote θ_{slip} (0° of slip), 1° of slip and 5° of slip of the block relative to liner. The data used to plot these curves is also contained in Appendix 7.

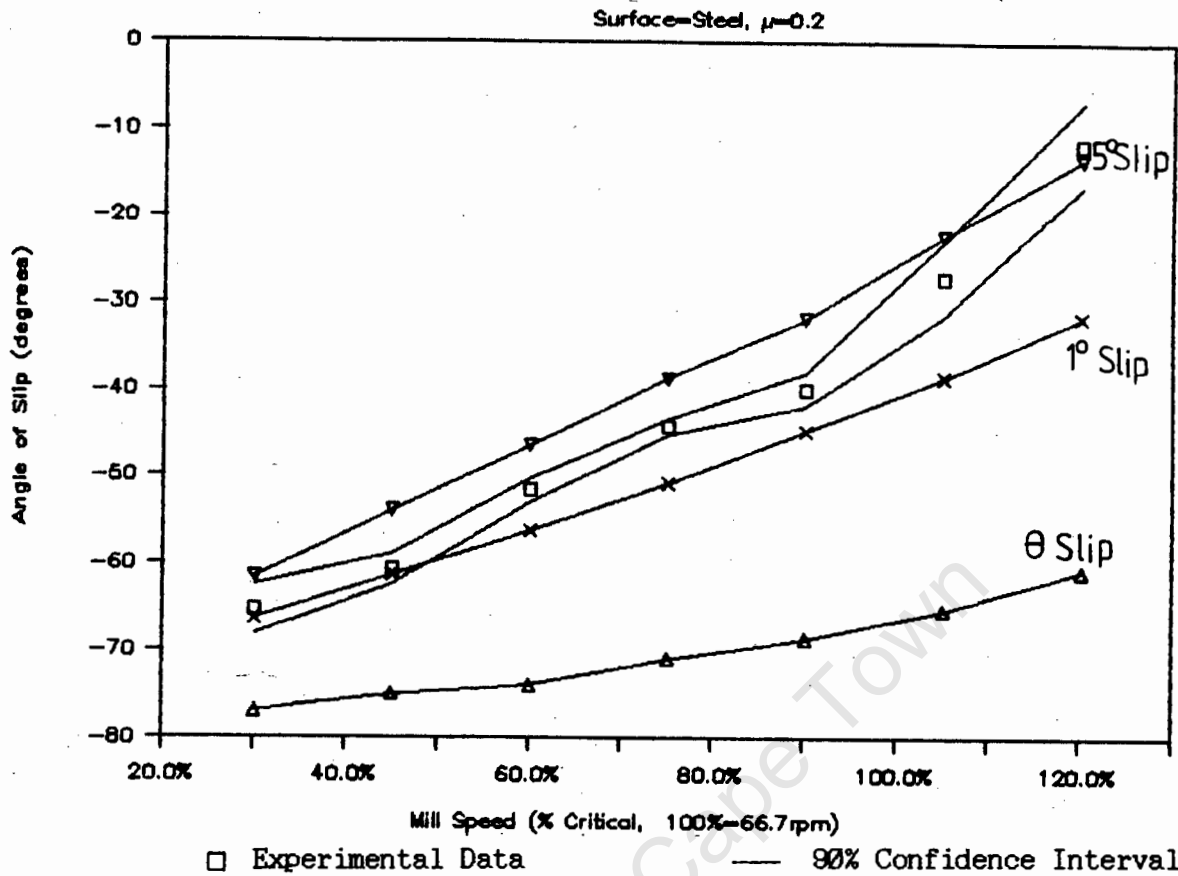


Figure 5.6: Graph of the Slip Angle versus Mill Speed on the Steel Surface

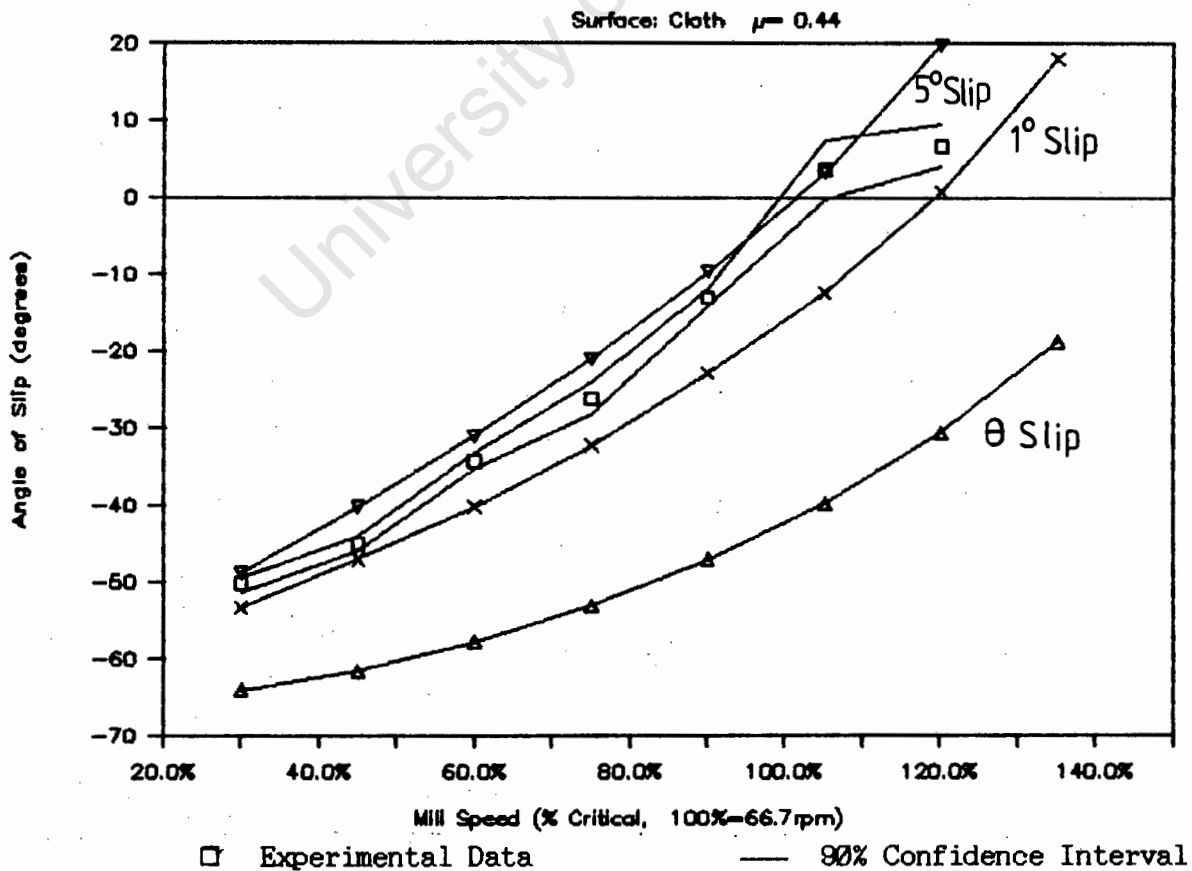


Figure 5.7: Graph of the Slip Angle versus Mill Speed on the Cloth Surface

Examining the two figures it is observed that all of the experimental confidence intervals (within a milling operational range $\Omega_m \leq 80\%$) fall between the 1° and 5° slip lines. None of the data points fall between the 0° and 1° lines. The two graphs illustrate the trends and uncertainties discussed above. The results all fall within the expected uncertainty range (the 1° and 5° slip ranges) and it can be concluded that no other significant experimental error might have been incorporated.

The following conclusions can be drawn from the above discussions:

1. The method employed to measure the Angle of Slip was not appropriate. A better method would be to define Slip as $\Omega_m - \dot{\epsilon}$. This would necessitate the continual measurement of $\dot{\epsilon}$ of the block, which would pose difficulties of its own.
2. The results do fall within the re-predicted theoretical ranges of 1° and 5° of Slip.
3. The ϵ_{slip} visibly detectable in an experimental situation is significantly different to the actual point of slipping. This implies that even though a block may *seem* to be moving without slipping, it may be slipping. This, in turn, suggests that previous measurements of the extent of the abrasion zone in a mill maybe incorrect and that the abrasion zone maybe more extensive.
4. The experimental procedure has highlighted the difficulties in measuring ϵ_{slip} . the theoretical formulation has provided the understanding required to interpret the experimental results. This fact supports McIvors [7] statement in favour of applied mechanics being used to study milling problems, instead of experimental investigations.

5.4 A Brief Discussion of the Experimentally observed Centrifuge Speeds of a Single Block.

One of the ending conditions of a block can have is to become centrifuged to the liner. Davis' original description predicted a constant Critical Velocity, that is only dependent on the mill size, and not on the magnitude of friction. The theory developed in this thesis includes the effects of friction, and is able to predict the centrifuge velocities for smooth liners varying roughness.

Two types of centrifuging have been defined, namely Slipping Centrifuged and Totally Centrifuged. The audio response of the test drum was used to distinguish between the two situations. An empty drum runs almost silent-

ly, because it was axially mounted on roller bearings. The only noise was due to windage. If a particle was added and the particle became Slipping Centrifuged, then it was accompanied by a audible ringing of the drum. The ringing was caused by the block slipping relative to the lining, and causing audible vibrations (a noise) to be emitted. During total centrifuging, there is no motion of the block relative to the lining and so no audio response was detectable.

<u>Velocity Ranges of Centrifuging</u>		
	<u>Slipping Centrifuged</u>	<u>Totally Centrifuged</u>
Steel	165% - 210%	225% - 232%
$\mu=0.2$	> 169%	> 226%
Cloth	135% - 142%	150% - 157%
$\mu=0.44$	> 139%	> 157%

Table 5.3: Tabulation of Experimental and Theoretical Centrifuge Speeds

Table 5.3 contains the ranges of speeds over which the two response were recorded. It was not possible to ascertain the exact speed of the onset of each response, so the approximate range has been presented. The theoretical predictions have been incorporated to allow for comparison to be made with the experimental results. They were evaluated by using the measured coefficients of friction for the two surfaces (steel: $\mu=0.2$ and cloth: $\mu=0.44$). All the mill speeds have been measured as a percentage of the Davis Critical Velocity. The test drum's Davis Critical Velocity is 66.7rpm.

As can be seen from Table 5.3 there is a good correspondence between the theory and experimental data. The uncertainty in the experimental data is because the drum's speed was only increased in 15% of Critical (10 rpm) increments. These results, once again, highlight the inadequacies of the Davis model. It can be concluded that the new formulation can predict the onset and nature of centrifuging occurring to a single block on a surface with a measurable coefficient of friction.

5.5 A Brief Discussion of the Results of the Rolling Scenario

The rolling situation, a ball rolling without skidding, was simulated experimentally with a cylinder rolling on the drum lining. The only alteration to the theory would be to substitute the angular second moment of inertia of a cylinder for that of the sphere.

During experimentation, the cylinder was placed at the bottom of the drum and released without an initial spin, ie $\dot{\theta}(0)=0$ and $\omega(0)=0$. The cylinder started moved with the drum and it began to spin. Once it had reached its apex, it rolled back down the lining and began to oscillate about the bottom of the mill. The prediction that a ball or cylinder, moving without skidding would become a divergent system, did not occur. The cylinder did not continue to rise ever higher, instead it tended to spin faster and "skip" along the lining.

The cylinder's behaviour implies that it might not have been moving without skidding. Re-examining the experimental initial conditions, it is apparent that if a stationary cylinder is introduced onto a moving liner, then initially it has to skid. The skidding would continue as the cylinder's angular velocity increases. There is no provision in the theory for a particle returning to a non-skid situation from a skidding situation. Hence for the present experimental scenario, it is not possible to analyse the motion of cylinder moving without skidding.

A possible test that could examine non-skid motion is as follows. The theory predicts that a high μ is required for the non-skid motion to continue for an observable time duration. If both the cylinder and the lining were coated in latex, then the required coefficient of friction might be attainable.

The difficulty of placing a initially spinning cylinder into a rotating drum could be over come by using a ramp. The ramp would be positioned, so that the cylinder would roll down it and then fall onto the rotating lining. A ramp of sufficient inclination and length could be constructed that would yield the required initial conditions, ie $\omega(0)=f(\Omega_m)$. This type of experimental arrangement might overcome the present difficulties of examining the non-skid rolling motion of a cylinder.

6. CONCLUSIONS AND RECOMMENDATIONS

6.1 Conclusions

At the end of each section of the thesis relevant comments were made and conclusions drawn. The aim of this chapter will be to summarise all the individual observations made throughout the text. The conclusions will be presented in point form in the approximate order they were made.

- i) The formulation derived by Davis [2] has been deemed inadequate by many authors [3,4,9,12]. In particular, the attempt made by Davis to predict the centrifuging velocity (N_c) does not take into account the effect of friction on a particle's motion. The Sliding Model developed by this author emphasises that Davis, by implication, assumes that the frictional force between a single particle and the mill liner is infinite.
- ii) Unlike past formulations, the Sliding model predicts two ways in which a particle can be centrifuged to the liner. The first way is the same as predicted by Davis and is defined as Totally Centrifuged. It occurs when the block's velocity is always equal to the mill velocity, ie a non-slip situation. Slipping Centrifuging is the other type of centrifuging predicted by the model. It is defined as the behaviour of a particle that becomes centrifuged to the liner, but whose velocity is less than the mill's velocity. Slipping Centrifuging is dependent on the magnitude of the frictional force acting between the block and the liner.
- iii) The Pure Rolling model developed is not adequate as it is only valid for the initial motion of a particle rolling along a liner. It breaks down as soon as the spinning ball would skid due to the insufficient friction between the ball and the liner. The model is valid for less than a second for a steel ball on a steel liner. Furthermore, the time period before it breaks down, decreases if either the mill speed is increased or the coefficient of friction decreases.
- iv) A simple combination of the Pure Rolling and Pure Sliding models does not overcome the inadequacies of the two individual models. The resulting combined model ignores the effects of the ball's spin

on its translational motion. The model that is required would have to incorporate both the effects of the ball's spin and its rotation, about the mill centre, into the final formulation that defines the balls' motion as a whole.

- v) The experimental investigation conducted yielded results that were in good agreement with the theoretical predictions. The trends discussed in section 3.1.5 can be considered to be valid. The three responses of a block; Sliding, Trajectory and Centrifuging, were all reproduced in the experimental testing.
- vi) The response of a block to changes in the coefficient of friction or the mill speed can be summarized as follows. For the Angle of Slip to increase, either the mill speed or the coefficient of friction must increase. Secondly, as the Angle of Slip increases, so the Point of Departure (if it occurs) increases. Associated with the increase in either mill speed or friction is an increase in the block's departure velocity. The larger the block's departure velocity, the further the block catarracts across the mill.
- vii) The experimental procedure used to measure the Angle of Slip was inadequate. It highlighted the difficulties of visually estimating when the relative velocity of two particles is non zero, by observing their relative displacements. The results indicate that previous investigators' measurements of slip might have been an under estimation of the true extent of the phenomena. The experimental results from this investigation indicated that slip occurs for approximately 30° before it is detected. The conclusion that can be drawn is that the abrasion zone may be larger than previously estimated.
- viii) The two types of centrifuging were both reproduced in the experimental situation. There was good agreement between the theoretical predictions and the experimental data. From this it can be concluded that the Sliding model provides an improved method for estimating the Centrifuge velocity of a single particle on surfaces of varying roughness.

6.2 Recommendations

The work contained in this thesis modelled the motion of a single particle on a smooth surface. This leads to two obvious areas where the model can be extended. They are to model the motion of more than one particle and to model the motion of a single particle on a unsmooth liner. These two topics will be discussed as well as the idea of developing a combined model for the behaviour of the block.

The first area that will be a logical extension of the developed theory is to add a second block or ball to the present model. When a block is added a reaction force will be introduced between the two particles because of their contact. Initially, when the particles are moving without sliding ($\dot{\theta} = \Omega_m$), then the force between the particle will be zero. Once the upper block has started to slip, it will retard the motion of the second block, while the lower block will provide an extra "push" to the upper block. The system of equations should be coupled and will need to be solved simultaneously. By adding extra blocks, the crowding or bunching action of the 'en masse' region will be modelled. This will permit a greater understanding of charge motion at the Point of Departure.

Another way in which the system could be transformed from a single to a multi particle system is to add balls instead of blocks. The extension will initially be the same as the extension to the block model. But instead of having only a reaction force between the two balls, there will also be a frictional force between the two balls. This is due to counter rotation occurring at the contact point between the balls. Once the system with two or three balls is understood, then a second layer of balls could be added. This process of adding additional balls will eventually permit the layer nature and dynamic pressure of the 'en masse' region to be modelled.

The second area where the Sliding model can be extended to, is to transform the smooth cylindrical liner into a corrugated liner. The type of liner shapes used in industry vary from sinusoids to ribbed. The modelling of a liner is relatively simple. The liner shape is periodic and so it is suited to a Fourier Analysis. Once the Fourier Analysis is completed, the resulting equation is "wrapped" around the circumference of the mill. Figure 7.1 contains a liner which is sinusoidal.

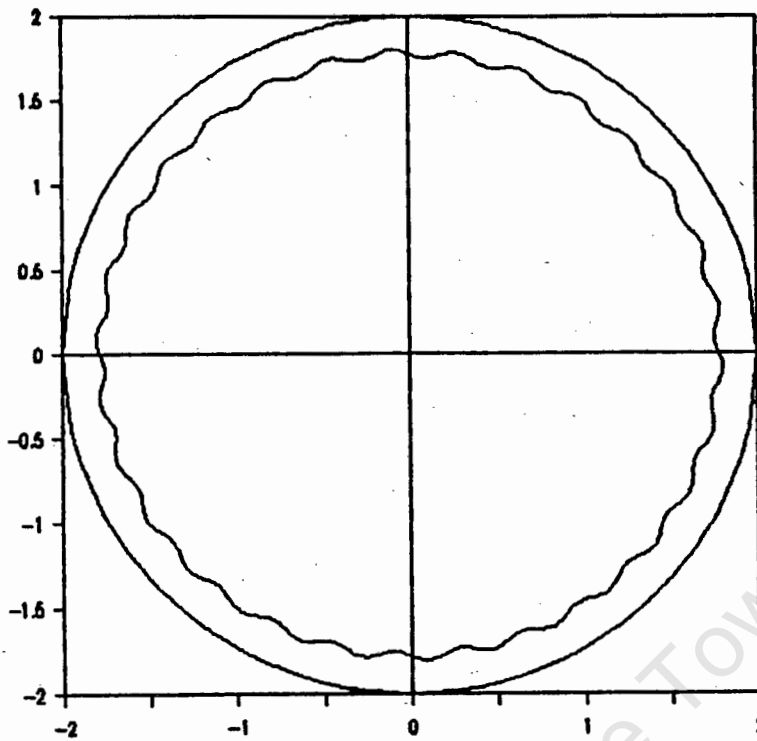


Figure 7.1: Mill with a Sinusoidal Liner Shape.

The next stage is to calculate the normal (a perpendicular line to the liner surface) to the surface at every point. This is done by using calculus and finding the Gradient to the liner surface. Once this is done, the system reduces to a situation that is very similar to that modelled by Powell [10]. Use could be made of the solved equations developed by Powell for a particle moving along a rotating lifter bar. In this way the effect of varied shaped liners on the motion of a single block could be analysed.

7. REFERENCES

1. White, H. A., "The Theory of the Tube Mill." The Journal of the Chemical, Metallurgical and Mining Society of South Africa. May, 1905 pp. 290-305.
2. Davis, E. W. "Fine Crushing in Ball Mills." Trans. of the American Inst. of Mining and Metallurgical Engineers. 1919, Vol. 61, pp 250-296.
3. Haultain, H. E. & Dyer, F. C., "Ball Paths in Tube Mills." Canadian Institute of Mining and Metallurgy Transactions, 1922, Vol. 25, pp 276-291
4. Gow, A. M., Campbell, A. B. & Coghill, W. H., "A Laboratory Investigation of Ball Milling." AIME Trans., October 1929, pp 51-81.
5. Fahrenwald, A.W. and Lee, H.E. "Ball Mill Studies", AIME Technical Publication No. 375, 1931.
6. Rose, H.E. and Sullivan, R. M. Ball, Tube and Rod Mills. Constable, London, 1958.
7. McIvor, R.E. "Effects of Speed and Liner Configuration on Ball Mill Performance." Mining Engineering, June 1983, pp 617-622.
8. Vermeulen, L. A.; Ohlson De Fine, M.J. and Schakowski, F. "Physical information from the inside of a Rotary Mill." J. S. Afr. Inst. Min. Metall., Vol. 84, no. 8, August 1984. pp 247-253 .
9. Vermuelen, L.A. "The Lifting Action of Lifter Bars in Rotary Mills." J. S. Afr. Inst. Min. Metall., 1985, Jan. pp 51-63.
10. Powell, M.S. The Effect of Liner Design upon Charge Motion in a Rotary Mill, MSc Dissertation, University of Cape Town, September 1988.
11. Gross, J. Crushing and Grinding. U.S.A. Department of the Interior, Bureau of Mines, 1938

12. Hukki, R.T. "Grinding at Supercritical Speeds in Rod and Ball Mills" Progress of Mineral Dressing, Trans. of 10th Int. Mineral Dressing Congress, Stockholm, 1958. In: Svensta Gruvgr reningen and Jernkontoret. Almqvist and Wiksell, Stockholm, pp 85-122.
13. Manz, R. "Experimental investigation into the slip of the charge of grinding medium in ball mills." Dechema Monographien Vol. 68 No. 1282-1326. 1972 pp 721-749. Mintek Translation from German, TR 1174.
14. Vermuelen, L.A. and Howat, D.D. "Effects of Lifter Bars on the Motion of 'En Masse' Grinding Media in Milling." Int. J of Mineral Processing. 1988, Vol 24, pp 143-159.
15. Henein, H.; Brimacombe, J.K. and Watkinson, A.P. "The Modeling of Transverse Solids Motion in a Rotary Kilns." Metallurgical Transactions B, Vol. 14B, June 1983, pp 207-220.
16. Vermuelen, L. A. and Howat, D.D. "Fluctuations in the slip of the Grinding Charge in Rotary Mills with Smooth Liners." Int. J. Miner. Process. 1986, Vol 16 pp 153-168.
17. Henein, H., Brimacombe, J.K. and Watkinson, A.P. "An Experimental Study of Segregation in Rotary Kilns." Metallurgical Trans. B: Vol. 16B, December 1985, pp 763-774.
18. Nityanand, N.B., Manley, B. and Henein, H. "An Analysis of Radial Segregation for different sized Spherical Solids in Rotary Cylinders." Metallurgical Trans. Vol. 17B, June 1986 pp 247-257.
19. Gerald, C. and Wheatley, P. Applied Numerical Analysis, 1984, Addison-Wesley Publishing Co.

8. BIBLIOGRAPHY

8.1 General Section

- Bignell, J.D. and Newton, S. "Recent Progress in Solids Processing: Comminution - A review." Chem Eng Res Des, Vol. 64, March 1986, pp 91-93.
- Bradley, A.A.; Hinde, A.L. and Lloyd, P.J. "The Determination of the Efficiency of the Milling Process." J. S.A. Inst. Min. Metall. June 1972, pp 277-281.
- Convey, R.F. "Attrition Milling of Industrial Minerals", Mineral and Resource Technology, Mountainside, New Jersey.
- Gross, J. Crushing and Grinding. U.S.A. Department of the Interior, Bureau of Mines, 1938
- Hoyer, D.I. "Particle Trajectories and Charge Shapes in Centrifugal Milling." Int. Conf. on Mineral Science and Technology "Mintek 50" 1985 Vol. 1 pp 401-409.
- Luckier, P. and Austin, L. Coal Grinding Technology. U.S.A. United States Energy Research and Development Administration
- Lynch, A.J.; Whiten, W.J. and Narayanan, S.S. "Ball Mill Models: Their Evolution and Present Status." Advances in Mineral Processing: A Half Century of Progress in Application of Theory to Practice. Proceedings of a Symposium Honoring Nathaniel Arbiter on his 75th Birthday. Publ. by: Soc. Mining Engineers of AIME. 1986 pp 48-66.
- Meaders, R. C. & MacPherson A.R., "Technical Design of Autogenous Mills." Mining Engineering (Canada), September 1964, pp 81-83
- Moys, M.H. "The control of Autogenous and Semi-autogenous Mills: The relationship between measurements of Bearing Pressure and parameters describing the Mill Load." J. S. Afr. Inst. Min. Metall., Nov. 1980, pp 401-408.

8.2 Motion of Charge in a Tube Mill (Wet and Dry)

Beke, B. Tumbling Ball Mills, The Process of Fine Grinding. Chp. 12, pp 74-83. Nijhoff and Junk Publishers, The Hague. 1981.

Davis, E. W. "Fine Crushing in Ball Mills." Trans. of the American Inst. of Mining and Metallurgical Engineers. 1919, Vol. 61, pp 250-296.

Fahrenwald, A.W. and Lee, H.E. "Ball Mill Studies", AIME Technical Publication No. 375. 1931.

Gow, A. M., Campbell, A. B. & Coghill, W. H., " A Laboratory Investigation of Ball Milling." AIME Trans., October 1929, pp 51-81.

Haultain, H. E. & Dyer, F. C., " Ball Paths in Tube Mills." Canadian Institute of Mining and Metallurgy Transactions. 1922, Vol. 25, pp 276-291

Henein, H.; Brimacombe, J.K. and Watkinson, A.P. "The Modeling of Transverse Solids Motion in a Rotary Kilns." Metallurgical Transactions B, Vol. 14B, June 1983, pp 207-220.

Henein, H., Brimacombe, J.K. and Watkinson, A.P. "An Experimental Study of Segregation in Rotary Kilns." Metallurgical Trans. B: Vol. 16B, December 1985, pp 763-774.

Hukki, R.T. "Grinding at Supercritical Speeds in Rod and Ball Mills" Progress of Mineral Dressing, Trans. of 10th Int. Mineral Dressing Congress. Stockholm, 1958. In: Svensta Gruvgröningen and Jernkontoret. Almqvist and Wiksell, Stockholm, pp 85-122.

Liddell, K.S. and Moys, M.H. "The Effects of Mill Speed and Filling on the behaviour of the Load in a Rotary Grinding Mill." J. S. Afr. Inst. Min. Metall., vol 88, no. 2, Feb 1985, pp 49-57.

Manz, R. "Experimental investigation into the slip of the charge of grinding medium in ball mills." Dechema Monographien Vol. 69 No. 1292-1326. 1972 pp 721-749. Mintek Translation from German, TR 1174.

McIvor, R.E. "Effects of Speed and Liner Configuration on Ball Mill Performance." Mining Engineering, June 1983, pp 617-622.

- Moys, M.H. and Montini, A. "The dynamic behaviour of the load in a pilot ball mill as a function of axial position and design and operating variables." 13th CMMI Congress-Metallurgy Vol. 4 pp 17-24.
- Nityanand, N.B., Manley, B. and Henein, H. "An Analysis of Radial Segregation for different sized Spherical Solids in Rotary Cylinders." Metallurgical Trans. Vol. 17B, June 1986 pp 247-257.
- Powell, M.S. The Effect of Liner Design upon Charge Motion in a Rotary Mill, MSc Dissertation, University of Cape Town, September 1988.
- Rose, H.E. and Sullivan, R. M. Ball, Tube and Rod Mills. Constable, London, 1958.
- Vermeulen, L. A.; Ohlson De Fine, M.J. and Schakowski, F. "Physical information from the inside of a Rotary Mill." J. S. Afr. Inst. Min. Metall., Vol. 84, no. 8, August 1984. pp 247-253 .
- Vermeulen, L.A. "The Lifting Action of Lifter Bars in Rotary Mills." J. S. Afr. Inst. Min. Metall., 1985, Jan. pp 51-63.
- Vermeulen, L. A. and Howat, D.D. "Fluctuations in the slip of the Grinding Charge in Rotary Mills with Smooth Liners." Int. J. Miner. Process. 1986, Vol 16 pp 153-168.
- Vermeulen, L.A. and Howat, D.D. "Effects of Lifter Bars on the Motion of 'En Masse' Grinding Media in Milling." Int. J of Mineral Processing. 1988, Vol 24, pp 143-159.
- White, H. A., " The Theory of the Tube Mill." The Journal of the Chemical, Metallurgical and Mining Society of South Africa. May, 1905 pp. 290-305.

8.3 Effects of Liner Configuration

Fuerstenau, D.W. and Abouzeid, A.Z.M. "Scale Up of Lifters in Ball Mills." Int. J. Miner. Process. 1985, 15: pp 183-192.

Howat, D.D. and Vermeulen, L.A. "The Effects of changes in liner design and mill speed on rod-mill parameters", Council for Mineral Technology, South Africa. Paper A2/4, No. 9596.

Howat, D.D. "A comparative study of the effects of changes in liner patterns and mill speeds on rod-mill parameters." Council for Mineral Technology, 1982. Report No. M6.

Howat, D.D. "Reduction in metal consumption by the use of alternating lines of higher and lower lifter bars in a rod mill", Council for Mineral Technology, 1983, Report No. M97.

Howat, D.D. and Vermeulen, L.A. "The Design of Lining for Rotary Mills: A Major Factor in Throughput and Consumption of Energy and Metal." J. S. Afr. Inst. Min. Metall. 1986, July, pp 251-259.

8.4 On Site Testing of Milling Variables

Fitch, J.H. "Effects of ball charge on mill output - 4B mill." C.E.G.B. Internal Report, Eggborough Power Station. March 1985, (R7C/92).

Fitch, J.H. "Effects of using two sizes of balls as make up on Unit 4 mills." C.E.G.B. Internal Report, Eggborough Power Station. May 1987, (R7D/118).

Todd, A.D. "The effect of a change in the ball charge size spectrum upon the performance of a "Foster Wheeler -D8" tumbling mill." C.E.G.B. Internal Report, N.E. Region, November 1973, (SSD/NE/N82).

Todd, A.D. "Further investigations into the relationship between the ball charge size spectrum and performance of a tumbling mill." C.E.G.B. Internal Report, N.E. Region, April 1974, (SSD/NE/N98)

Ready, A.B. "Cottam Mills:- Effects of ball make up and ball hardness on the variation of ball size distribution with time." C.E.G.B. Internal Report, Midlands Region, May 1977 (0540/77/CS)

APPENDIX 1: Resume of Reviewed Literature

<u>Ref</u>	<u>Author</u>	<u>Year</u>	<u>Nature of Contribution</u>
A1.1	<u>Ball Paths and Trajectories in a Tube Mill.</u>		
1	White, H.A.	1905	Contains experimental investigation and first theoretical modelling. Results using photography.
2	Davis, E.W.	1919	Contains theoretical modelling of ball paths, substantiated by experimental results. Results using photography.
3	Haultain, H.E. Dyer, F.C.	1922	Only experimental. Results obtained using photography.
4	Gow, A.M. Campbell, A.B. Coghill, W.H.	1929	Contains theoretical modelling of ball paths including the effects of crowding. Experimental results from photography.
5	Fahrenwald, A.W. Lee, H.E.	1931	Contains theoretical modelling, including friction induced ball spin. Experimental results from batch tests
6	Rose, H.E. Sullivan, R.M.	1958	A book that covers most areas of milling. Theoretical modelling is presented on ball paths and charge shapes. Experimental results from batch tests or referenced results.
7	McIvor, R.E.	1983	Theoretical modelling of ball paths including the effects of lifter face angle.
8	Vermeulen, L.A. Ohlson De Fine, M. Schakowski, F.	1984	Theoretical modelling of ball paths including the effects of adhesion. Experimentation by using a piezo-electric sensor placed in liner.
9	Vermeulen, L.A.	1985	Theoretical modelling of rod paths, including the effects of lifter bars. Experimentation done using high speed cinema-tography.
10	Powell, M.S.	1988	Theoretical modelling of rod paths including the effects of changes in lifter bar face angle. Experimentation done by high speed cinema-tography.
A1.2	<u>Charge Slippage in a Tube Mill.</u>		
3	Haultain, H.E. Dyer, F.C.	1922	Only experimental. Results obtained using photography.
4	Gow, A.M. Campbell, A.B. Coghill, W.H.	1929	Experimental investigation into centrifuge (critical) velocities as effected by slip and percentage fill. Experimental results from photography using a batch test mill.

- | | | | |
|----|---|------|---|
| 11 | Gross, J. | 1938 | Contains experimentation on slip. Observations made through an end-plate on a test mill. |
| 12 | Hukki, R.T. | 1958 | Contains theoretical modelling of ball mechanics. Experiments done on a batch test mill. |
| 13 | Manz, R. | 1972 | Contains experimental results on slip in a mill. Experimentation done by inserting electrical probes into the mill. |
| 14 | Henein, H.
Brimacombe, J.K.
Watkinson, A.P. | 1983 | Theoretical modelling of the motion of charges in rotary kilns. Various types of motion are defined. Experimental results by photographs and a partitioning device. |
| 15 | Vermuelen, L.A.
Howat, D.D. | 1988 | Theoretical modelling of the 'en Masse' region with the development of an expression for dynamic pressure. Experimentation done using high speed cinematography, with the effect of parallax being accounted for. |

A1.3 Charge Surge in a Tube Mill.

- | | | | |
|----|--------------------------------|------|--|
| 6 | Rose, H.E.
Sullivan, R.M. | 1958 | Theoretical modelling is developed on the surging in a mill. Experimental results are referenced to other experimenters. |
| 16 | Vermuelen, L.A.
Howat, D.D. | 1986 | Theoretical modelling of the surge of a mill charge using rods. Experimentation done using high speed cinematography. |

A1.4 Radial Segregation in a Tube Mill.

- | | | | |
|----|---|------|---|
| 17 | Henein, H.
Brimacombe, J.K.
Watkinson, A.P. | 1985 | Experimental investigation of segregation in kilns. Photograph and a radial partitioning device within the mill. |
| 18 | Nityanand, N.B.
Manley, B.
Henein, H. | 1986 | Experimental investigation into the characteristics of radial segregation of a mill charge. High speed cinematography was used. |

Notes: i) "Contains" implies that the reference covers more areas than referred to in this report.
ii) Articles appearing in two sections are referenced in both sections.

APPENDIX 2: Resume of Mathematical FormulationsA2.1 Ball Paths and TrajectoriesWhite [1] 1905

Balance of Forces (See Fig. 2.1)

$$m\Omega_m^2 \rho = mgsin\theta + R$$

Critical Velocity: $\dot{\theta}c^2 = g/\rho$ rad/s or $N_c = \frac{29.9}{\sqrt{\rho}}$ rpmDavis [2] 1919Parabolic trajectory with origin at POD. [$\alpha = \text{POD}$] (See Fig. 2.4)

The equation of the parabola trajectory is:

$$y = x \tan(\alpha) - \frac{gx^2}{2V^2 \cos^2(\alpha)}$$

Point of Impact (or the Point of Return) will have coordinates

$$x = 4\rho \cos\alpha \cdot \sin^2\alpha$$

$$y = -4\rho \cos^2\alpha \cdot \sin\alpha$$

Gow et al [4] 1929Constant velocity of ascent: $y = \frac{V^2}{g} \left[\ln\left(\cos\left(\beta - \frac{57.29gx}{V^2}\right)\right) - \ln(\cos\beta) \right]$ At highest point ($dy/dx=0$): $x = V^2\beta/g$
 $y = 2.3025(V^2/g)\log\sec\beta$

From this point, until contact, a parabolic path is assumed

Fahrenwald and Lee [5] 1931

Forces acting at P.O.D., including friction induced spin

$$F_1 + F_4 \left(\frac{R-r}{(R^2+2r^2-2Rr)^{1/2}} \right) + mgsin\alpha = \frac{QV^2}{R-r}$$

 $F_1 = \text{Centripetal Force}$ $F_4 = \text{Friction} = \mu mgsin\alpha$ $V = \text{Ball Velocity}$ If $R \gg r$ and at the P.O.D. $F_1 = 0$, then:

$$V^2 = g(R-r)(\mu sin\alpha + \cos\alpha)$$

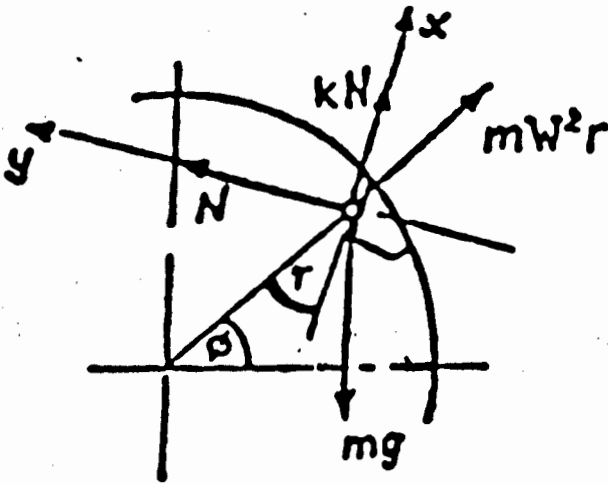
Hence a measure of slip (for a particular α) can be analysed.

Von Steiger using a similar formulation as Gow et al:

Coordinates as apex: $y_s - y_o = (V^2/g)\log\sec\alpha_o$

$$x_s - x_o = (V^2/g)\alpha_o$$

McIvor [7] 1983



A Force Balance yields:

$$\Sigma x: \mu N + mR\Omega_m^2 \cos\tau - mg\sin(\phi - \tau) = 0$$

$$\Sigma y: N - mR\Omega_m^2 \sin\tau - mg\cos(\phi - \tau) = 0$$

where: τ = Tilt of lifter

μ = Coeff. of Friction

N = Normal to lifter face

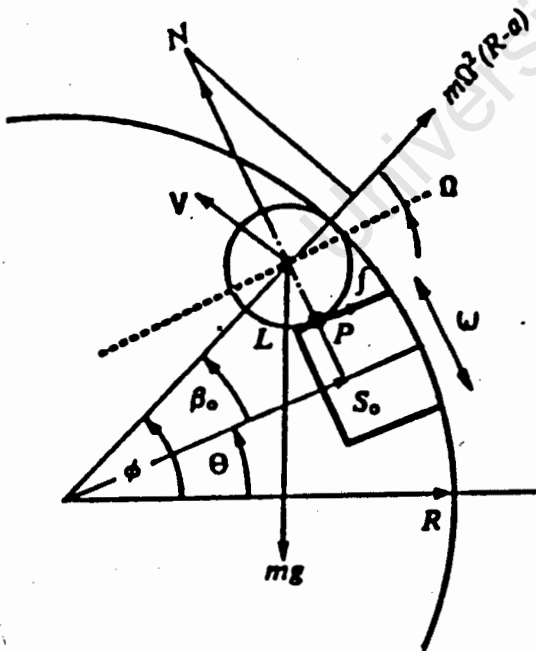
e = Angle of Friction

$$= \arctan(\mu)$$

Solving for ϕ , ($\phi = \text{AOD}$):

$$\phi = \arcsin\left\{\left[\frac{R\Omega_m^2}{g}\right]\cos(e - \tau)\right\} + (e - \tau)$$

Vermuelen et al [9] 1985



A Force balance on a rod yields:

$$\Omega_m^2(R-a)(\cos\beta_o - \mu\sin\beta_o) - g(\sin e_o - \mu\cos e_o) = 0$$

Boundary conditions:

- i) $t=0$ at $e=e_o$
- ii) $t=t_L$ when rod on lifter edge

For Sliding Motion:

$$\frac{d^2s}{dt^2} = \Omega_m^2 s + g(\mu\cos\phi - \sin\phi) - \Omega_m^2 \delta$$

where: $\phi = \Omega t + e_o$

$$\delta = \mu\sin\beta = \mu(a + \frac{1}{2}w)$$

Boundary Conditions:

$$s(0) = (R-a)\cos\beta$$

$$\frac{ds}{dt}(0) = 0$$

Solving for s yields:

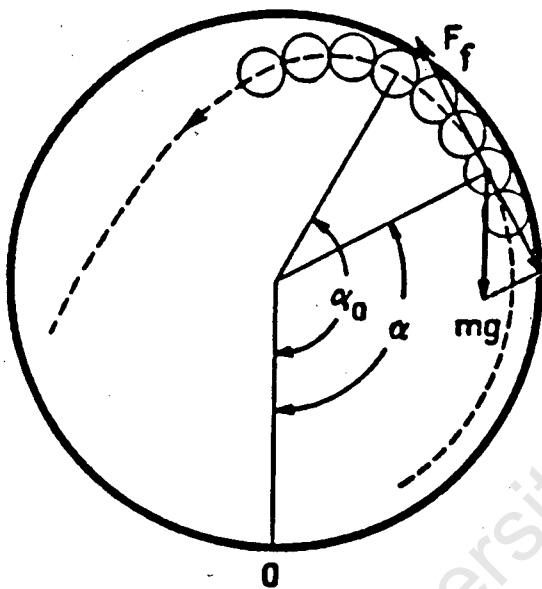
$$s(t) = [s(0) - \delta + \{g/2\Omega_m^2\}(\mu \cos e_0 - \sin e_0)] \cosh \Omega_m t - \{g/2\Omega_m^2\}[(\mu \sin e_0 + \cos e_0) \sinh \Omega_m t + \{\mu \cos A - \sin A\}] + \delta$$

The rod velocity relative to the lifter is given by ds/dt which can be evaluated from s(t) and yields:

$$ds/dt = \Omega_m [s(0) - \delta + (\mu g \cos e_0 - g \sin e_0) / 2\Omega_m^2] \sinh \Omega_m t - (g/2\Omega_m) [(\mu \sin e_0 + \cos e_0) \cosh(\Omega_m t + e_0) - \{\mu \sin(\Omega_m t + e_0) + \cos(\Omega_m t + e_0)\}]$$

A2.2 CHARGE SLIPPAGE

Hukki [12] 1958



Frictional Force:

$$F_f = \frac{\Phi(n_0 - n)(mg \cos \alpha + M\Omega_m^2 R)}{n_0}$$

where: m = Ball Mass

M = Large Effective Mass

n_0 = mill speed

n = ball speed

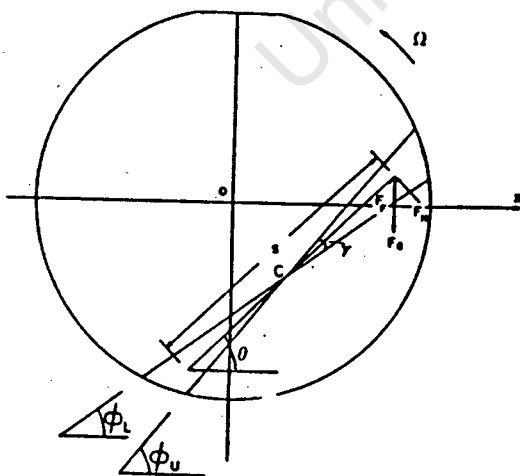
Phi = proportionality constant

After integrating alpha from 0 to alpha_0,

The following expression is

obtained: $\frac{n_0}{n_c} = \frac{1}{1 - \left(\frac{2m}{mM\Phi}\right)}$

Henein et al [14] 1983



A: Slipping/Rolling boundary

$$d^2s/dt^2 = g(\sin e - \mu \cos e)$$

Boundary Conditions: i) t=0 when V=0

ii) t=0 when s=0

The time required to replenish the

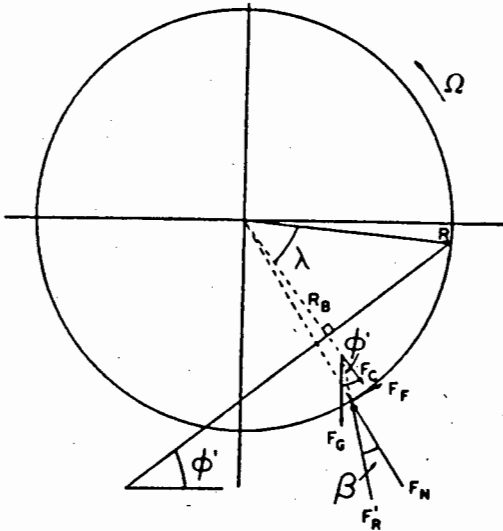
wedge is: $t_0 = (30/\pi)\{\tau_0/\Omega\}$

where: $\tau = \phi_u - \phi_L$

Solving yields:

$$1 - \frac{1}{2} \frac{(gR)}{V^2} \left(\frac{R}{s} \right) \left(\frac{300\tau_0^2}{V^2} \right) (\sin e - \tan \phi_L \cos e) = 0$$

Froude number Material Parameters
 Scale Up factor (% fill)



B: Slipping Conditions

$$\tan \phi_s = A - \{\cos(\arcsin[A])\}^{-1}$$

where:

ϕ = Bed Inclination

ϕ_s = Slip Angle

ϕ_u = Upper angle of Repose

ϕ_d = Dynamic angle of Repose

$$A = (R_b/R) [F_g \sin \phi] \{F_c^2 + 2F_c F_g \cos \phi + F_g\}^{-1/2}$$

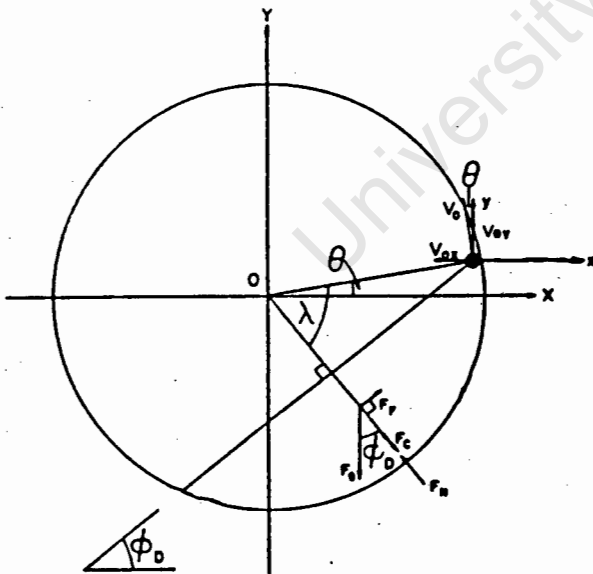
If $\phi > \phi_u > \phi_d$ then no slipping occurs

$\phi_u > \phi > \phi_d$ then slipping occurs rather than slumping

$\phi_u > \phi_d > \phi$ then the bed only slips, (no other type of motion)

C: For Rolling: compare ϕ to ϕ_d and F_c is negligible

$$\text{Hence: } \tan \phi = \frac{3 \tan \phi (\lambda - \cos \lambda \sin \lambda)}{2 \sin^3 \lambda}$$



D: Cascading/Cataracting Conditions

If ϵ (the A.O.D. measured from the bottom of the mill) $\epsilon > \theta$ then V_0 is angled inwards and ball can depart from charge body. Hence the boundary between cascading and cataracting occurs at $\epsilon = \theta$.

Hence, for this condition:

$$\Omega_{r/c}^2 R = \left(\frac{3g}{2} \left[\frac{\tan \phi_d}{\mu_d} - 1 \right] \left[\frac{\frac{1}{2}\pi - \phi_d - \tan \phi_d}{\cos^2 \phi_d} \right] \right)$$

E: Centrifuging of Charge:

$$N_c = \frac{\{30\} (2g)^{1/2}}{\pi D}$$

By definition $\Delta V = V_J - V_0$; where: V_J is velocity at time $t = t_J$

$$\begin{aligned}
 \text{Hence: } V_J &= V_0 + c\Delta p_d \\
 &= V_0 + c(\rho_0\Delta f + f_0\Delta\rho) \\
 &= V_0 + c\left[\rho_0\left(\left(\frac{df}{d\alpha}\right)_0 \cdot \Delta\alpha + \left(\frac{df}{d\lambda}\right)_0 \cdot \Delta\lambda\right) + f_0\Delta\lambda\right]
 \end{aligned}$$

$$\text{where: } \Delta\alpha = \alpha_J - \alpha_0$$

$$\Delta\lambda = \lambda_J - \lambda_0$$

$$\Delta\rho = \rho_J - \rho_0$$

University of Cape Town

APPENDIX 3: Solution of the Sliding Governing Equations using an Euler Forward.

The decomposition of the one 2nd Order Differential Equation (Equation 3.11) into two 1st Order equations, can be done as follows:

$$\ddot{\theta} \rho - \mu_k \dot{\theta}^2 \rho + g(\mu_k \sin \theta + \cos \theta) = 0 \quad \dots (3.11)$$

$$\text{Let } \dot{\theta} = \phi \quad \dots (A3.1)$$

$$\therefore \ddot{\theta} = \dot{\phi} \quad \dots (A3.2)$$

$$\therefore \dot{\phi} = \mu_k \dot{\theta}^2 - \frac{g(\mu_k \sin \theta + \cos \theta)}{\rho} \quad \dots (A3.3)$$

Equations (A3.1) and (A3.3) make up the system of first order differential equations that are solved simultaneously.

The Euler Forward Step is of the form [19]:

$$y(x_0 + h) = y(x_0) + hy'(x_0) + \text{Error} \quad \dots (A3.4)$$

where: $y(x)$ is the function value at x

$y'(x)$ is the derivative of the function at x

h is the interval size, $h = x - x_0$

For small h the error term becomes small, so re-writing with subscripts:

$$y_{n+1} = y_n + hy'_n \quad \dots (A3.5)$$

Using the Euler Forward Step to numerically approximate the derivatives of the governing equations yields:

$$\dot{\theta}_{n+1} = \frac{d\theta_{n+1}}{dt} \approx \frac{\theta(t+h) - \theta(t)}{\delta t} = \frac{\theta_{n+1} - \theta_n}{h} \quad \dots (A3.6)$$

$$\dot{\phi}_{n+1} = \frac{d\phi_{n+1}}{dt} \approx \frac{\phi(t+h) - \phi(t)}{\delta t} = \frac{\phi_{n+1} - \phi_n}{h} \quad \dots (A3.7)$$

where:

$\theta_{n+1}, \dot{\theta}_{n+1}, \phi_{n+1}, \dot{\phi}_{n+1}$ are the values at time increment $n+1$

$\theta_n, \dot{\theta}_n, \phi_n, \dot{\phi}_n$ are the values at time increment n

$\delta t = h$ is the time increment

At time increment $n=0$ the values of $\theta, \dot{\theta}, \ddot{\theta}$ are known (initial conditions) and hence the values at time increment $n=1$ can be calculated. Therefore at any increment n , one is able to solve (by "stepping forward") for the values at $n+1$. This is the basis of a forward step, numerical solution procedure. Equations (A3.6) and (A3.7) are only valid for small δt or h . The underlying assumption is that the rate of change of the function is linear over a sufficiently small time increment. The size of a suitable h is discussed in Appendix 4.

Substituting (A3.6) and (A3.7) into (A3.1) and (A3.3) yields:

$$\theta_{n+1} = \theta_n + h\dot{\theta}_n \quad \dots (A3.8)$$

$$\ddot{\theta}_{n+1} = \dot{\theta}_n + h\left\{\frac{\mu_k(\dot{\theta}_n)^2 - g\mu_k \sin\theta_n - g\cos\theta_n}{\rho}\right\} \quad \dots (A3.9)$$

The value of $\ddot{\theta}$ at any time increment can be numerically approximated by:

$$\ddot{\theta}_{n+1} = \frac{\dot{\theta}_{n+1} - \dot{\theta}_n}{h} \quad \dots (A3.10)$$

Finally using the above equations the values of R and T can be evaluated at any time.

$$R_{n+1} = m(\dot{\theta}_{n+1})^2 \rho - mg \sin\theta_{n+1} \quad \dots (A3.11)$$

$$T_{n+1} = m(\ddot{\theta}_{n+1}) \rho + mg \cos\theta_{n+1} \quad \dots (A3.12)$$

These four equations (A3.8 - A3.11) are the basis of the algorithm used in the computer program used to analyze the block's motion.

APPENDIX 4: Worked Example of the Numerical Solution of the Sliding Equations

The problem will be worked through using a large time increment. This will result in significant inaccuracies occurring. The convergence of the solution, by reducing the time increment, will be presented and discussed after the conclusion of the worked example.

The Milling parameters used are: $\mu=0.5$ $r=1.5\text{m}$ $m=0.5\text{kg}$ $\Omega_m=30$ rpm $H=0.1\text{s}$
Let the block initially be moving with the mill and start at the mill bottom.

So: $\theta(0) = -90^\circ$; $\dot{\theta}(0) = 30$ rpm = 3.142 rad/s ; $\ddot{\theta}(0) = 0$ rad/s²

Hence the values for N=1 are: $\theta_1=-72.0^\circ$; $\dot{\theta}_1=3.142$ rad/s ; $\ddot{\theta}_1=0$ rad/s²

Using Equations (3.8) & (3.9):

R at the end of time step 1 is: $R_1 = 12.307$ N

T at the end of time step 1 is: $T_1 = 0.0$ N

$\therefore \mu R > T$ and so the block is not sliding

Therefore using equations (3.5), (3.6) & (3.7):

$\theta_2=-54.0^\circ$; $\dot{\theta}_2=3.142$ rad/s ; $\ddot{\theta}_2=0$ rad/s²

Tabulating the results for the time steps:

N	θ	$\dot{\theta}$	$\ddot{\theta}$	R	T	Comments
1	-72.0°	3.142	0	12.307	0.0	$\mu R > T$, \therefore No Sliding
2	-54.0°	3.142	0	12.067	1.516	$\mu R > T$, \therefore No Sliding
3	-36.0°	3.142	0	11.370	2.883	$\mu R > T$, \therefore No Sliding
4	-18.0°	3.142	0	10.285	3.968	$\mu R > T$, \therefore No Sliding
5	0.0°	3.142	0	8.918	4.665	$\mu R < T$, \therefore Sliding

Solving equation (3.18) yields: $\theta_{\text{slip}} = -20.989^\circ$

This numerical solution shows that $-18^\circ \leq \theta_{\text{slip}} \leq 0^\circ$, which exhibits the expected inaccuracy due to the large time increment.

The block has started to slide, so the numerical solutions of the governing differential equations are used from here on. Therefore using Equations (A3.8) to (A3.12):

$\theta_B = 0.0^\circ$; $\dot{\theta}_B = 2.981$ rad/s ; $\ddot{\theta}_B = -1.605$ rad/s² (Note: $\dot{\theta} < \Omega_m$)

and $R_B = 7.402$ N and $T_B = 4.905$ N

$\mu R > T$, so the block continues to slide.

Tabulating the results for the time steps:

N	θ	$\dot{\theta}$	$\ddot{\theta}$	R	T	Comments
6	18.0°	2.981	-1.605	7.402	4.905	$\mu R < T$, ∴ Sliding
7	35.1°	2.702	-2.787	5.149	4.665	$\mu R < T$, ∴ Sliding
8	50.6°	2.344	-3.580	2.658	4.014	$\mu R < T$, ∴ Sliding
9	64.0°	1.951	-3.932	0.334	3.116	$\mu R < T$, ∴ Sliding
10	75.2°	1.561	-3.803	-1.553	2.151	$R < 0$ ∴ Departed Liner

The values of the parameters at departure are found by averaging the iterations before and after the iteration when $R=0$.

$$\therefore \text{AOD} = 69.6^\circ \quad \text{and} \quad \dot{\theta} = 1.756 \text{ rad/s}$$

$$\therefore \text{Velocity at departure} = 2.621 \text{ m/s}$$

With these two values the block's parabolic trajectory can be determined. The solution process is terminated when the centre of the block comes into contact with the mill liner.

The solution that has been presented used $H=0.1$ seconds. Due to the large increment size, there was a significant inaccuracy between the analytical and numerical values at θ_{slip} . Presented below is a table of the numeric solution's results for different increment sizes. The values are tabulated are θ and N before and after friction is exceeded. The analytic solution predicts that $\theta_{\text{slip}} = -20.989^\circ$

H	θ_{slip} Numeric	N_{slip}
0.1s	-18.0° to 0.0°	4 - 5
0.05s	-18.0° to -9.0°	8 - 9
0.01s	-19.8° to -18.0°	39 - 40
0.005s	-20.70° to -19.80°	77 - 78
0.001s	-20.88° to -20.70°	384 - 385
0.0005s	-20.90° to -20.88°	767 - 768
0.0001s	-20.958° to -20.955°	3835 - 3836

The numeric solution converges to the analytic solution as H decreases. The convergence at $H=0.0001$ seconds is to the second decimal place. The cost of this accuracy is that 3835 iterations were performed before this result was reached. The result for $H=0.001$ seconds is within 0.5% of the analytic result, but only 384 iterations were required. This example has been presented to highlight the rapid increase in computational time that accompanies any extra accuracy in a numerical solution process.

APPENDIX 5: Derivation of the Toppling Equations.

The block can topple down the liner either before or after sliding has begun. Both cases will be presented as the forces involved are not the same.

A5.1 Toppling before the start of Sliding:

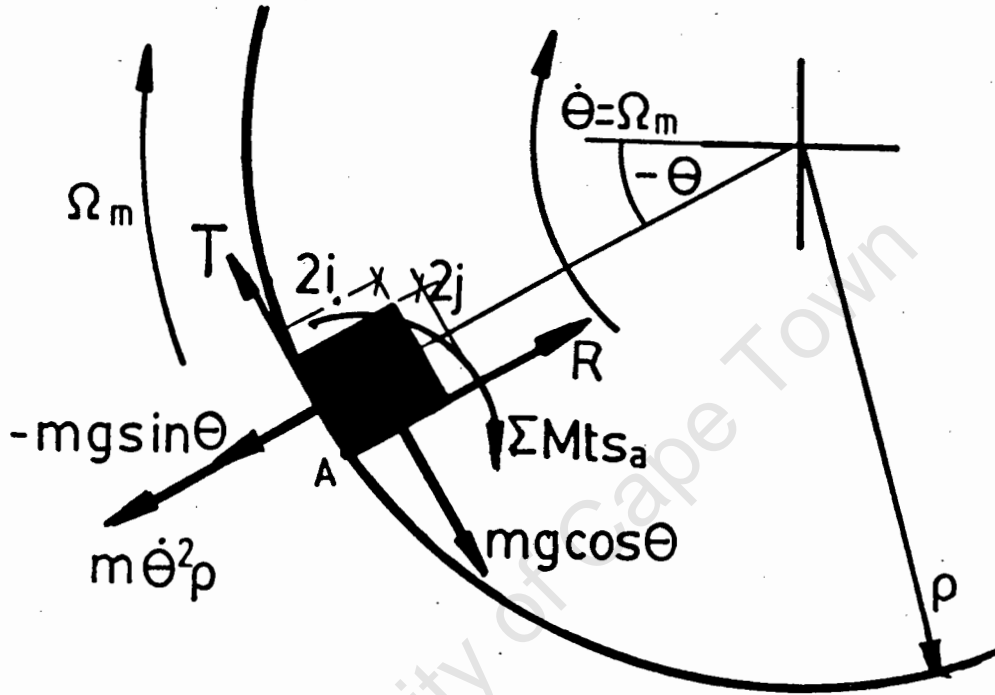


Figure A5.1: Orientation of forces acting on a Block on the Point of Toppling ($\dot{\theta} = -\Omega_m$)

Using d’Lambert’s Principle, the Radial Angular Acceleration has been replaced by an equivalent inertial force. In this case the force is an outward acting force of magnitude $m\dot{\theta}^2\rho$. The tangential angular acceleration is zero as $\dot{\theta} = -\Omega_m$. As the block is on the verge of toppling, it can be assumed that the Normal reaction (R) acts at the extremity of the block, ie point A.

Taking moments to be positive in the clockwise direction. There is no external moment, so the sum of moments about any point must equal zero. The size of the block in the tangential direction is $2j$ and in the radial direction $2i$.

$$\therefore \Sigma Mts_A : \quad i(mg\cos\theta) - j(m\dot{\theta}^2\rho - mg\sin\theta) = 0 \quad \dots (A5.1)$$

$$\text{But } \dot{\theta} = -\Omega_m \quad \therefore \quad g(\cos\theta + j\sin\theta) - j\Omega_m^2\rho = 0 \quad \dots (A5.2)$$

For the block to topple over $\Sigma Mts_A > 0$

$$\therefore \text{For Toppling } g(\cos\theta + j\sin\theta) - j\Omega_m^2\rho > 0 \quad \dots (A5.3)$$

Using a Newton-Cotes Numerical Solution Technique to solve for θ_{topple} :

$$\theta_{n+1} = \theta_n - \frac{g(i\cos\theta + j\sin\theta) - j\Omega_m^2\rho}{g(j\cos\theta - i\sin\theta)} \quad \dots(5.4)$$

This solution technique is used in the computer implementation to calculate the Toppling Angle for a block moving without sliding.

Summing moments about the Centre of Gravity (CG) of the block yields the following: $\Sigma M_{ts} \cos \alpha : iT - jR = 0 \quad \dots (A5.5)$

$$\text{For toppling } \Sigma M_{ts} > 0 \quad \therefore iT - jR > 0 \quad \dots (A5.6)$$

Assuming that the block starts to slide and topple simultaneously, then the frictional force is such that $T = \mu R$. Combining this with A5.5 yields:

$$i\mu R - jR = 0 \quad \therefore \mu = j/i \quad \dots (A5.7)$$

The magnitude of μ defined in equation A5.7 is the coefficient of friction required to allow the block to start sliding and toppling simultaneously.

Therefore: $\mu < j/i$ then the block will slide before toppling
 $\mu > j/i$ then the block will topple before sliding.

Hence for a square block if $\mu < 1$ the block will slide before toppling
 while if $\mu > 1$ the block will topple before sliding

This result is significant as the operating parameters (Ω_m , ρ or m) do not effect the interaction of toppling and sliding. The only factors that determine whether a particle will slide or topple are the dimensions of the particle and the coefficient of friction between the particle and the surface. As expected, tall narrow blocks ($j > i$) will topple, while short broad ($i > j$) blocks will slide. Similarly, smooth surfaces (μ small) will result in the block sliding, while rough surfaces (μ larger) will result in the block toppling.

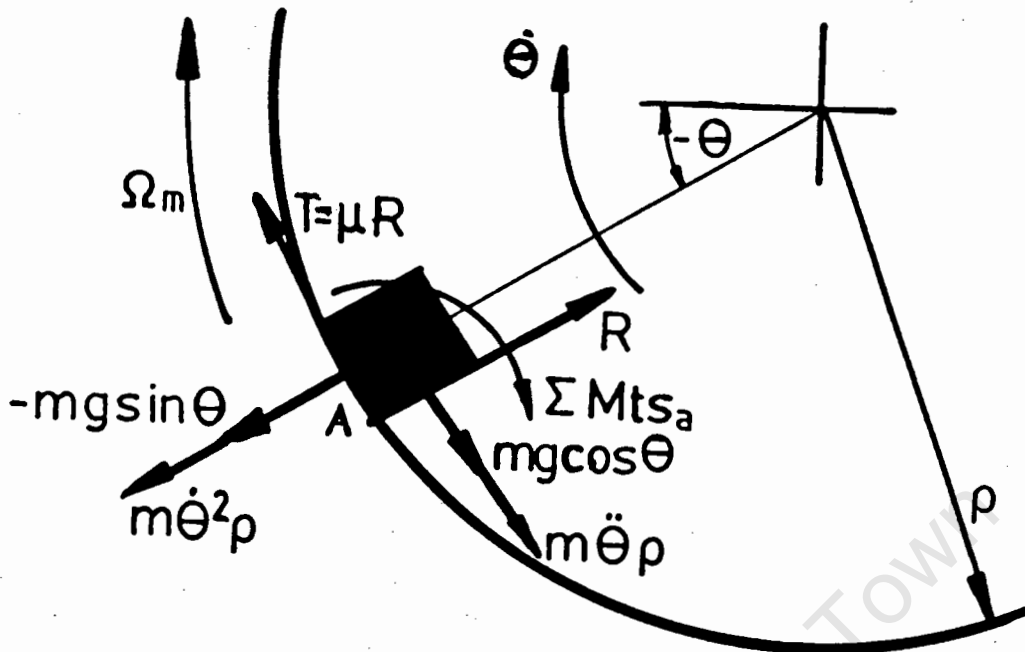
A5.2 Toppling after the start of Sliding:

Figure A5.2: Orientation of forces acting on a Block on the Point of Toppling ($\dot{\theta} \neq \Omega_m$)

At the point of toppling the normal reaction acts through the point A. Using d'Lambert's Principle both the tangential and radial accelerations ($m\dot{\theta}^2\rho$ and $m\ddot{\theta}\rho$ respectively) have been replaced with equivalent inertial forces.

Taking moments to be positive in the clockwise direction. There is no external moment, so the sum of moments about any point must equal zero. The size of the block in the tangential direction is $2j$ and in the radial direction $2i$.

$$\therefore \Sigma Mts_A : i(m\ddot{\theta}\rho + mg\cos\theta) - j(m\dot{\theta}^2\rho - mg\sin\theta) = 0 \dots (A5.8)$$

For toppling to occur $\Sigma Mts > 0$

$$\therefore \text{For toppling: } i\ddot{\theta}\rho - j\dot{\theta}^2\rho + g(i\cos\theta + j\sin\theta) > 0 \dots (A5.9)$$

The computer implementation uses equation A5.8 and at the end of each time increment the inequality is checked. If the sum of the moments is greater than zero then it signals that the block has started to topple down the liner. It does not terminate the run, but continues to implement the sliding equations. The reason being that $\Sigma Mts > 0$ does not imply that the block has toppled over, but that it has only started to topple. So there is still time before the block will topple over and during this time the sliding equations would still be applicable. The motion of the toppling block was considered to be outside of the scope of thesis investigation.

APPENDIX 6: Solution of the Rolling Governing Equations using an Euler Forward Step.

The system of 2nd Order Differential Equation is the following:

$$\Omega_m \rho = \dot{e} \rho + \omega a \quad \dots (3.23)$$

$$7\dot{\omega} a = 5g \cos e \quad \dots (3.25)$$

Equations (3.23) and (3.25) are a pair of coupled differential equations, ($\dot{e} = f\{\Omega_m, \omega\}$ and $\dot{\omega} = f\{e\}$). This necessitates that they are solved simultaneously. The two 1st Order Differential Equations will be numerically solved using an Euler Forward Step.

The Euler Forward Step is of the form [19]:

$$y(x_0 + h) = y(x_0) + hy'(x_0) + \text{Error} \quad \dots (A6.1)$$

where: $y(x)$ is the function value at x

$y'(x)$ is the derivative of the function at x

h is the interval size, $h = x - x_0$

For small h , the error term becomes small, so re-writing with subscripts:

$$y_{n+1} = y_n + hy'_n \quad \dots (A6.2)$$

Using the Euler Forward Step to numerically approximate the derivatives of the governing equations yields:

$$\dot{e}_{n+1} = \frac{de_{n+1}}{dt} \approx \frac{e(t+h) - e(t)}{\delta t} = \frac{e_{n+1} - e_n}{h} \quad \dots (A6.3)$$

$$\dot{e}_{n+1} = \frac{d\dot{e}_{n+1}}{dt} \approx \frac{\dot{e}(t+h) - \dot{e}(t)}{\delta t} = \frac{\dot{e}_{n+1} - \dot{e}_n}{h} \quad \dots (A6.4)$$

$$\dot{\omega}_{n+1} = \frac{d\omega_{n+1}}{dt} \approx \frac{\omega(t+h) - \omega(t)}{\delta t} = \frac{\omega_{n+1} - \omega_n}{h} \quad \dots (A6.5)$$

where:

$e_{n+1}, \dot{e}_{n+1}, \ddot{e}_{n+1}, \omega_{n+1}, \dot{\omega}_{n+1}$ are the values at time increment $n+1$

e_n, \dot{e}_n, ω_n are the values at time increment n

$\delta t = h$ is the time increment

Substituting (A6.3) and (A6.5) into (3.23) and (3.25) yields:

$$\omega_{n+1} = \omega_n + \frac{h\{5g \cos e_n\}}{7a} \quad \dots (A6.6)$$

$$\dot{e}_{n+1} = \dot{e}_n + \frac{h\{\Omega_m \rho - a\omega_n\}}{\rho} \quad \dots (A6.7)$$

Hence at the end of the step:

$$R_{n+1} = m(\dot{\theta}_{n+1})^2 \rho - mg \sin(\theta_{n+1}) \quad \dots \text{(A6.8)}$$

$$T_{n+1} = m(\ddot{\theta}_{n+1}) \rho - mg \cos(\theta_{n+1}) \quad \dots \text{(A6.9)}$$

These equations are the basis of the algorithm used in the computer program used to analyze a ball moving with pure rolling.

University of Cape Town

APPENDIX 7: Listing of Experimental and Theoretical ResultsList of Results of the Angle of Departure on a Steel Lining

Ω_m (% N_c)	<u>Theoretical Predictions</u>		<u>Experimental Results</u>			
	Uncertainty in Expt. μ		N	Mean	90% Confidence Range	
	$\mu=0.194$	$\mu=0.268$			Lower	Upper
30	-61.1°	-57.0°	7	-59.4°	-61.6°	-57.8°
45	-51.5°	-47.1°	4	-50.8°	-51.9°	-49.6°
60	-41.3°	-36.5°	10	-40.4°	-41.3°	-39.7°
75	-30.4°	-25.0°	4	-30.0°	-31.7°	-28.3°
90	-18.5°	-12.1°	8	-18.4°	-19.1°	-17.7°
105	- 5.2°	- 1.6°	3	- 4.7°	- 5.6°	- 3.7°
120	6.8°	13.7°	4	12.0°	6.4°	17.6°
135	19.3°	28.9°	3	21.7°	17.4°	25.8°
150	35.7°	52.1°	4	36.5°	32.8°	40.2°
165	62.4°	Cent.	3	49.0°	37.4°	60.0°

List of Results of the Angle of Departure on a Cloth Lining

Ω_m (% N_c)	<u>Theoretical Predictions</u>		<u>Experimental Results</u>			
	Uncertainty in Expt. μ		N	Mean	90% Confidence Range	
	$\mu=0.384$	$\mu=0.466$			Lower	Upper
30	-50.9°	-47.0°	3	-39.7°	-41.6°	-37.7°
45	-40.7°	-36.6°	5	-34.8°	-36.5°	-33.1°
60	-29.5°	-25.0°	6	-23.8°	-25.4°	-22.2°
75	-17.1°	-12.0°	6	-11.2°	-12.0°	-10.4°
90	- 2.9°	2.2°	9	- 2.7°	- 4.0°	- 1.4°
105	9.7°	14.9°	8	11.8°	10.6°	12.9°
120	24.6°	32.3°	7	28.3°	26.9°	29.6°
135	46.8°	66.4°	6	57.5°	53.2°	61.8°

List of Results of the Angle of Slip on a Steel Lining

Ω_m (% N_c)	<u>Theoretical Predictions</u>			<u>Experimental Results</u>			
	$\mu_{\text{experimental}} = 0.2$			N	Mean	90% Confidence Range	
	0° Slip	1° Slip	5° Slip			Lower	Upper
30	-77.0°	-66.4°	-61.6°	8	-65.4°	-68.2°	-62.5°
45	-75.0°	-61.4°	-54.0°	4	-60.8°	-62.5°	-59.0°
60	-74.0°	-56.4°	-46.4°	8	-51.8°	-53.1°	-50.4°
75	-71.0°	-50.9°	-38.8°	3	-44.3°	-45.3°	-43.4°
90	-68.7°	-44.9°	-31.9°	4	-40.0°	-41.9°	-38.1°
105	-65.4°	-38.7°	-22.4°	3	-27.3°	-31.6°	-23.1°
120	-61.0°	-31.8°	-13.3°	3	-11.7°	-16.5°	- 6.8°

List of Results of the Angle of Slip on a Cloth Lining

Ω_m (% N_c)	<u>Theoretical Predictions</u>			<u>Experimental Results</u>			
	$\mu_{\text{experimental}} = 0.44$			N	Mean	90% Confidence Range	
	0° Slip	1° Slip	5° Slip			Lower	Upper
30	-64.1°	-53.3°	-48.8°	3	-50.3°	-51.3°	-49.4°
45	-61.6°	-47.1°	-40.2°	7	-45.1°	-45.8°	-44.5°
60	-57.9°	-40.2°	-31.0°	6	-34.3°	-35.3°	-33.3°
75	-53.1°	-32.3°	-21.0°	5	-26.2°	-28.3°	-24.1°
90	-47.1°	-22.9°	- 9.7°	8	-13.0°	-14.1°	-11.9°
105	-39.8°	-12.4°	3.2°	5	3.6°	- 0.3°	7.5°
120	-30.7°	0.7°	19.7°	4	6.8°	4.0°	9.5°

APPENDIX 8: Listing of the Computer Program used for the Solution and Animation of the Sliding Equations.

A listing has been included of the computer program that was used to solve the governing equations of a block sliding on the inside of a rotating cylinder. The program is written in Fortran 77. An executable version is contained on the disk attached to this thesis. The program has been called BALLS.EXE and needs DOS 3.2 or more to run. The program looks for the file BALLS.DAT, so the two files must be in the same directory to run the program. The output files and their characteristics have been discussed in the thesis and at the start of the subroutine BALLFILE.FOR

To use the animation subroutines one or two other executable programs must be run before BALLS.EXE is executed. If the computer that you are using has a Colour monitor (of any kind), then the file WGKS.EXE must be run before starting BALLS.EXE. If the computer has a Hercules Card the two files WGKS.EXE and HERCBIOS.COM must both be run before the program BALLS.EXE is begun.

The animation section of the program can be speeded up by increasing the size of the time increment used by the Euler Solution. This has a side effect that the Euler Solution becomes unstable and the animated response of the block can become fictitious. For example if h is too large the animated response can cause the block (represented by a circle on the screen) to travel straight through the liner. When the program is executed without the animation, then it is advisable to reduce h , so that the results contained in the output files do not suffer from inaccuracies. On the other hand, if no documented output is required, then one can adjust the size of h accordingly.

When large output files are generated by the program, it is recommended that the files be copied to a Hard Drive. The reason is that the program will stop running, if it can not find any more free space on the disk to which it is writing the results. To stop this and to allow the program to run faster, the programs can be down loaded onto a Hard Drive.

```

c.....
c   File = BALLS.FOR
c.....
c   Purpose ..... The Controlling routine for BALLS Program
c   Developer ..... M. Nates, UCT
c   Date ..... September 1989
c   Referenced by .. NONE
c   References to .. BALLTITL.FOR, BALLFILE.FOR, CURED, BALLINPU.FOR,
c                   BALLVARA.FOR, SOLVE.FOR, BALLINCR.FOR,
c                   BALLOUTP.FOR, YESNO
c   Language ..... Fortran 77 (WATFOR77)
c   Installation ... IBM PC with DOS 3.3
c.....
c   Description of module function:
c   -----
c   This is the calling or controlling routine of the entire numerical
c   solution and computer implementation. The various subroutines are
c   called inturn, as required.
c.....
c   Description of the Variables used throughout the program
c   -----
c   A           = Size of 'Ball' used for Animation  $[(Anorm^2+Atang^2)^{1/2}]$ 
c   ANIM        = Marker [Flag] to show if animation is required
c   ANORM       = Normal dimension of the block
c   ATANG       = Tangential dimension of the block
c   BALLIN     = Character name of Data Input file [ BALL.DAT ]
c   BALLOUT    = Character name of Full Output File
c   BALLSUM    = Character name of Summary Output File
c   COMBALL.INC= File that contains the common block used by the program
c   CORD(N,1)  = X co-ordinate of the ball relative to the mill centre
c   CORD(N,2)  = Y co-ordinate of the ball relative to the mill centre
c   CORD(N,3)  = Total rotation of the mill from starting time.
c   DUMMY/DUM  = General character string used, changes as required.
c   FINALN    = Final increment number
c   G          = Gravitational constant [9.81]
c   H          = Size of time increment used while block on liner
c   HP        = Size of time increment used during flight
c   IMAX      = Maximum Number of Iterations
c   MARKER    = Used as a general flag
c   MARKPR1   = Marker [Flag] to show if a Full Output file is open
c   MARKPR2   = Marker [Flag] to show if a Co-ordinate File is open
c   MARKPR3   = Marker [Flag] to show if a Summary Output file is open
c   MASS      = Mass of the block [m]
c   MCORDN    = New mill rotation [used for animation - exor put]
c   MCORDO    = Old mill rotation [used for animation - exor put]
c   MUS       = Static coefficient of friction [ $\mu_s$ ]
c   MUK       = Kinetic coefficient of friction [ $\mu_k$ ]
c   NPOD      = Increment number at the point of departure (POD)
c   OMEGA(N,1) = Increment number N
c   OMEGA(N,2) = Theta_dot of block [ $\dot{\theta}$ ] at time N
c   OMEGA(N,3) = Theta of block [ $\theta$ ] at time N
c   OMEGA(N,4) = Reaction of liner on block [R] at time N
c   OMEGA(N,5) = Tangential force [T] on block at time N
c   OMEGA(N,6) = Toppling moment about A at time N
c   OMEGAI    = Initial theta_dot of block [ $\dot{\theta}(\theta)$ ]
c   OMEGAM    = Rotational velocity of the mill [ $\Omega_m$ ]
c   PI       =  $\pi$  (3.141592854)
c   RHO      = Radius of the mill [ $\rho$ ]
c   THETA0    = Theta at which sliding should start [ $\theta_{slip}$ ]

```

```

C   THETA1      = Initial theta of block [ $\theta(0)$ ]
C   THETA1TOP  = Angle at which Toppling will occur, but only for  $\theta = 0$ 
C   THETAADD   = Angular Acceleration of the Block [ $\ddot{\theta}$ ]
C   XCORDN     = New X co-ordinate [used for animation - exor put]
C   XCORDO     = Old X co-ordinate [used for animation - exor put]
C   YCORDN     = New Y co-ordinate [used for animation - exor put]
C   YCORDO     = Old Y co-ordinate [used for animation - exor put]

```

```
c
```

```
c.....
      program BALLS

```

```
c.....
```

```

c$include comball.inc
      character*1 dummy,dum
      equivalence(dummy,dum)
      call curini

```

```
c
```

```

c---  Display program title page
      call BALLTITL

```

```
c
```

```

c---  Initialise
      markpr1=0
      markpr2=0
      markpr3=0
      anim=0

```

```
5.   continue
```

```
c
```

```

c---  input of data output file names
      call BALLFILE(markpr1,markpr2,markpr3,anim)
      call cured

```

```
c
```

```
      call BALLINPU
```

```
c
```

```
      call BALLVARA
```

```
c
```

```

c---  Solve for  $\theta_0$  for given variables
      call SOLVE

```

```
c
```

```

      if(anim.eq.1)then
      call millini
      endif

```

```
c
```

```

      if(anim.eq.0)then
      write(*,*)
      write(*,*) 'Program Running - Please Wait'
      endif
      call Ballincr

```

```
c
```

```

c---  Close all animation workstations if required
      if(anim.eq.1)then
      call finish()
      endif

```

```
c
```

```

      write(*,*)
      write(*,*) 'Writing the Results to the required Output Files'
      write(*,*) 'Please Wait'

```

```
c
```

```
      call balloutp
```

```
c
```

```

c---  Close all the files that where opened
      close(7)

```

```
    if(markpr1.eq.1)then
    close(8)
    end if
    if(markpr2.eq.1)then
    close(9)
    end if
c
c--- Possibility of re-running program from within itself, but only if
c--- the block's motion has not been animated
    if(anim.eq.0)then
    write(*,*)
    write(*,*) Do you wish to re-run the package?
75    format(' Y or N \')
    write(*,75)
    call YESNO(dum)
    if(dummy.eq.'Y'.or.dummy.eq.'y')then
    write(*,*) Note:
    write(*,*) The new output files to be specified will
    write(*,*) be written over those just created if their
    write(*,*) names are not altered.
    write(*,*)
    pause - Press Enter to continue
    goto 5
    end if
    endif
c
    stop
    end
c$include BALLMISC.FOR
```

```

c.....
c   File = BALLTITL.FOR
c.....
c   Purpose ..... To display an introductory Screen
c   Developer ..... M. Nates, UCT
c   Date ..... September 1989
c   Referenced by .. BALLS.FOR
c   References to .. CURED, CURCUP
c   Language ..... Fortran 77 (WATFOR77)
c   Installation ... IBM PC with DOS 3.3
c.....
SUBROUTINE BALLTITL
c.....
   call cured
15  format(10x, '*****')
25  format(10x, 'Program to Numerically Solve the Governing ')
35  format(10x, 'Differential Equation of a Single Block ')
45  format(10x, 'Sliding on the inside of a Smooth Cylinder ')
55  format(10x, '*****')
65  format(10x, 'Theory Developed by: M. Nates')
75  format(10x, 'G. Nurick')
85  format(10x, 'D. Reddy')
95  format(10x, 'Please Wait')

   call curcup(2,0)
   write(*,15)
   call curcup(5,0)
   write(*,25)
   call curcup(6,0)
   write(*,35)
   call curcup(7,0)
   write(*,45)
   call curcup(9,0)
   write(*,55)
   call curcup(12,0)
   write(*,65)
   call curcup(13,0)
   write(*,75)
   call curcup(14,0)
   write(*,85)
c--- delay to keep the front page on the screen
   do 10 i=1,20000
       j=j+1
10  continue
   call curcup(16,0)
   write(*,95)
   do 20 i=1,10000
       k=k+1
20  continue
   call cured
   return
   end

```

```

c.....
c   File = BALLFILE.FOR
c.....
c   Purpose ..... To handle the opening of the various data files
c   Developer ..... M. Nates, UCT
c   Date ..... September 1989
c   Referenced by .. BALLS.FOR
c   References to .. CURED, CURCUP, YESNO
c   Language ..... Fortran 77 (WATFOR77)
c   Installation ... IBM PC with DOS 3.3
c.....
c   Description of module function:
c   -----
c   The module opens the various output data files requested by the
c   user (listed below). It sets the flags of the files that are
c   opened. It process the users responses with the aid of the
c   utility subroutine YESNO. The module also enquires wether the
c   user wishes to animate the block's motion. The relevant flag
c   is set for the animation process.
c.....
c
c   Description of parameters :
c o MARKPR1 - Flag to denote wether a Full Data Output File is open
c o MARKPR2 - Flag to denote wether a Summary Output File is open
c o MARKPR3 - Flag to denote wether a Co-ordinate Output File is open
c o ANIM    - Flag to denote wether Animation is required
c List of Files: 1. BALLIN: This is the file that the program stores
c                   the default input variables in. It is not
c                   changable, and is called BALL.DAT
c                   2. BALLOUT: This is the Full Output File. It contains
c                   all the variables incremental values. It
c                   also contains information of the Blocks
c                   fight trajectory and velocity.
c                   3. BALLSUM: This file contains the only a listing of
c                   the input variables and specific values
c                   at significant increments (eg At POD).
c                   It is useful for quick analysis of the
c                   block's response
c                   4. CORDOUT: This file contains the block's centre's
c                   co-ordinates at each increment. It is
c                   used to plot the Block's motion path.
c.....
c   SUBROUTINE BALLFILE(MARKPR1,MARKPR2,MARKPR3,anim)
c.....
c   character*12 BALLIN, BALLOUT, CORDOUT, BALLSUM
c   character*1 dummy,dum
c   equivalence(dummy,dum)
c   integer markpr1,markpr2,markpr3,anim
c
c--- initialise
c   markpr1=0
c   markpr2=0
c   markpr3=0
c   anim=0
c
c--- Default input data deck called BALL.DAT
c   BALLIN='BALL.DAT'
c
c---- Create page for file handling

```

File Specification for Output Files

```

call cured
write(*,*)
write(*,*)
write(*,*)
c
c--- input of data output file name
c
15  format(a)
25  format('Is a data ouput file required? Y or N -'\)
    write(*,25)
    call YESNO(dum)
    if(dummy.eq.'Y'.or.dummy.eq.'y')then
c--- set print marker 1 to 1 ie markpr1=1 and read in name of output file
        markpr1=1
        write(*,*)
35  format('Enter name of output data file.-'\)
        write(6,35)
        read(*,15) BALLOUT
        end if
        write(*,*)
c
c--- input of data output summary file name
c
45  format('Is a condensed data ouput file required? Y or N -'\)
    write(*,45)
    call YESNO(dum)
    if(dummy.eq.'Y'.or.dummy.eq.'y')then
c--- set print marker 1 to 1 ie markpr3=1 and read in name of output file
        markpr3=1
        write(*,*)
55  format('Enter name of condensed data output file.-'\)
        write(6,55)
        read(*,15) BALLSUM
        end if
        write(*,*)
c
c--- input of cordinate output file name
c
65  format('Is a cordinate ouput file required? Y or N -'\)
    write(*,65)
    call YESNO(dum)
    if(dummy.eq.'Y'.or.dummy.eq.'y')then
c--- set print marker 2 to 1 ie markpr2=1 and read in name of output file
        markpr2=1
        write(*,*)
75  format('Enter name of cordinate output data file.-'\)
        write(6,75)
        read(*,15) CORDOUT
        end if
c
c--- Determine wether animation is required
c
    write(*,*)
    write(*,*)
    write(*,*)
    write(*,*) Note 1. With Animation the ratio of ball size to mill
    write(*,*) size must be such that (ball/mill)<0.1
    write(*,*) 2. For an acceptable animation speed H>=0.01
    write(*,*)
85  format('Is the Blocks motion to be animated ? Y or N -'\)

```

```
write(*,85)
call YESNO(dum)
if(dummy.eq.'Y'.or.dummy.eq.'y')then
c--- set animation marker to 1 ie anim=1
      anim=1
endif
c
c--- open required files
      open(7,file=BALLIN)
c
      if(markpr1.eq.1)then
        open(8,file=BALLOUT)
      end if
c
      if(markpr2.eq.1)then
        open(9,file=CORDOUT)
      end if
c
      if(markpr3.eq.1)then
        open(10,file=BALLSUM)
      end if
c
      return
end
```

University of Cape Town

```

c .....
c   File = BALLINPUT.FOR
c .....
c   Purpose ..... To read and display the default input variables
c   Developer ..... M. Nates, UCT
c   Date ..... September 1988
c   Referenced by .. BALLS.FOR
c   References to .. None
c   Language ..... Fortran 77 (WATFOR77)
c   Installation ... IBM PC with DOS 3.3
c .....
c   Description of module function:
c   -----
c   This routine reads the input from a data deck BALL.DAT
c   It then displays the input variables for modification by
c   BALLVARA.FOR if required. It is used as a buffer routine before
c   BALLVARA.FOR
c .....
c   Subroutine BALLINPU
c .....
c$include comball.inc
c   Initilise all variables
c .....
c       Do 10 i = 1,5000
c           Do 20 j = 1,6
c               omega(i,j)=0
20          continue
10         continue
c
c---      Read input from data deck
          read(7,* ) OMEGAM,MASS,MUS,MUK,RHO,G,H,OMEGAI,THETAI,HP,Atang,
          &anorm,imax
c .....
C       Output the input for display
c .....
          write(*,*)
          write(*,*)
          write(*,*) Listing of the Problem Variables.
          write(*,*)
15      Format( 5x, Size of time increments {s} (H) = ',F11.5,/,
+          5X, Mass of ball {kg} (MASS) = ',F11.5,/,
+          5X, Static Coeff. of Friction (MUS) = ',F11.4,/,
+          5X, Kinetic Coeff. of Friction (MUK) = ',F11.4,/,
+          5X, Mill Speed {rpm} (OMEGAM) = ',F11.2,/,
+          5X, Gravity {m/s2} (G) = ',F11.2,/,
+          5X, Mill Radius {m} (RHO) = ',F11.3,/,
+          5X, Ball Dim. (Tangential) {m} (ATANG) = ',F11.4,/,
+          5X, Ball Dim. (Normal) {m} (ANORM) = ',F11.4,/,
+          5X, Initial Ball Omega {rpm} (OMEGAI) = ',F11.2,/,
+          5X, Initial Theta {degrees} (THETAI) = ',F11.2,/,
+          5x, Time increments for flight {s}(HP) = ',F11.5,/,
+          5x, Max. Number of Iterations{N}(IMAX) = ',F11.0,/)
          write(6,15)H,MASS,MUS,MUK,OMEGAM,G,RHO,Atang,anorm,omegai,
          &thetai,hp,imax
c
c       return
c       end

```

```

c.....
c   File = BALLVARA.FOR
c.....
c   Purpose ..... To assist with the processing of the Input Data
c   Developer ..... M. Nates, UCT
c   Date ..... September 1989
c   Referenced by .. BALLS.FOR
c   References to .. BALLCHAN.FOR, CURED, CURCUP
c   Language ..... Fortran 77 (WATFOR77)
c   Installation ... IBM PC with DOS 3.3
c.....
c   Description of module function:
c   -----
c   This program is used to help with the altering and managment of the
c   BALLCHAN routine. It also writes the changed input variables to the
c   required output files. It specifies the size of the animation 'Ball'
c   Its final task is to convert the input data from degrees and rpm to
c   to rads and rads/s.
c.....
c   Subroutine BALLVARA
c.....
c$include comball.inc
character*1 dum,dummy
equivalence (dummy,dum)

10  continue
C
C---- Check wether the initial default values need changing
write(*,*) 'Are the default values of the variables suitable ?'
75  format(' Y or N '\)
write(*,75)
call YESNO(dum)
if(dummy.eq.'Y'.or.dummy.eq.'y')then
goto 60
end if
call BALLCHAN
call cured
write(*,*)
write(*,*) Listing of the New Default Problem Variables.
write(*,*)
85  Format( 5x, Size of time increments {s} (H) = ',F11.5,/,
+        5X, Mass of ball {kg} (MASS) = ',F11.5,/,
+        5X, Static Coeff. of Friction (MUS) = ',F11.4,/,
+        5X, Kinetic Coeff. of Friction (MUK) = ',F11.4,/,
+        5X, Mill Speed {rpm} (OMEGAM) = ',F11.2,/,
+        5X, Gravity {m/s2} (G) = ',F11.2,/,
+        5X, Mill Radius {m} (RHO) = ',F11.3,/,
+        5X, Ball Dim. (Tangential) {m} (ATANG) = ',F11.4,/,
+        5X, Ball Dim. (Normal) {m} (ANORM) = ',F11.4,/,
+        5X, Initial Ball Omega {rpm} (OMEGAI) = ',F11.2,/,
+        5X, Initial Theta {degrees} (THETAI) = ',F11.2,/,
+        5x, Time increments for flight {s}(HP) = ',F11.5,/,
+        5x, Max. Number of Iterations{N}(IMAX) = ',F11.0,/)
write(6,85) H,MASS,MUS,MUK,OMEGAM,G,RHO,ATANG,ANORM,OMEGAI,
&THETAI,hp,inax
goto 10
60  continue
c
c---- write final values to ouput files,if required

```

```

if(markpr1.eq.1)then
  write(8,*)
  write(8,*)      Listing of the Problem Variables.
  write(8,*)
  write(8,85) H,MASS,MUS,MUK,OMEGAM,G,RHO,ATANG,ANORM,OMEGAI,
&THETAI,hp,imax
end if

c
if(markpr2.eq.1)then
  write(9,*)
  write(9,*)      Listing of the Problem Variables.
  write(9,*)
  write(9,85) H,MASS,MUS,MUK,OMEGAM,G,RHO,ATANG,ANORM,OMEGAI,
&THETAI,hp,imax
end if

c
if(markpr3.eq.1)then
  write(10,*)
  write(10,*)     Listing of the Problem Variables.
  write(10,*)
  write(10,85) H,MASS,MUS,MUK,OMEGAM,G,RHO,ATANG,ANORM,OMEGAI,
&THETAI,hp,imax
end if

c
c--- Prepare screen for problem solution
call cured
  write(*,*)      Problem Variables
  write(*,*)
  write(*,85) H,MASS,MUS,MUK,OMEGAM,G,RHO,ATANG,ANORM,OMEGAI,
&THETAI,hp,imax

c
c--- Convert the input variables from degrees & rpm to rad & rad/s
c--- Convert thetai to radians
  thetai=thetai*3.141592654/180
c--- convert omegam and omegai from rpm to radians
  omegai=omegai*3.141592654/30
  omegam=omegam*3.141592654/30
c---- Let the variable A=(tang/2) ie the radius of the block/ball
  A=0.5*sqrt(atang*atang+anorm*anorm)

c
return
end

```

```

c.....
c   File = BALLCHAN.FOR
c.....
c   Purpose ..... To allow a default value to be entered as input
c   Developer ..... M. Nates, UCT
c   Date ..... September 1989
c   Referenced by .. BALLVARA.FOR
c   References to .. CURED, GETREAL.FOR
c   Language ..... Fortran 77 (WATFOR77)
c   Installation ... IBM PC with DOS 3.3
c.....
c   Description of module function:
c   -----
c   The module is used if the input variables require changing.
c   The module presents the default value and calls for a new
c   value. If none is entered, then the default value is used.
c   The module calls the subroutine GETREAL.FOR, which is used (with
c   the aid of CHRTOR) to parse the input string into a real number
c.....
c   subroutine BALLCHAN
c.....
c   character*12 BALLIN
c$include comball.inc
c   INTEGER MARKDEF,numval
c   real num,pi

c--- initialise
c   MARKDEF=0
c   numval=1
c   num=0.0
c   pi=3.14159265

C   Output the old input for display and change
c.....
*   write(*,*)
*   write(*,*)
*   write(*,*) Listing of the Problem Variables.
*   write(*,*)
5   Format(a)
15  Format( 2x, Size of time increments {s} (H) [',F9.5,'] = ',\ )
25  Format( 2X, Mass of ball {kg} (MASS) [',F9.5,'] = ',\ )
35  Format( 2X, Static Coeff. of Friction (MUS) [',F9.4,'] = ',\ )
135 Format( 2X, Kinetic Coeff. of Friction (MUK) [',F9.4,'] = ',\ )
45  Format( 2X, Mill Speed {rpm} (OMEGAM) [',F9.2,'] = ',\ )
55  Format( 2X, Gravity {m/s2} (G) [',F9.2,'] = ',\ )
65  Format( 2X, Mill Radius {m} (RHO) [',F9.3,'] = ',\ )
75  Format( 2X, Ball Dim. (Tangential) {m} (ATANG) [',F9.4,'] = ',\ )
125 Format( 2X, Ball Dim. (Normal) {m} (ANORM) [',F9.4,'] = ',\ )
85  Format( 2X, Initial Ball Omega {rpm} (OMEGAI) [',F9.2,'] = ',\ )
95  Format( 2X, Initial Theta {degrees} (THETAI) [',F9.2,'] = ',\ )
105 Format( 2x, Time increments for flight {s}(HP) [',F9.5,'] = ',\ )
145 Format( 2x, Max. Number of Iterations{N}(IMAX) [',F9.0,'] = ',\ )
115 Format(f12.6)
c   call cured

c   write(*,*) *****
&*****
c   write(*,*) *** Input the new value at the equals sign,
& ***

```

```

write(*,*)'*** or press return for the bracketted default value
& ***'
write(*,*)'*****'
&*****'

```

c

```

write(*,*)
write(*,*)
write(*,15) H
call GETREAL(NUM,MARKDEF)
IF(MARKDEF.NE.1)THEN
C--- MAKE H=NEW VALUE AND DO NOT USE DEFAULT
H=NUM
END IF

```

c

```

write(*,25) mass
call GETREAL(NUM,MARKDEF)
IF(MARKDEF.NE.1)THEN
C--- MAKE mass=NEW VALUE AND DO NOT USE DEFAULT
mass=NUM
END IF

```

c

```

write(*,35) mus
call GETREAL(NUM,MARKDEF)
IF(MARKDEF.NE.1)THEN
C--- MAKE mus=NEW VALUE AND DO NOT USE DEFAULT
mus=NUM
END IF

```

c

```

write(*,135) muk
call GETREAL(NUM,MARKDEF)
IF(MARKDEF.NE.1)THEN
C--- MAKE muk=NEW VALUE AND DO NOT USE DEFAULT
muk=NUM
END IF

```

c

```

write(*,45) omegan
call GETREAL(NUM,MARKDEF)
IF(MARKDEF.NE.1)THEN
C--- MAKE omegan=NEW VALUE AND DO NOT USE DEFAULT
omegan=NUM
END IF

```

c

```

write(*,55) g
call GETREAL(NUM,MARKDEF)
IF(MARKDEF.NE.1)THEN
C--- MAKE g=NEW VALUE AND DO NOT USE DEFAULT
g=NUM
END IF

```

c

```

write(*,65) rho
call GETREAL(NUM,MARKDEF)
IF(MARKDEF.NE.1)THEN
C--- MAKE rho=NEW VALUE AND DO NOT USE DEFAULT
rho=NUM
END IF

```

c

```

write(*,75) atang
call GETREAL(NUM,MARKDEF)
IF(MARKDEF.NE.1)THEN
C--- MAKE a=NEW VALUE AND DO NOT USE DEFAULT

```

```

atang=NUM
END IF

c
write(*,125) anorm
call GETREAL(NUM,MARKDEF)
IF(MARKDEF.NE.1)THEN
C--- MAKE a=NEW VALUE AND DO NOT USE DEFAULT
anorm=NUM
END IF

c
write(*,85) omegai
call GETREAL(NUM,MARKDEF)
IF(MARKDEF.NE.1)THEN
C--- MAKE omegai=NEW VALUE AND DO NOT USE DEFAULT
omegai=NUM
END IF

c
write(*,95) thetai
call GETREAL(NUM,MARKDEF)
IF(MARKDEF.NE.1)THEN
C--- MAKE thetai=NEW VALUE AND DO NOT USE DEFAULT
thetai=NUM
END IF

c
write(*,105) Hp
call GETREAL(NUM,MARKDEF)
IF(MARKDEF.NE.1)THEN
C--- MAKE HP=NEW VALUE AND DO NOT USE DEFAULT
HP=NUM
END IF

C
write(*,145) Imax
call GETREAL(NUM,MARKDEF)
IF(MARKDEF.NE.1)THEN
C--- MAKE HP=NEW VALUE AND DO NOT USE DEFAULT
Imax=NUM
END IF

C
C--- WRITE NEW VALUES TO DATA FILE, but first and then rewind file
rewind(7)
WRITE(7,* ) OMEGAM, MASS, MUS, MUK, RHO, G, H, OMEGAI, THETA I, HP,
&ATANG, ANORM, imax
rewind(7)

c
RETURN
END

```

```

c.....
c   File = GETREAL.FOR
c.....
c   Purpose ..... To interface with between BALLCHAN and CHRTOR
c   Developer ..... M. Nates, UCT
c   Date ..... September 1989
c   Referenced by .. BALLCHAN.FOR
c   References to .. CHRINI.FOR, CHRSTR, CHRTOR, CHRRED, CHRERR
c   Language ..... Fortran 77 (WATFOR77)
c   Installation ... IBM PC with DOS 3.3
c.....
c   Description of module function:
c   -----
c   To get a real value, by first buffering the input using the CHRINI
c   routines, from the keyboard. The CHRINI routines were written by
c   J. Vos, and parse a character string into a real variable. It allows
c   a value in the form -2.5e-3 (-0.0025) to be entered and interpreted.
c.....
c   Description of parameters :
c o N          - Real value returned by to BALLCHAN.FOR
c o MARKDEF    - Flag to indicate whether the default value is to be used
c.....
c   SUBROUTINE GETREAL(N,MARKDEF)
c.....
c
c   real a(100),n
c   integer iferr,numchr,maxchr,markdef
c   parameter (maxchr=10)
c   character*1 chrbuf(maxchr)
c
c---- initialize module
c   call CHRINI
c   markdef=0
c
c 10 continue
c
c---- get the real value to be read
c   iofset = 48
c   call CHRRED (iferr)
c   if(iferr.ne.0)then
c   write(*,*)'Error in reading input'
c   goto 100
c   end if
c   call CHRSTR (chrbuf,maxchr,numchr,iferr)
c   if(iferr.ne.0) then
c     call CHRERR (iofset)
c     write(*,1001) maxchr
c 1001 format(1h, '=> Maximum number of characters in token = ',i2)
c     goto 10
c   else if(numchr.eq.0) then
c     write(*,1003)
c 1003 format('\, '=> Used Default Value ',\ )
c     write(*,*)
c     markdef=1
c     goto 100
c   endif
c
c

```

```
call CHRTOR (chrbuf,numchr,n,iferr)
if(iferr.ne.0) then
  call CHRERR (iofset)
  write(*,1002)
1002  format(1h , => Invalid real value specified, re-enter - ',\))
      goto 10
endif
c
100  continue
c
return
end
```

University of Cape Town


```

15      format(5x, 'The theta at which slipping should start is ',f8.3,/)
      if(markpr1.eq.1)then
      write(8,15)theta0*180/3.14159
      end if
c---- Write the value of theta-slip to screen
      write(*,*)
      write(*,15)theta0*180/3.14159
c
500    continue
c
c---- Solve for theta-topple at theta-dot=omegan - Using a Newton-Cotes
c*****
      y2=0.0
      y1=-3.14159/2
      cons2= (atang/2)*omegan*omegan*rho
c
30     continue
      y1=y2
      numer=cons2-g*((atang/2)*sin(y1)+(anorm/2)*cos(y1))
      denom=g*((anorm/2)*sin(y1)-(atang/2)*cos(y1))
      y2=y1-numer/denom
      j=j+1
      If(j.gt.100) then
      write(*,*)          !!! unable to solve for theta-topple !!!
      write(8,*)          !!! unable to solve for theta-topple !!!
      goto 1000
      else if (abs(y2-y1).gt.0.0001) then
      goto 30
      endif
c
      thetatop=y2
c
c---- make sure that -3.14159< theta-topple < 3.14139
      If(theta0.gt.3.14159.or.thetatop.lt.-3.14159)then
      const=thetatop/3.14159
      thetatop= thetatop-int(const)*3.14159
      end if
c
35     format(5x, 'The theta at which toppling should occur is ',f8.3,/)
      if(markpr1.eq.1)then
      write(8,35)thetatop*180/3.14159
      end if
c
c---- Write the value of theta-topple to screen
      write(*,35)thetatop*180/3.14159
c
c---- Compare theta topple and theta-sliding (if they are available)
      If(pointer.eq.1) goto 1000
      If(theta0.lt.thetatop)then
      if(markpr1.eq.1)then
      write(8,*)          Hence the block should slide before toppling
      endif
      write(*,*)          Hence the block should slide before toppling
      Elseif(theta0.eq.thetatop)then
      if(markpr1.eq.1)then
      write(8,*)          The block should slide and topple simultaneously
      endif
      write(*,*)          The block should slide and topple simultaneously
      Else
      if(markpr1.eq.1)then

```

```
write(8,*) Hence the block should topple before sliding
endif
write(*,*) Hence the block should topple before sliding
Endif
c
1000 continue
c
return
end
```

University of Cape Town

```

c.....
c   File = MILLINI.FOR
c.....
c   Purpose ..... To initialise the animation process
c   Developer ..... M. Nates, UCT
c   Date ..... September 1988
c   Referenced by .. BALLS.FOR
c   References to .. Various GKSCOVER.FOR Routines
c   Language ..... Fortran 77 (WATFOR77)
c   Installation ... IBM PC with DOS 3.3
c.....
c   Description of module function:
c   -----
c   The module is used to initialise the animation process with the aid
c   the GKSCOVER.FOR routines. The graphic routines employed use the
c   General Kernel System developed by WATCOM. This module first opens
c   the type of screen required and then draws the mill. The size of the
c   mill never changes (as its radius changes), only a scale line
denotes
c   the change in the mill size. The next stage is to draw the block to
c   the same scale as the mill, and the to place it in its starting
c   position on the mill liner. The final task done is to draw two
markers
c   that represent the rotation of the mill. These markers are also
placed
c   in a starting position.
c.....
c
c   Description of parameters :
c   XAXIS   - The size of the X axis, proportional to the mill size
c   YAXIS   - The size of the Y axis, proportional to the X axis
c   XC      - The centre of the X axis (the centre of the screen)
c   YC      - The centre of the Y axis (the centre of the screen)
c.....
c           subroutine millini
c.....
c$include gksdefn.inc
c$include comball.inc
c   INTEGER M,i,j,n
c   REAL xc,yc,xaxis,yaxis
c   CHARACTER*80 PIC1(1:PIC_SIZE), PIC2(1:PIC_SIZE), pic3(1:PIC_SIZE)
c   character*12 CORDIN
c   COMMON /PICTURE/ PIC1, PIC2, pic3
c   common/mill/xc,yc,xaxis,yaxis
c
c   * Initialization.
c   *
c           xaxis=4*rho
c           yaxis=xaxis*0.75
c           xc=xaxis/2
c           yc=yaxis/2
c
c   CALL INIT( 0 )
c
c--- set colours if required
c       if(gkswk_type.ne.10)then
c   CALL COLOURMAP( 0, BLACK )
c   CALL COLOURMAP( 1, LIGHT_GREEN )
c   CALL COLOURMAP( 2, LIGHT_RED )

```

```

CALL COLOURMAP( 3, LIGHT_YELLOW )
endif
*
c--- redefine screen with a linear transformation
call gswm(1, 0.0, xaxis, 0.0, yaxis)
call gselnt(1)
*
c--- draw outside and inside of mill
*
call circle(xc,yc,rho,1)
call circle(xc,yc,rho*1.1,1)
call paint (xc+rho*1.05,yc,3)
c
c--- put in mill centre
call LINE(xc-rho/4,yc,xc+rho/4,yc,1)
call LINE(xc,yc+rho/4,xc,yc-rho/4,1)
c
c--- draw first ball and label it as such
*
set text attributes
CALL GSTXFP(2,2)
CALL GSCHH(0.1*rho)
call gstxp(tp_right)
CALL GSTXAL(left,BOTTOM)
call text(xc*0.05,0.25*yc,'Position Markers',1)
call text(xc*0.05,0.1*yc,'Block:',1)
call circle(0.3*xc,0.15*yc,a,1)
call paint (0.3*xc,0.15*yc,2)
c
c--- draw mill marker and label it as such, sized rho/10
call text(xc*0.6,0.1*yc,'Mill:',1)
call circle(0.85*xc,0.15*yc,0.05*rho,1)
call paint (0.85*xc,0.15*yc,3)
c
c--- put in scale line of 0.5 metre in length
CALL GSTXAL(right,bottom)
call text(1.95*xc,0.1*yc,'Scale: 0.5 metre',2)
call line(1.95*xc,0.01*yc,1.9*xc-0.5,0.01*yc,2)
c
c--- getpic ball, ball=pic1
call getpic(0.3*xc-a,0.15*yc+a,0.3*xc+a,0.15*yc-a,pic1)
c
c--- getpic mill marker, mill marker =pic2
call getpic(0.85*xc-0.05*rho,0.15*yc+0.05*rho,
& 0.85*xc+0.05*rho,0.15*yc-0.05*rho,pic2)
c
c--- place first ball on liner (and marker) at starting point
xcordn=(rho-a)*cos(thetai)
ycordn=(rho-a)*sin(thetai)
mcordn=thetai
c
c place ball and mill marker
c--- ball
call putpic_action(xc+xcordn-a,yc+ycordn+a,pic1,3)
c-- marker
call putpic_action(xc+(cos(mcordn))*rho*1.2-0.05*rho,
$yc+(sin(mcordn))*rho*1.2+0.05*rho,pic2,3)
call putpic_action(xc+(cos(mcordn+pi))*rho*1.2-0.05*rho,
$yc+(sin(mcordn+pi))*rho*1.2+0.05*rho,pic2,3)
return
end
*$include gkscover

```

```

c.....
c   File = BALLINCR.FOR
c.....
c   Purpose ..... To Solve the Governing Equations Numerically
c   Developer ..... M. Nates, UCT
c   Date ..... September 1989
c   Referenced by .. BALLS.FOR
c   References to .. BALLPARA.FOR, MILLMOVE.FOR
c   Language ..... Fortran 77 (WATFOR77)
c   Installation ... IBM PC with DOS 3.3
c.....
c
c   Description of module function:
c   -----
c
c   This subroutine uses an Euler Method to step forward with
c   increment h in time. The path of the ball is traced until the
c   until one of the possible ending conditions in reached. After
c   each increment the block (ball) is moved on the screen by
c   MILLMOVE.FOR. If the block leaves the liner then BALLPARA.FOR
c   is called.
c.....
c
c   Description of parameters :
c   omega(i,1) = Increment Number
c   omega(i,2) = Theta dot of the block at each time increment
c   omega(i,3) = Theta of the block at each time increment
c   omega(i,4) = Normal Reaction on the block at each time increment
c   omega(i,5) = Tangential Force on the block at each time increment
c   omega(i,6) = Toppling Moment on the block at each time increment
c.....
c   SUBROUTINE BALLINCR
c.....
c
c$include comball.inc
c---  Initialise required values
      integer i,marker,para,j
      real THETADD
      THETADD=0
      marker=0
      Do 110 i = 1,5000
        Do 120 j = 1,3
          cord(i,j)=0
120      continue
110      continue
c
      finaln=0
      npod = 0
      para=0
c
c---  Values of the variables at time t=0 or N=1
      i=1
      omega(1,1)=0
      omega(1,2)=omegai
      omega(1,3)=thetai
      omega(1,4)=mass*omegan*omegan*rho-mass*g*sin(omega(1,3))
      omega(1,5)=mass*g*cos(omega(1,3))
      omega(1,6)=(atang/2)*rho*omegan*omegan-g*((atang/2)*sin(
& omega(1,3)) + (anorm/2)*cos(omega(1,3)))

```

```

cord(1,3)=thetai
c
c--- Check if Omegai=Omegan if not go immediately to slipping
If(omegai.ne.omegan)then
  write(*,*)      Ball slips immediatley, Omegai.ne.Omegan
  if(markpr1.eq.1)then
    write(8,*)    Ball slips immediatley, Omegai.ne.Omegan
  endif
  if(markpr3.eq.1)then
    write(10,*)   Ball slips immediatley, Omegai.ne.Omegan
  endif
  goto 10
endif
c*****
c  Implimentation of the Numerical Sol'n of the Non-Sliding Case
c*****
c
5  continue
c
c--- calculate the values of the variables at time N+1
  omega(i+1,1)=i
  omega(i+1,2)=omegai
  omega(i+1,3)=omega(i+1,2)*H+omega(i,3)
  omega(i+1,4)=mass*omegan*omegan*rho-mass*g*sin(omega(i,3))
  omega(i+1,5)=mass*g*cos(omega(i,3))
  omega(i+1,6)=(atang/2)*rho*omegan*omegan-g*((atang/2)*sin(
& omega(i,3)) + (anorm/2)*cos(omega(i,3)))
c
c--- calculate the cordinates of the ball centre
  cord(i+1,1)=(rho-a)*cos(omega(i,3))
  cord(i+1,2)=(rho-a)*sin(omega(i,3))
  cord(i+1,3)=cord(i,3)+h*omegan
c
c--- move ball on the screen
c  first make the past increments old
  xcordo=xcordn
  ycordo=ycordn
  mcordo=mcordn
c  then make the new cords from this iteration
  xcordn=cord(i+1,1)
  ycordn=cord(i+1,2)
  mcordn=cord(i+1,3)
c  then call 'moving' routine but only if required
  if(anim.eq.1)then
    call millmove
  endif
c
c--- Check Number 1
c--- If no 'event' after 1000 iterations end routine
c--- Also note to screen when a further 500 iterations are completed
  If(0.eq.mod(i+1,500).and.i+1.ne.0.and.anim.eq.0)then
    write(*,101) i+1
  endif
  If(i+1.gt.inax)then
    write(*,*)      !!! Block has not started to slide      !!!
115  format(' !!! But the maximum iterations exceeded=',f5.0,' !!!')
    write(*,115) inax
    write(*,*)      !!! therefore the run is terminated.    !!!
    if(markpr1.eq.1)then
      write(8,*)    !!! Block has not started to slide      !!!

```

```

write(8,115) imax
write(8,*)'   !!! therefore the run is terminated.   !!!'
  end if
  if(markpr3.eq.1)then
write(10,*)'   !!! Block has not started to slide   !!!'
write(10,115) imax
write(10,*)'   !!! therefore the run is terminated.   !!!'
  end if
c--- End run because number of iterations has been exceeded
      Npod=i+1
      Finaln=i+1
      goto 899
  End if

c
c--- Check Number 2
c--- check if theta>89,9 and omega>=0
c--- then ball never leaves rim, but sticks to it
  If(omega(i+1,3).ge.1.569051.and.omega(i+1,2).gt.0)then
write(*,*)'   !!! Ball is centrifuged to liner   !!!'
write(*,*)'   !!! before it has started to slide !!!'
write(*,*)'   !!! therefore the run is terminated !!!'
  if(markpr1.eq.1)then
write(8,*)'   !!! Ball is centrifuged to liner   !!!'
write(8,*)'   !!! before it has started to slide !!!'
write(8,*)'   !!! therefore the run is terminated !!!'
  end if

c
  if(markpr3.eq.1)then
write(10,*)'   !!! Ball is centrifuged to liner   !!!'
write(10,*)'   !!! before it has started to slide !!!'
write(10,*)'   !!! therefore the run is terminated !!!'
  end if
c--- End run because ball is centrifuged
      Npod=i+1
      Finaln=i+1
      goto 999
  End if

c
c--- Check Number 3
c--- Check wether the toppling moment has changed sign
  If(omega(i+1,6).lt.0.and.marker.eq.0)then
  if(markpr1.eq.1)then
write(8,*)'   Block starting to toppled before sliding.'
write(8,51) omega(i,1),omega(i,2),omega(i,3)*180/3.14159,
&          omega(i,4),omega(i,5),omega(i,6)
write(8,51) omega(i+1,1),omega(i+1,2),omega(i+1,3)*180/3.14159,
&          omega(i+1,4),omega(i+1,5),omega(i+1,6)
  end if

c
  if(markpr3.eq.1)then
write(10,*)'   Block starting to toppled before sliding.'
write(10,51) omega(i,1),omega(i,2),omega(i,3)*180/3.14159,
&          omega(i,4),omega(i,5),omega(i,6)
write(10,51) omega(i+1,1),omega(i+1,2),omega(i+1,3)*180/3.14159,
&          omega(i+1,4),omega(i+1,5),omega(i+1,6)
  end if
c--- toggle marker so that the message is not re-written
      marker=1
  End if
c--- Check Number 4

```

```

c--- Check wether mus*R>=T if so slipping begun
      If(omega(i+1,4)*MUS.le.omega(i+1,5))then
        write(*,*) Slipping about to begin, mus*R=T
51   format(4x,f5.0,4x,f8.4,4x,f8.4,4x,f8.4,4x,f8.4,4x,f8.4)
        if(markpr1.eq.1)then
          write(8,*)
          write(8,*) Slipping about to begin, mus*R=T
          write(8,51) omega(i+1,1),omega(i+1,2),omega(i+1,3)*180/3.14159,
*omega(i+1,4),omega(i+1,5),omega(i+1,6)
          end if
c
          if(markpr3.eq.1)then
            write(10,*)
            write(10,*) Slipping about to begin, mus*R=T
            write(10,51) omega(i+1,1),omega(i+1,2),omega(i+1,3)*180/3.14159,
*omega(i+1,4),omega(i+1,5),omega(i+1,6)
            end if
c--- Increment N to N+1
      i=i+1
      goto 10
c
c--- No sliding so increase increment and re-iterate
      Else
        i=i+1
        goto 5
      End if
c
10   continue
c
c*****
c   Implimentation of the Numerical Solution of the Sliding D.E.
c*****
c   The kinetic Coefficient of Friction is used for sliding MUK
c
c--- record increased increment number [time = t + ih]
      omega(i+1,1)=i
c
c--- theta_dot [omega] at time t + ih
      omega(i+1,2)=omega(i,2)+h*(muk*omega(i,2)**2-muk*g*
+sin(omega(i,3))/rho-g*cos(omega(i,3))/rho)
c
c--- theta_dot_dot at time t + ih
      THETADD = (omega(i+1,2)+omega(i,2))/2
c
c---- theta at time t + ih {only used to calculate Toppling Moment}
      omega(i+1,3)=omega(i,3)+h*omega(i,2)
c
c--- calculate reaction r = omega(i,4) at time t + ih
      omega(i+1,4)=mass*(omega(i,2)**2*rho-g*sin(omega(i,3)))
c
c--- calculate tangential force T omega(i,4) at time t + ih
      omega(i+1,5)=mass*g*cos(omega(i,3))
c
c--- calculate the toppling moment
      omega(i+1,6)=(atang/2)*rho*omega(i,2)**2-g*((atang/2)*sin(
& omega(i,3)+(anorm/2)*cos(omega(i,3)))-(anorm/2)*rho*thetadd
c
c--- calculate the cordinates of the ball centre
      cord(i+1,1)=(rho-a)*cos(omega(i,3))
      cord(i+1,2)=(rho-a)*sin(omega(i,3))

```

```

cord(i+1,3)=cord(i,3)+h*omegam
c
c--- move ball on the screen
c   first make the past increments old
      xcordo=xcordn
      ycordo=ycordn
      mcordo=mcordn
c   then make the new cords from this iteration
      xcordn=cord(i+1,1)
      ycordn=cord(i+1,2)
      mcordn=cord(i+1,3)
c   then call 'moving' routine
      if(anim.eq.1)then
        call millmove
      endif
c
c*****
c   Start checks to determine the nature of the block's motion
c*****
c--- Check Number 1
c--- Check if the block has started to toppled over, M>0
c--- write only once to the screen and file, i.e. use marker
      If((omega(i+1,6)).lt.0.and.marker.eq.0)then
        if(markpr1.eq.1)then
          write(8,*) ' The block has started to toppled down the liner'
          write(8,51) omega(i,1),omega(i,2),omega(i,3)*180/3.14159,
            & omega(i,4),omega(i,5),omega(i,6)
          write(8,51) omega(i+1,1),omega(i+1,2),omega(i+1,3)*180/3.14159,
            & omega(i+1,4),omega(i+1,5),omega(i+1,6)
          end if
          if(markpr3.eq.1)then
            write(10,*) ' The block has started to toppled down the liner'
            write(10,51) omega(i,1),omega(i,2),omega(i,3)*180/3.14159,
              & omega(i,4),omega(i,5),omega(i,6)
            write(10,51) omega(i+1,1),omega(i+1,2),omega(i+1,3)*180/3.14159,
              & omega(i+1,4),omega(i+1,5),omega(i+1,6)
            end if
          end if
          toggle marker so that the message is not re-written
          marker=1
        end if
c
c--- Check Number 2
c--- Print omega if sliding down the liner is about to start, the
c   interval of "omega=0" decreases as the increment time decreases
      if(abs(omega(i+1,2)).lt.(0.045+0.015*(h-0.001/0.001)))then
101 format(5x,i6.0,' iterations have been completed')
      if(anim.eq.0)then
        write(*,*)
        write(*,101) i+1
      endif
      write(*,*) ' Theta_dot [Omega] of the Ball is ≈ zero'
      if(markpr1.eq.1)then
        write(8,*) ' Theta-dot [Omega] of the Ball is ≈ zero'
        write(8,51) omega(i+1,1),omega(i+1,2),omega(i+1,3)*180/3.14159,
          *omega(i+1,4),omega(i+1,5),omega(i+1,6)
        end if
      if(markpr3.eq.1)then
        write(10,*) ' Theta-dot [Omega] of the Ball is ≈ zero'
        write(10,51) omega(i+1,1),omega(i+1,2),omega(i+1,3)*180/3.14159,
          *omega(i+1,4),omega(i+1,5),omega(i+1,6)

```

```

        end if
    end if

c
c--- Check Number 3
c--- If no 'event' after imax iterations end routine
c--- Also note to screen when a further 500 iterations are completed
        If(0.eq.mod(i+1,500).and.i+1.ne.0)then
            write(*,101) i+1
        endif
    If(i+1.gt.imax)then
111  write(*,*) '    !!! Block has not departed from the liner !!!'
        format('    !!! or centrifuged after',f5.0,'iterations, !!!')
        write(*,111) imax
        write(*,*) '    !!! therefore the run is terminated.    !!!'
        if(markpr1.eq.1)then
            write(8,*) '    !!! Block has not departed from the liner !!!'
            write(8,111) imax
            write(8,*) '    !!! therefore the run is terminated.    !!!'
        end if
        if(markpr3.eq.1)then
            write(10,*) '    !!! Block has not departed from the liner !!!'
            write(10,111) imax
            write(10,*) '    !!! therefore the run is terminated.    !!!'
        end if
c--- End run because number of iterations has been exceeded
        Finaln=i+1
        Npod=i+1
        goto 999
    End if

c
c--- Check Number 4
c--- check if theta>89,9
c--- then ball never leaves rim, but sticks to it
        If(omega(i+1,3).ge.1.569051.and.omega(i+1,2).gt.0)then
            write(*,*) '    !!! Ball is centrifuged to liner    !!!'
            write(*,*) '    !!! therefore the run is terminated !!!'
            if(markpr1.eq.1)then
                write(8,*) '    !!! Ball is centrifuged to liner !!!'
                write(8,*)
            end if
c
            if(markpr3.eq.1)then
                write(10,*) '    !!! Ball is centrifuged to liner !!!'
                write(10,*)
            end if
c--- End run because ball is centrifuged
        Finaln=i+1
        Npod=i+1
        goto 999
    End if

c
c
c--- Check Number 5
c--- check sign of reaction and see if required to 'kick-out'
        If(omega(i+1,4).ge.0)then
            i=i+1
c--- pass final increment number
        npod=i
        goto 10
    Endif

```

```

c
c--- Normal P.O.D. has occurred write it to screen and file
write(*,*)'   Ball follows normal path and leaves liner.'
      if(markpr1.eq.1)then
write(8,*)'   Ball follows normal path and leaves liner.'
      end if
c
      if(markpr3.eq.1)then
write(10,*)'  Ball follows normal path and leaves liner.'
      end if
c-- mark that ball left liner "normally"
Npod=i
para=1
50 continue
      if(markpr1.eq.1)then
write(8,51) omega(i,1),omega(i,2),omega(i,3)*180/3.14159,
*omega(i,4),omega(i,5),omega(i,6)
write(8,51) omega(i+1,1),omega(i+1,2),omega(i+1,3)*180/3.14159,
*omega(i+1,4),omega(i+1,5),omega(i+1,6)
      end if
c
      if(markpr3.eq.1)then
write(10,51) omega(i,1),omega(i,2),omega(i,3)*180/3.14159,
*omega(i,4),omega(i,5),omega(i,6)
write(10,51) omega(i+1,1),omega(i+1,2),omega(i+1,3)*180/3.14159,
*omega(i+1,4),omega(i+1,5),omega(i+1,6)
      end if
c
c--- Call BALLPARA to calculate the ball parabolic path if the ball
c leaves the liner
c If(para.eq.1)then
call BALLPARA
endif
c
999 continue
c
return
end

```

```

c.....
c   File = BALLPARA.FOR
c.....
c   Purpose ..... To numerically solve the Parabolic trajectory of
c                   block after it has left the liner.
c   Developer ..... M. Nates, UCT
c   Date ..... September 1989
c   Referenced by .. BALLINCR.FOR
c   References to .. MILLMOVE.FOR
c   Language ..... Fortran 77 (WATFOR77)
c   Installation ... IBM PC with DOS 3.3
c.....
c   Description of module function:
c   -----
c   Subroutine to numerically simulate the parabolic flight path of
c   block. An Forward Step is used to solve the equations of. The
c   The Point of Departure is found by averaging the angle of the
c   block before and after  $R=0$ . The initial velocity is found by
c   assuming that it is purely tangential. The average of Theta_dot
c   before and after  $R=0$  is used to find the velocity. The subroutine
c   call the animation subroutine MILLMOVE.FOR after each increment
c   to animate the blocks's motion.
c.....
c
c   Description of parameters :
c   POD   = Angle or Point of Departure of the Block from the liner
c   Vini  = Initial Tangential Velocity
c   Ux,Uy = Initial components of velocity in the X and Y directions
c   Sx,Sy = Block's displacement in the X and Y directions
c   V     = Block's Total Velocity at each time increment
c   Vy    = Block's Vertical Velocity at each time increment
c           (Vx is constant)
c.....
c           Subroutine BALLPARA
c.....
c$include comball.inc
c   real SX,SY,UX,UY,VINI,POD,V
c   integer i
c--- Use the average of the last two iteration on the liner surface
c   POD=(omega(NPOD+1,3)+omega(NPOD,3))/2
c   Sx = cos(POD)*(rho-A)
c   Sy = sin(POD)*(rho-A)
c   Vini = ((omega(NPOD+1,2)+omega(NPOD,2))/2)*(rho-a)
c   Ux = -Vini*sin(POD)
c   Uy = Vini*cos(POD)
c   vy = uy
c   i = 0
c
c--- Output initial conditions to file
c   write(8,*)
c   write(8,*)          Initial values at the start of Flight.
c   write(8,*)
15  Format( 5X, Point of Departure {degrees} (POD) = ,F11.5,/,
+      5X, Initial Velocity {m/s} (Vini) = ,F11.5,/,
+      5X, Init. Horiz. displacement {m} (Sx) = ,F11.5,/,
+      5X, Init. Vert. displacement {m} (Sy) = ,F11.5,/,
+      5X, Init. Horiz. velocity {m/s} (Ux) = ,F11.5,/,
+      5X, Init. Vert. velocity {m/s} (Uy) = ,F11.5,/)
c   write(8,15)POD*180/3.14159,VINI,SX,SY,UX,UY

```

```

c -- write heading
write(8,*)
write(8,*) Incremental Flight Path and Velocity Results
write(8,*)
write(8,*) No          Sx          Sy          Vy          V
write(8,*)          (m)          (m)          (m/s)        (m/s)
c
10 continue
c
c--- Increment one time step using time increment of HP
i=i+1
sx=sx+ux*hp
sy=sy+vy*hp-g*hp*hp/2
vy=vy-g*hp
v=sqrt(vy*vy+ux*ux)
cord(i+1+NPOD,1)=SX
cord(i+1+NPOD,2)=SY
cord(i+1+NPOD,3)=cord(i+NPOD,3)+hp*omegam
c
c--- move ball on the screen
c first make the past increments old
xcordo=xcordn
ycordo=ycordn
mcordo=mcordn
c then make the new cords from this iteration
xcordn=cord(i+1+npod,1)
ycordn=cord(i+1+npod,2)
mcordn=cord(i+1+npod,3)
if(anim.eq.1)then
call millmove
endif
c
c--- Check if against liner
If(sx*sx+sy*sy.lt.rho*rho.or.i.lt.10)then
c-- print this steps values
11 format(4x,i4,4x,f8.4,4x,f8.4,4x,f8.4,4x,f8.4)
write(8,11)i+Npod,sx,sy,vy,v
goto 10
endif
c
c--- Print final value and record Finaln
write(8,11)i+Npod,sx,sy,vy,v
Finaln=1+I+NPOD
c
return
end

```

```

c.....
c   File = MILLMOVE.FOR
c.....
c   Purpose ..... To animate the block after each increment
c   Developer ..... M. Nates, UCT
c   Date ..... September 1989
c   Referenced by .. BALLINCR.FOR, BALLPARA.FOR
c   References to .. Various GKSCOVER.FOR Routines
c   Language ..... Fortran 77 (WATFOR77)
c   Installation ... IBM PC with DOS 3.3
c.....
c   Description of module function:
c   -----
c   This routine animates the block after each increment. It removes
c   the block from its old position (?CORDO) and puts it at its new
c   position (?CORDN).
c.....
c       subroutine millmove
c.....
c$include comball.inc
*$include gksdefn
  INTEGER M,i,j,n
  REAL xc,yc,xaxis,yaxis
  CHARACTER*80 PIC1(1:PIC_SIZE), PIC2(1:PIC_SIZE), pic3(1:PIC_SIZE)
  COMMON /PICTURE/ PIC1, PIC2, pic3
  common/mill/xc,yc,xaxis,yaxis
c---  remove old ball and marker and redraw new ball and new marker
c---  ball
      call putpic_action(xc+xcordo-a,yc+ycordo+a,pic1,1)
c----  marker
      call putpic_action(xc+(cos(mcordo))*rho*1.2-0.05*rho,
$yc+(sin(mcordo))*rho*1.2+0.05*rho,pic2,1)
      call putpic_action(xc+(cos(mcordo+pi))*rho*1.2-0.05*rho,
$yc+(sin(mcordo+pi))*rho*1.2+0.05*rho,pic2,1)
c
c   move ball and mill marker
c---  ball
      call putpic_action(xc+xcordn-a,yc+ycordn+a,pic1,3)
c--   marker
      call putpic_action(xc+(cos(mcordn))*rho*1.2-0.05*rho,
$yc+(sin(mcordn))*rho*1.2+0.05*rho,pic2,3)
      call putpic_action(xc+(cos(mcordn+pi))*rho*1.2-0.05*rho,
$yc+(sin(mcordn+pi))*rho*1.2+0.05*rho,pic2,3)
*
      return
      end

```

```

c.....
c   File = BALLOUTPUT.FOR
c.....
c   Purpose ..... To process the relavent output data.
c   Developer ..... M. Nates, UCT
c   Date ..... September 1989
c   Referenced by .. BALLS.FOR
c   References to .. None
c   Language ..... Fortran 77 (WATFOR77)
c   Installation ... IBM PC with DOS 3.3
c.....
c   Description of module function:
c   -----
c   The module writes the incremental results to the Full Output
c   Data file and the Co-ordinate Data Output File. The data is
c   written at the end of the numeric solution, therefore if the run
c   is terminaed before it comes to an end (eg by CTRL-BREAK), then
c   the results will not be written to the files. The data for the
c   Summary Output file is written during the solution process, and so
c   no specific ouput needs to be written after the solution comes
c   to an end.
c.....
c       Subroutine BALLOUTP
c$include comball.inc
c
c---   write array to output file
       if(markpr1.eq.1)then
           write(8,*)
           write(8,*)          Pre-Departure Incremental Results
           write(8,*)
           write(8,*) Number   Theta dot   Theta   Reaction   Tangential
&Toppling Mom.   Mill Rot.
           write(8,*)   N       (rad/s)   (degrees)   (N)       (N)
&   (Nm)   (degrees)
51   format(2x,f4.0,3x,f8.4,4x,f9.4,3x,f8.4,3x,f8.4,4x,f8.4,3x,f8.3)
       do 20 j=1,Npod+1
           write(8,51) omega(j,1),omega(j,2),omega(j,3)*180/3.14159,
*omega(j,4),omega(j,5),omega(j,6),cord(j,3)*180/3.14159
20   continue
       end if
c
c
c---   write cords to file cords file
61   if(markpr2.eq.1)then
       format(7x,i4.0,4x,f9.4,4x,f9.4,4x,f9.4)
       write(9,*)
       write(9,*)           N           X Cord           Y Cord           Mill Rot.
       write(9,*)           (m)           (m)           (degrees)
       do 60 j=1,Finaln
           write(9,61)j-1,cord(j,1),cord(j,2),cord(j,3)*180/3.14159
60   continue
       end if

       return
       end

```

```

c .....
c   File = BALLMISC.FOR
c .....
c   Purpose ..... Contains miscellaneous utility subroutines
c   Developer ..... M. Nates, UCT
c   Date ..... September 1989
c   Referenced by .. Included in BALLS.FOR
c   References to .. None
c   Language ..... Fortran 77 (WAITFOR77)
c   Installation ... IBM PC with DOS 3.3
c .....
c   Description of modules
c   -----
c   WAIT:
c   Used as an automatic non interactive pausing routine
c   YESNO:
c   Used to return the letters Y/y/N/n only for a yes/no question,
c   so that a decision can be made from the response.
c .....
c   SUBROUTINE WAIT( SECONDS )
c .....
c   REAL SECONDS
c   INTEGER LPS, TICS, add
c
c 'LPS' is the number of do-loop iterations required to delay 1 second.
c This number varies between CPUs.
c
c   PARAMETER (LPS=500000)
c   SECONDS = SECONDS*LPS
c   DO 11 TICS=1, INT( SECONDS )
c     add=add+1
11  continue
c   return
c   END
c .....
c   Subroutine YESNO(dum)
c .....
c   character*1 dum
c
10  continue
15  format(a)
c   read(*,15) dum
c   if(dum.eq.'Y')then
c     goto 20
c   endif
c   if(dum.eq.'y')then
c     goto 20
c   elseif(dum.eq.'N')then
c     goto 20
c   elseif(dum.eq.'n')then
c     goto 20
c   else
c     write(*,*) 'Enter Y or N only -
c     goto 10
c   end if
c
c   continue
20  continue
c
c   return
c   end

```

```
c---- Common block for BALLMILL Problem
real OMEGAM,MASS,H,RHO,G,theta0,xcordo,ycordo,mcordo
real OMEGA,OMEGAI,THETAI,HP,CORD,A,mcordn,xcordn,ycordn
real ATANG,ANORM,MUK,MUS,imax
integer finaln,markfirs,markpr1,markpr2,Npod,markpr3,anim
common/COMball/OMEGAM,H,G,RHO,MASS,OMEGA(5000,6),A,anim,
+      theta0,thetai,omegai,finaln,HP,CORD(5000,3),imax,
+      xcordo,ycordo,mcordo,xcordn,ycordn,mcordn,mus,muk,
+      markfirs,markpr1,markpr2,atang,anorm,Npod,markpr3
```

University of Cape Town

APPENDIX 9: Listing of the Computer Program used for the Solution of the Rolling Equations.

A listing has been included of the computer program that was used to solve the governing equations of a ball moving with pure rolling. The program is written in Fortran 77. An executable version is contained on the disk attached to this thesis. The program has been called ROLLS.EXE and needs DOS 3.2 or more to run. The program looks for the file ROLLS.DAT, so the two files must be in the same directory to run the program. The output file and its characteristics has been discussed in the thesis.

```

c.....
c   File = ROLLS.FOR
c.....
c   Purpose ..... The Controlling routine for the ROLLS Program
c   Developer ..... M. Nates, UCT
c   Date ..... September 1989
c   Referenced by .. NONE
c   References to .. ROLLTITL.FOR, ROLLINPU.FOR,
c                   ROLLVARA.FOR, ROLLINCR.FOR,
c   Language ..... Fortran 77 (WATFOR77)
c   Installation ... IBM PC with DOS 3.3
c.....
c   Description of module function:
c   -----
c   This is the calling or controlling routine of the entire numerical
c   solution and computer implementation of the Rolling model. The various
c   subroutines are called inturn, as required. The routine calls for
c   the name of the Output File (Unlike in Balls.for were a subroutine
c   does the calling
c
c.....
c           program ROLLS
c.....
c--- Common block for BALLMILL Problem, rolling case
real OMEGAM,MASS,MU,H,RHO,G,theta,thetad,thetadd,a,imax
real data,OMEGA,OMEGAI,THETAI,thetadi,thetaddi,marker
common/COMROLL/OMEGAM,MU,H,G,RHO,MASS,data(2000,7),theta,
+         thetad,thetadd,thetai,omegai,thetadi,thetaddi,
+         omega,a,marker,imax
character*12 ROLLIN, ROLLOUT
character*1 dummy
call curini

c
c           call rolltitl
c--- open input and output data files
25  format( 'Enter name of output data file.-\' )
35  format(a)
45  format( 'Is the output file to be condensed? Y or N -\' )
write(6,25)
read(*,35) ROLLOUT
write(6,45)
call YesNo(dummy)
  if(dummy.eq. 'Y'.or.dummy.eq. 'y')then
    marker=0
  else
    marker=1
  endif

c
c           rollin = 'roll.dat'
c           open(7,file=ROLLIN)
c           open(8,file=ROLLOUT)

c
c           call ROLLINPUT

c
c           call ROLLINCR

c
c           stop
c           end

```

```

c.....
c   File = ROLLTITL.FOR
c.....
c   Purpose ..... To display an introductory Screen for the Rolling
c                   program
c   Developer ..... M. Nates, UCT
c   Date ..... September 1989
c   Referenced by .. ROLLS.FOR
c   References to .. CURED, CURCUP
c   Language ..... Fortran 77 (WATFOR77)
c   Installation ... IBM PC with DOS 3.3
c.....
c   SUBROUTINE ROLLTITL
c.....
c   call cured
15  format(lx, '*****')
25  format(lx, 'Program to Numerically Solve the Governing ')
35  format(lx, 'Differential Equation of a Single Ball ')
45  format(lx, 'Rolling on the inside of a Smooth Cylinder ')
55  format(lx, '*****')
65  format(lx, 'Theory Developed by: M. Nates')
75  format(lx, 'G. Nurick')
85  format(lx, 'D. Reddy')
95  format(lx, 'Please Wait')
    call curcup(2,15)
    write(*,15)
    call curcup(5,15)
    write(*,25)
    call curcup(6,15)
    write(*,35)
    call curcup(7,15)
    write(*,45)
    call curcup(9,15)
    write(*,55)
    call curcup(12,15)
    write(*,65)
    call curcup(13,15)
    write(*,75)
    call curcup(14,15)
    write(*,85)
c--- delay to keep the front page on the screen
    do 10 i=1,10000
        j=j+1
10  continue
    call curcup(16,15)
    write(*,95)
    do 20 i=1,5000
        k=k+1
20  continue
    call cured
    return
end

```

```

c.....
c   File = ROLLINPUT.FOR
c.....
c   Purpose ..... To read and display the default input variables
c   Developer ..... M. Nates, UCT
c   Date ..... September 1989
c   Referenced by .. ROLLS.FOR
c   References to .. ROLLVARA.FOR
c   Language ..... Fortran 77 (WATFOR77)
c   Installation ... IBM PC with DOS 3.3
c.....
c   Description of module function:
c   -----
c
c   This routine reads the input from a data deck ROLL.DAT
c   It then displays the input variables for modification by
c   ROLLVARA.FOR if required. It is used as a buffer routine before
c   ROLLVARA.FOR. Finally it converts the input data from degrees and
c   rpm to rads and rads/s
c.....
c   Subroutine ROLLINPUT
c.....
c   This routine reads the input from a data deck ??????.???
c   It then creates the time increment and initialises
c   all the other variables.
c.....
c--- Common block for BALLMILL Problem, rolling case
real OMEGAM,MASS,MU,H,RHO,G,theta,thetad,thetadd,a
real data,OMEGA,OMEGAI,THETAI,thetadi,thetaddi,marker,imax
common/COMROLL/OMEGAM,MU,H,G,RHO,MASS,data(2000,7),theta,
+   thetad,thetadd,thetadi,omegai,thetadi,thetaddi,
+   omega,a,marker,imax
c   Initilise all variables
c.....
      Do 10 i = 1,2000
        Do 20 j = 1,7
          data(i,j)=0
20      continue
10      continue

c--- Read input from data deck
read(7,*) OMEGAM,MASS,MU,RHO,G,H,thetadi,thetadi,
&   thetaddi,omegai,a,imax
      omegadi=0
c
c.....
C   Output the input for display
c.....
      write(*,*)
      write(*,*) Listing of the Problem Variables.
      write(*,*)
15      Format( 1x, 'Size of time increments {s} (H) =',F7.3,
+           4X, 'Theta {degrees} (THETAI) =',F7.3,/,
+           1X, 'Mass of ball {kg} (MASS) =',F7.3,
+           4X, 'Theta Dot {rpm} (THETADI) =',F7.3,/,
+           1X, 'Coeffecient of Friction (MU) =',F7.3,
+           4X, 'Theta Dot Dot (THETADDI) =',F7.3,/,
+           1X, 'Mill Speed {rpm} (OMEGAM) =',F7.3,
+           4X, 'Ball Spin {rpm} (OMEGAI) =',F7.3,/,

```

```

+          1X, 'Gravity {m/s2)                (G) = ',F7.3,
+          4X, 'Max Iterations                (IMAX) = ',F7.3,/,
+          1X, 'Mill Radius {m}              (RHO) = ',F7.3,
+          4X, 'Ball Radius {m}              (A) = ',F7.3,/)
write(6,15) H,thetai,mass,thetadi,mu,thetaddi,omegam,omegai,
+          g,imax,rho,a

```

```

c
c---- Check whether the default values are acceptable
      CALL ROLLVARA

```

```

c
      write(8,*)
      write(8,*)                               Listing of the Problem Variables.
      write(8,*)
write(8,15) H,thetai,mass,thetadi,mu,thetaddi,omegam,omegai,
+          g,imax,rho,a

```

```

c
c---- Convert thetai to radians
      thetai=thetai*3.14159/180
c---- convert omegam, thetadi and omegai from rpm to radians
      omegai=omegai*3.14159/30
      thetadi=thetadi*3.14159/30
      omegam=omegam*3.14159/30
c---- Convert thetaddi and omegadi from rpm/s to rad/s2
      omegadi=omegadi*3.14159/30
      thetaddi=thetaddi*3.14159/30
return
end

```

```

c.....
c   File = ROLLVARA.FOR
c.....
c   Purpose ..... To assist with the processing of the Input Data
c   Developer ..... M. Nates, UCT
c   Date ..... September 1989
c   Referenced by .. ROLLINPUT.FOR
c   References to .. ROLLCHAN.FOR, CURED, CURCUP
c   Language ..... Fortran 77 (WATFOR77)
c   Installation ... IBM PC with DOS 3.3
c.....
c   Description of module function:
c   -----
c   This program is used to help with the altering and managent of the
c   ROLLCHAN routine.
c.....
c   Subroutine ROLLVARA
c.....
c---- Common block for BALLMILL Problem, rolling case
real OMEGAM,MASS,MU,H,RHO,G,theta,thetad,thetadd,a,imax
real data,OMEGA,OMEGAI,THETAI,thetadi,thetaddi,marker
common/COMROLL/OMEGAM,MU,H,G,RHO,MASS,data(2000,7),theta,
+      thetad,thetadd,thetai,omegai,thetadi,thetaddi,
+      omega,a,marker,imax
character*1 dum,dummy
equivalence (dummy,dum)
10  continue
C
C---- Check wether the initial default values need changing
write(*,*) 'Are the default values of the variables suitable ?'
75  format(' Y or N \')
write(*,75)
call YESNO(dum)
if(dummy.eq.'Y'.or.dummy.eq.'y')then
goto 60
end if
call ROLLCHAN
call cured
write(*,*)
write(*,*) Listing of the Problem Variables.
write(*,*)
15  Format( 1x, 'Size of time increments {s} (H) =',F7.3,
+      4X, 'Theta {degrees} (THETAI) =',F7.3,/,
+      1X, 'Mass of ball {kg} (MASS) =',F7.3,
+      4X, 'Theta Dot {rpm} (THETADI) =',F7.3,/,
+      1X, 'Coefficient of Friction (MU) =',F7.3,
+      4X, 'Theta Dot Dot (THETADDI) =',F7.3,/,
+      1X, 'Mill Speed {rpm} (OMEGAM) =',F7.3,
+      4X, 'Ball Spin {rpm} (OMEGAI) =',F7.3,/,
+      1X, 'Gravity {m/s2} (G) =',F7.3,
+      4X, 'Max. Iterations {N}(IMAX) =',F7.3,/,
+      1X, 'Mill Radius {m} (RHO) =',F7.3,
+      4X, 'Ball Radius {m} (A) =',F7.3,/)
write(6,15) H,thetai,mass,thetadi,mu,thetaddi,omegam,omegai,
+      g,imax,rho,a
goto 10
60  continue
return
end

```

```

c      File = ROLLCHAN.FOR
c.....
c      Purpose ..... To allow a default value to be entered as input
c      Developer ..... M. Nates, UCT
c      Date ..... September 1989
c      Referenced by .. ROLLVARA.FOR
c      References to .. CURED, GETREAL.FOR
c      Language ..... Fortran 77 (WATFOR77)
c      Installation ... IBM PC with DOS 3.3
c.....
c      Description of module function:
c      -----
c      The module is used if the input variables require changing.
c      The module presents the default value and calls for a new
c      value. If none is entered, then the default value is used.
c      The module calls the subroutine GETREAL.FOR, which is used (with
c      the aid of CHRTOR) to parse the input string into a real number
c.....
      subroutine ROLLCHAN
c.....
c--- Common block for BALLMILL Problem, rolling case
      real OMEGAM,MASS,MU,H,RHO,G,theta,thetad,thetadd,a
      real data,OMEGA,OMEGAI,THETA,thetadi,thetaddi,marker,imax
      common/COMROLL/OMEGAM,MU,H,G,RHO,MASS,data(2000,7),theta,
+          thetad,thetadd,thetadi,omegai,thetadi,thetaddi,
+          omega,a,marker,imax
      INTEGER MARKDEF,numval
      real num,pi

c--- initialise
      MARKDEF=0
      numval=1
      num=0.0
      pi=3.14159265

C      Output the old input for display and change
c.....
5      Format(a)
15     Format( 2x, ' Size of time increments {s}      (H) [',F9.5,']= ',\ )
25     Format( 2X, ' Mass of ball {kg}                (MASS) [',F9.5,']= ',\ )
35     Format( 2X, ' Coefficient of Friction          (MU) [',F9.4,']= ',\ )
45     Format( 2X, ' Mill Speed {rpm}                 (OMEGAM) [',F9.2,']= ',\ )
55     Format( 2X, ' Gravity {m/s2}                   (G) [',F9.2,']= ',\ )
65     Format( 2X, ' Mill Radius {m}                   (RHO) [',F9.3,']= ',\ )
75     Format( 2X, ' Ball Radius {m}                   (A) [',F9.4,']= ',\ )
85     Format( 2X, ' Initial Theta {degrees}          (THETA) [',F9.2,']= ',\ )
95     Format( 2X, ' Initial Theta Dot {rpm}          (THETADI) [',F9.2,']= ',\ )
105    Format( 2X, ' Initial Theta Dot Dot           (THETADDI) [',F9.2,']= ',\ )
115    Format( 2X, ' Initial Ball Spin {rpm}          (OMEGAI) [',F9.2,']= ',\ )
125    Format( 2x, ' Max. Number of Increments{s}(IMAX) [',F9.5,']= ',\ )
135    Format(f12.6)
      call cured

      write(*,*)'*****'
&*****'
      write(*,*)'*** Input the new value at the equals sign,
& ***'
      write(*,*)'*** or press return for the bracketted default value
& ***'

```

```

write(*,*)'*****
&*****'

```

c

```

write(*,*)
write(*,*)
write(*,15) H
call GETREAL(NUM,MARKDEF)
IF(MARKDEF.NE.1)THEN
C--- MAKE H=NEW VALUE AND DO NOT USE DEFAULT
H=NUM
END IF

```

c

```

write(*,25) mass
call GETREAL(NUM,MARKDEF)
IF(MARKDEF.NE.1)THEN
C--- MAKE mass=NEW VALUE AND DO NOT USE DEFAULT
mass=NUM
END IF

```

c

```

write(*,35) mu
call GETREAL(NUM,MARKDEF)
IF(MARKDEF.NE.1)THEN
C--- MAKE mu=NEW VALUE AND DO NOT USE DEFAULT
mu=NUM
END IF

```

c

```

write(*,45) omegam
call GETREAL(NUM,MARKDEF)
IF(MARKDEF.NE.1)THEN
C--- MAKE omegam=NEW VALUE AND DO NOT USE DEFAULT
omegam=NUM
END IF

```

c

```

write(*,55) g
call GETREAL(NUM,MARKDEF)
IF(MARKDEF.NE.1)THEN
C--- MAKE g=NEW VALUE AND DO NOT USE DEFAULT
g=NUM
END IF

```

c

```

write(*,65) rho
call GETREAL(NUM,MARKDEF)
IF(MARKDEF.NE.1)THEN
C--- MAKE rho=NEW VALUE AND DO NOT USE DEFAULT
rho=NUM
END IF

```

c

```

write(*,75) a
call GETREAL(NUM,MARKDEF)
IF(MARKDEF.NE.1)THEN
C--- MAKE a=NEW VALUE AND DO NOT USE DEFAULT
a=NUM
END IF

```

c

```

write(*,85) thetai
call GETREAL(NUM,MARKDEF)
IF(MARKDEF.NE.1)THEN
C--- MAKE thetai=NEW VALUE AND DO NOT USE DEFAULT
thetai=NUM
END IF

```

```
c      write(*,95) thetadi
      call GETREAL(NUM,MARKDEF)
      IF(MARKDEF.NE.1)THEN
C---  MAKE thetai=NEW VALUE AND DO NOT USE DEFAULT
      thetadi=NUM
      END IF

c      write(*,105) thetaddi
      call GETREAL(NUM,MARKDEF)
      IF(MARKDEF.NE.1)THEN
C---  MAKE thetai=NEW VALUE AND DO NOT USE DEFAULT
      thetaddi=NUM
      END IF

C      write(*,115) omegai
      call GETREAL(NUM,MARKDEF)
      IF(MARKDEF.NE.1)THEN
C---  MAKE omegai=NEW VALUE AND DO NOT USE DEFAULT
      omegai=NUM
      END IF

c      write(*,125) imax
      call GETREAL(NUM,MARKDEF)
      IF(MARKDEF.NE.1)THEN
C---  MAKE omegai=NEW VALUE AND DO NOT USE DEFAULT
      imax=NUM
      END IF

c
C---  WRITE NEW VALUES TO DATA FILE, but first and then rewind file
      rewind(7)
      write(7,*) OMEGAM, MASS, MU, RHO, G, H, thetai, thetadi,
&          thetaddi, omegai, a, imax
      rewind(7)

c
      RETURN
      END
```

```

c.....
c   File = ROLLINCR.FOR
c.....
c   Purpose ..... To Solve the Governing Equations of the Pure
c                   Rolling Motion
c   Developer ..... M. Nates, UCT
c   Date ..... September 1989
c   Referenced by .. ROLLS.FOR
c   References to .. None
c   Language ..... Fortran 77 (WATFOR77)
c   Installation ... IBM PC with DOS 3.3
c.....
c
c   Description of module function:
c   -----
c   This subroutine uses an Euler Method to step forward with
c   increment h in time. The path of the ball is traced until the
c   reaction becomes negative and the ball leaves the liner. An out-
put
c   matrix of, as shown below, is created and is written to the output
c   file, named in ROLLS.FOR (ie ROLLOUT)
c.....
c
c   Description of parameters :
c   Matrix called DATA [the columns are filled up with increments]
c
c   Row 1: The number of the increment
c   " 2: Theta, i.e. the angle the ball makes with the horizontal
c   " 3: Thetad, the angular velocity of the ball about mill centre
c   " 4: Thetadd, the angular acc/n " " " " "
c   " 5: Omega, the spin velocity of the ball about its own centre
c   " 6: The normal REACTION of the ball on the liner [R]
c   " 7: The TANGENTIAL force acting on the ball [T]
c.....
c   SUBROUTINE ROLLINCR
c.....
c--- Common block for BALLMILL Problem, rolling case
real OMEGAM, MASS, MU, H, RHO, G, theta, thetai, thetadi, thetadd, a
real data, OMEGA, OMEGAI, THETA, thetai, thetadi, thetaddi, marker, imax
common/COMROLL/OMEGAM, MU, H, G, RHO, MASS, data(2000,7), theta,
+ thetai, thetadi, thetaddi, thetai, omegai, thetadi, thetaddi,
+ omega, a, marker, imax
c--- Initialise required values
integer i, ans
real mill
mill = -3.14159/2
i=1
ans=0
data(1,1)=0
data(1,2)=theta
data(1,3)=thetadi
data(1,4)=thetaddi
data(1,5)=omegai
data(1,6)=mass*thetadi**2*rho-mass*g*sin(theta)
data(1,7)=mass*thetaddi*rho+mass*g*cos(theta)
c
write(*,*) ' No Theta Thetad Thetadd Omega Reac
*tion Tangent Mill Rot.'
write(8,*) ' No Theta Thetad Thetadd Omega Reac

```

```

*tion Tangent Mill Rot.
c
51   format(1x,f5.0,2x,f9.3,2x,f8.4,2x,f8.4,2x,f8.4,2x,f8.4,
*       2x,f8.4)
      write(*,51) data(i,1),data(i,2)*180/3.14159,data(i,3),
*data(i,4),data(i,5),data(i,6),data(i,7)
      write(8,51) data(i,1),data(i,2)*180/3.14159,data(i,3),
*data(i,4),data(i,5),data(i,6),data(i,7)
c
c
10  continue
c
c--- Increment for a step
      data(i+1,1)=i
c--- evaluate theta
      data(i+1,2)=data(i,2)+H*(omegam-(data(i,5)*a/rho))
c--- evaluate theta dot
      data(i+1,3)=(data(i+1,2)-data(i,2))/H
c--- evaluate omega
      data(i+1,5)=data(i,5)+(H*g*5*cos(data(i,2))/(7*a))
c--- evaluate theta dot dot
      data(i+1,4)=-((data(i+1,5)-data(i,5))*a/(H*rho))
c--- evaluate R and T for new thetas, ie at end of step N+1
      data(i+1,6)=mass*data(i+1,3)**2*rho-mass*g*sin(data(i+1,2))
      data(i+1,7)=mass*data(i+1,4)*rho+mass*g*cos(data(i+1,2))
      mill=omegam*h+mill
c
c--- write to output
c
52   format(1x,f5.0,2x,f9.3,2x,f8.4,2x,f8.4,2x,f8.4,2x,f8.4,
*       2x,f8.4,1x,f8.4)
      if(marker.eq.1)then
        write(8,52) data(i+1,1),data(i+1,2)*180/3.14159,data(i+1,3),
*data(i+1,4),data(i+1,5),data(i+1,6),data(i+1,7),mill*180/3.14159
      endif
c
      if(i.gt.imax.or.data(i+1,6).le.0.or.data(i+1,2).ge.1.5708)then
c
        write last three increments only (marker=0)
          if(marker.eq.0)then
            write(8,52) data(2,1),data(2,2)*180/3.14159,data(2,3),
*data(2,4),data(2,5),data(2,6),data(2,7)
            write(*,52) data(2,1),data(2,2)*180/3.14159,data(2,3),
*data(2,4),data(2,5),data(2,6),data(2,7)
            write(8,52) data(i-1,1),data(i-1,2)*180/3.14159,data(i-1,3),
*data(i-1,4),data(i-1,5),data(i-1,6),data(i-1,7)
            write(*,52) data(i-1,1),data(i-1,2)*180/3.14159,data(i-1,3),
*data(i-1,4),data(i-1,5),data(i-1,6),data(i-1,7)
            write(8,52) data(i,1),data(i,2)*180/3.14159,data(i,3),
*data(i,4),data(i,5),data(i,6),data(i,7)
            write(*,52) data(i,1),data(i,2)*180/3.14159,data(i,3),
*data(i,4),data(i,5),data(i,6),data(i,7)
            write(8,52) data(i+1,1),data(i+1,2)*180/3.14159,data(i+1,3),
*data(i+1,4),data(i+1,5),data(i+1,6),data(i+1,7)
            write(*,52) data(i+1,1),data(i+1,2)*180/3.14159,data(i+1,3),
*data(i+1,4),data(i+1,5),data(i+1,6),data(i+1,7)
          endif
          goto 999
        else if(abs(data(i+1,7)).ge.abs(mu*data(i+1,6)))then
c
          write last three increments only (marker=0)
            if(marker.eq.0)then

```

```
    write(8,52) data(2,1),data(2,2)*180/3.14159,data(2,3),
*data(2,4),data(2,5),data(2,6),data(2,7)
    write(*,52) data(2,1),data(2,2)*180/3.14159,data(2,3),
*data(2,4),data(2,5),data(2,6),data(2,7)
    write(8,52) data(i-1,1),data(i-1,2)*180/3.14159,data(i-1,3),
*data(i-1,4),data(i-1,5),data(i-1,6),data(i-1,7)
    write(*,52) data(i-1,1),data(i-1,2)*180/3.14159,data(i-1,3),
*data(i-1,4),data(i-1,5),data(i-1,6),data(i-1,7)
    write(8,52) data(i,1),data(i,2)*180/3.14159,data(i,3),
*data(i,4),data(i,5),data(i,6),data(i,7)
    write(*,52) data(i,1),data(i,2)*180/3.14159,data(i,3),
*data(i,4),data(i,5),data(i,6),data(i,7)
    write(8,52) data(i+1,1),data(i+1,2)*180/3.14159,data(i+1,3),
*data(i+1,4),data(i+1,5),data(i+1,6),data(i+1,7)
    write(*,52) data(i+1,1),data(i+1,2)*180/3.14159,data(i+1,3),
*data(i+1,4),data(i+1,5),data(i+1,6),data(i+1,7)
    endif
    write(8,*) ' !! Ball begins to slide, static friction exceeded !!'
    write(*,*) ' !! Ball begins to slide, static friction exceeded !!'
    goto 999
    else
    i=1+i
    goto 10
    endif
c
999    continue
    return
    end
```

```
c--- Common block for BALLMILL Problem, rolling case
real OMEGAM,MASS,MU,H,RHO,G,theta,thetad,thetadd,a
real data,OMEGA,OMEGAI,THETAI,thetadi,thetaddi,marker,imax
common/COMROLL/OMEGAM,MU,H,G,RHO,MASS,data(2000,7),theta,
+      thetad,thetadd,thetadi,omegai,thetadi,thetaddi,
+      omega,a,marker,imax
```

University of Cape Town